UNIVERSITY OF SÃO PAULO
INSTITUTE OF ARCHITECTURE AND URBANISM SÃO CARLOS

Camila Chagas Anchieta

Regression Models to Assess the Thermal Performance of Brazilian Low-Cost Houses: Consideration of Solar Incidence and Shading Devices

Dissertation submitted to the Institute of Architecture and Urbanism of São Carlos, in the University of São Paulo, in partial fulfillment of the requirements for the degree of Master of Architecture and Urbanism.

Concentration field:
Architecture, Urbanism and Technology

Adviser:
Karin M. S. Chvatal

Financial Support:
CAPES - Coordenação de Aperfeiçoamento de Pessoal de Nível Superior

Corrected Version

São Carlos
2016

A539r

Anchieta, Camila Chagas
Regression models to assess the termal performance of Brazilian low-cost houses : consideration of solar incidence and shading devices / Camila Chagas Anchieta ; advisor Karin Maria Soares Chvatal. – São Carlos, 2015.

Thesis (MA) – Graduate Program in Architecture and Urbanism and Concentration Área in Architecture, Urbanism and Technology – Institute of Architecture and Urbanism of São Carlos University of São Paulo, 2015.

1. Thermal comfort. 2. Building performance simulation. 3. Meta - model. 4. Brazilian low-cost houses. 5. Solar incidence. 6. Shading devices. I. Title.

52
4

FOLHA DE JULGAMENTO

Candidato(a): Arquiteta e Urbanista **Camila Chagas Anchieta**

Título da dissertação: **"Regression models to assess the thermal performance of Brazilian low-cost houses: consideration of solar incidence and shading devices"**

Data da defesa: **01/02/2016**

Comissão Julgadora:	**Resultado:**
Profa. Dra. Karin Maria Soares Chvatal (Orientador) (Instituto de Arquitetura e Urbanismo - USP)	APROVADA
Profa. Dra. Rosana Maria Caram (Instituto de Urbanismo e Urbanismo - USP)	
Prof. Dr. Jopseph F. DeCarolis (North Carolina State University)	APROVADA

Coordenadora e Presidente da Comissão de Pós-Graduação do Programa de Pós-Graduação em Arquitetura e Urbanismo: Profa. Dra. **Cibele Saliba Rizek.**

To my parents, for the love, constant support and belief in me. To my brother, for being a real partner at all times.

Acknowledgments

I thank God for the opportunity I was given, and for capacitating me to fulfill the challenge I faced. I thank for His faithfulness in never letting me down, always by my side.

I thank the constant love and support of my parents, Nelma and Pedro, and of my brother, Pedro H., who were always present, for the good and the bad times, never leaving my side. I thank every phone call with prayers, words of encouragement and sometimes just silliness to make my day better.

To all my family, who are always participating in my life, cheering with me and always encouraging me. A special thank you to my grandmothers, Maura and Mariana, who are so involved in my life and so happy with every accomplishment.

I thank my fiancé Valdir, for being so supportive and understanding of my time away, always calming me and believing everything would be all right.

I thank my adviser, Karin Chvatal, for believing I would be able to do the job and for giving me the opportunity.

I would like to thank everyone who was somehow involved in this work, you each had a participation and are here acknowledged.

I'd like to thank the contributions of everyone at NCSU, Dr. Ranji Ranjithan, Dr. Joseph De Carolis, David Hill, Dr. Soolyeon Cho, Janelle Hygh, Yifan Yang, Sedighehsadat (Nasim) Mirianhosseinabadi and Jeffrey Thomas, as well as Dr. Victor Roriz.

This research was funded by CAPES and the financial support was highly appreciated.

ANCHIETA, C.C. **Regression Models to Assess the Thermal Performance of Brazilian Low-Cost Houses: Consideration of Solar Incidence and Shading Devices**. 2016. 160f. Dissertation (Master) – Institute of Architecture and Urbanism, University of São Paulo, São Carlos, 2016.

Abstract

Building performance simulation (BPS) tools are significant and helpful during all design stages, especially during the early ones. However, there are obstacles to the full implementation and use of such tools, causing them not to become an effective part of the design process. In order to overcome this barrier, this research is presented, with the creation of regression models (meta-models) that allow to predict the discomfort by heat and/or by cold in a Brazilian low-cost house (LCH) in three distinct bioclimatic zones in Brazil, represented by the cities of Curitiba/PR, São Paulo/SP and Manaus/AM. The focus of this work was to analyze the impact of solar incidence and shading devices on thermal comfort by applying the meta-models. The method consisted in a) collecting data from projects referring to the type of building aforementioned to aid in the creation of the base model; b) definition of the key parameters and their ranges to be varied; c) simulations run on EnergyPlus using the Monte Carlo method to randomly create parameters' combinations within their defined ranges; d) regression analysis and meta-models' elaboration, followed by their validation with reliability tests; and lastly, e) a case study, consisting in applying the meta-models to a standard LCH to verify the impact of shading devices in a unit in regards to thermal comfort and the their potential as support tool in the design process. In general, all R^2 values for the meta-models were above 0.95, except for the ones for São Paulo and Curitiba for discomfort by heat, 0.74 and 0.61, respectively. In regards to the case study, the meta-models predicted a decrease of approximately 50% in discomfort by heat for Manaus when a given combination of orientation, quantity and size of the devices was used. For the remaining locations, the meta-models predicting discomfort by heat and by cold require further investigation to properly assess some unexpected predictions and the meta-models' sensitivity to the parameters related to shading devices.

Key words: thermal comfort, building performance simulation, meta-model, Brazilian Low-cost houses, solar incidence, shading devices.

ANCHIETA, C.C. **Regression Models to Assess the Thermal Performance of Brazilian Low-Cost Houses: Consideration of Solar Incidence and Shading Devices**. 2016. 160f. Dissertation (Master) – Institute of Architecture and Urbanism, University of São Paulo, São Carlos, 2016.

Resumo

Ferramentas de simulação computacional são importantes e uteis durante todas as etapas de projeto, especialmente durante as iniciais. No entanto. Há obstáculos para a completa implementação e uso de tais ferramentas, fazendo com que não sejam uma parte efetiva do processo de projeto. Para superar esta barreira, esta pesquisa é apresentada, com a criação de modelos de regressão (meta-modelos) que permitem a predição do desconforto por frio e/ou por calor em uma habitação de interesse social (HIS) no Brasil em três zonas bioclimáticas, representadas pelas cidades de Curitiba/PR, São Paulo/SP e Manaus/AM. O foco deste trabalho foi analisar o impacto da incidência solar e das proteções solares no conforto térmico utilizando os meta-modelos. O método consistiu em a) coletar dados referentes ao tipo de edifício mencionado para auxiliar na criação do modelo de base; b) a definição dos parâmetros chave e suas faixas de variação; c) simulações no EnergyPlus usando o método de Monte Carlo para aleatoriamente combinar valores de parâmetros dentro de suas faixas; d) análise de regressão e elaboração dos meta-modelos, seguida da validação dos mesmos por testes de confiabilidade; e por fim, e) um estudo de caso, consistindo na aplicação dos meta-modelos a uma HIS padrão para verificar o impacto das proteções solares em uma unidade em relação ao conforto térmico da mesma, assim como o potencial dos meta-modelos em serem utilizados como uma ferramenta de auxílio nas fases iniciais de projeto. No geral, todos os valores de R2 foram acima de 0.95, exceto para os meta-modelos de São Paulo e Curitiba para desconforto por calor, com 0.74 e 0.61, respectivamente. Em relação ao estudo de caso, os meta-modelos previram uma queda de aproximadamente 50% no desconforto por calor para Manaus, dada uma combinação entre orientação, quantidade e dimensão das proteções. Para as demais localidades, os meta-modelos prevendo desconforto por frio e por calor requerem maiores estudos para avaliar predições inesperadas e a sensibilidade dos meta-modelos em relação aos parâmetros de proteções solares.

Palavras-chave: conforto térmico, simulação computacional, incidência solar, proteções solares, meta-modelo.

List of Figures

List of Tables

List of Equations

Nomenclature

BPS : Building Performance Simulation

LR_KIT : Living Room and Kitchen

BDR : Bedroom

SZM : Single Zone Model

MZM : Multi-Zone Model

PR : Paraná

SP : São Paulo

AM ; Amazonas

°Ch : Degree-Hour

U : U-value

HC : Heat capacity

LCH : Low-cost houses

NZ : non-zero

EWVA : Effective Window Ventilation Area

EP : EnergyPlus

TRNSYS : Transient System Simulation Tool

ID : identification

WWR : Window to Wall Ratio

HVAC : Heating, Ventilating and Air Conditioning

ABNT: Associação Brasileira de Normas Técnicas

ASHRAE: American Society of Heating, Refrigerating and Air-Conditioning Engineers

INMETRO: Instituto Nacional de Metrologia, Normalização e Qualidade Industrial

NBR: Norma Brasileira

RTQ: Requisitos Técnicos da Qualidade para o Nível de Eficiência Energética

PMCMV: Programa Minha Casa Minha Vida

CFD: Computational Fluid Dynamic

GDP: Gross Domestic Product

idf: input data format

epw: EnergyPlus weather data

csv: cooma separated value

Symbols

˚C : Degress Celsis

F : Fahrenheit

α : Solar absorptance

Kg : Kilogram

W : Watt

J : Joule

f : function

x_1 : regressor

y : response

ΔTa^{room} : Average difference in air temperature

$T_{a,i}^{S}$: Hourly air temperature

$T_{a,i}^{M,room}$: Hourly air temperature

ΔTo^{room} : Average difference in operative temperature

$T_{o,i}^{S}$: Hourly operative temperature

$T_{o,i}^{M,room}$: Hourly operative temperature for each long-stay room

ΔDc^{room} : Average difference in discomfort by cold

$D_{c,i}^{S}$: Hourly discomfort by cold

$D_{c,i}^{M,room}$: Hourly discomfort by cold for each long-stay room

ΔDh^{room} : Average difference in discomfort by heat

$\mathrm{D}_{\mathrm{h,i}}^{\mathrm{S}}$: Hourly discomfort by heat

$\mathrm{D}_{\mathrm{h,i}}^{\mathrm{M,room}}$: Hourly discomfort by heat for each long-stay room

T_n : Neutral temperature (ideal internal operative temperature)

$T_{pma(out}$: prevailing mean outdoor air temperature.

Table of Contents

1 Introduction

Human beings are constantly exposed to climatic changes, and even though they are able to tolerate different types of climate, the limits for comfort are very restricted regarding environmental conditions. To be in a comfortable environment is one of mankind's aspirations, which also guarantees a person's well being.

According to Wu and Sun (2012), thermal comfort can influence the health, satisfaction and productivity of a building's occupants. The authors highlight the importance of ensuring the users' comfort and health by showing that people spend over 90% of their time indoor. To provide a comfortable environment and, at the same time, save energy and money, passive strategies compose a wise solution when designing. Among such strategies, one can highlight the use of natural ventilation, specific choice of materials that respond better to the surrounding environment and climatic conditions, as well as shading devices.

It is the responsibility of architects and engineers to design adequate, comfortable, healthy spaces for users. Such professionals must adapt the solutions they propose according to the design limitations they are presented with. When designing, one must explore a large set of parameters, and consider a building's form, function, material, fenestration and orientation, among others. Building Performance Simulation (BPS) tools are important to aid designers and architects to make informed decisions and find the best solutions to achieve thermal comfort in an environment. According to Struck and Hensen (2007) simulation tools are a powerful way to generate quantitative information to guide professionals during the early stages, providing a rich feedback at a time when it is important and useful to have different design solutions for comparison. The choices made early in the process are very significant to determine a building's performance, making it important for designers to be aware of their initial decisions (PETERSEN; SVENDSEN, 2010). There is an emphasis on the use of BPS tools, since it becomes increasingly difficult to change or implement new improvement strategies as the design approaches its final stage.

Despite the advantages and importance of such tools in the design process, there are still obstacles to their application and implementation, mainly because of their high level of difficulty and costs (HONG; CHOU; BONG, 2000). Such tools require a large quantity of input data describing in detail the model's construction, thermo-physical properties, geometry and control strategies, for example. Carlos and Nepomuceno (2012), state that the user can have difficulties in two distinct moments; when choosing which software to use, and later, when actually using it.

Hong, Chou and Bong (2000) state some important factors to be considered from the user's point of view, justifying why BPS tools are not a common practice, most importantly; (a) Need or purpose: to understand the nature of the problem one intends to solve by using the software is an important consideration to be made. Choosing a software that exceeds the needs presented by the design can be costly and result in more expenses due to its complexity; and (b) Budget: the budget available to buy the software must also include expenses made during its use, such as maintenance, and, if necessary, costs with an adequate computer with the appropriate configuration to run the desired program.

Due to the many difficulties that designers are faced with when using simulation software to predict a building's performance, several studies have been conducted to develop simplified methods as a way to overcome the obstacles presented by such tools. Mathematical methods, more specifically statistical ones, allow users to estimate a building's performance faster, as opposed to the complete simulation process. Architects and engineers can use such simplified methods during the early stages of design as a way to guide important decisions pertaining a building's key elements (WESTPHAL, 2007).

A number of studies have been conducted employing statistical methods to create simplified solutions for designers to use during the early design stages. Hygh et al. (2012) used the software EnergyPlus (EP) within a

Monte Carlo simulation framework to create a linear regression energy model. It was based on a set of parameters considered relevant during the early design stages, and it accurately predicts a rectangular building's annual energy performance for four distinct US climate zones. The model can be the basis of a tool that can provide architects and engineers with real time feedback when modifying basic elements in the building's design.

Other studies on the same field had slightly different approaches to the same problem, and all suggested mathematical methods to create a simplified model to be used during the early design stages. AlGharably et al. (2015) reformulated the model developed by Hygh et al. (2012) and tested different geometries; Asadi et al. (2014) developed seven different geometries for one climate (Houston, TX); Ourghi et al. (2007) compared two types of geometry considering a building's energy consumption in relation to its compactness; Lam et al. (2010) simulated office buildings for different climates in China, varying a total of twelve variables as input; Catalina et al. (2008) developed a regression model to predict heating demands for a single-family residence in temperate climates; Catalina et al. (2013) used a regression model to predict heating demands for residential buildings in three different cities (Moscow, Nice and Bucharest) based on the most influential factors they identified; and Wu and Sun (2012) used a regression model to measure thermal comfort in office buildings that use Heating, Ventilating and Air Conditioning (HVAC) systems. In Brazil, the Brazilian Energy Labeling Schemes for Residential Buildings[1] (RTQ-R; INMETRO, 2012) was developed to assess the energy efficiency of residencies according to the climate they are in. The regulation provides two evaluation methods, one of them being an equation that was developed using regression models.

In this context, this work is developed, aiming the creation of a simplified model that can be applied to the Brazilian reality. The meta-model intends to include a combination of parameters that show a higher impact on the results, and thus inform the user which combination of the available

[1] Regulamento Técnico da Qualidade para o Nível de Eficiência Energética de Edificações Residenciais – RTQ-R

parameters yields the most thermally comfortable design option. The simplified model is a way to provide several options for designers to compare the possible solutions and make an informed decision that will display a high impact on thermal comfort.

The majority, or nearly totality, of the studies developed in this area provides models for buildings with artificial air-conditioning systems, and most of them are focused on office buildings. This research differs from the previously mentioned studies, and intends to fill this gap, because it presents a simplified model to be applied to naturally ventilated residencies, with no use of HVAC systems. The work has developed a meta-model for low-cost houses (LCH) in Brazil, considering three distinct Brazilian climates (Curitiba, PR; São Paulo, SP; Manaus, AM), and it intends to measure the thermal comfort, and not energy use, of a residence that uses solely natural ventilation for thermal control. When natural ventilation is included in the model, it adds a complexity to the model's development. Natural ventilation is an intricate phenomenon to be simulated and the simplifications that can be made to it are very limited.

The focus of the present study is the use of shading devices as a passive strategy, by creating a meta-model that is able to identify the impact of such elements on thermal comfort.

Shading devices are an important element in low-cost houses because such buildings usually do not dispose of any type of HVAC systems. Brazil is a large country encompassing latitudes with intense solar exposure; therefore shading devices are of extreme importance in such climates. The Brazilian regulation NBR 15 220 (ABNT, 2005), presents recommendations to include shading devices in projects for all bioclimatic zones, highlighting the importance of such elements when designing.

All projects can benefit from the use of passive strategies, especially those with budget restrictions and in extreme climate conditions. In Brazil, low-cost houses are built as a solution for the housing deficit, and are an example of where architects and engineers can apply such strategies to improve the thermal comfort for the users, while maintaining the project economically viable. Traditionally, in Brazil, this type of building is restricted to a low budget and lacks in design quality, revealing itself as a field for improvement with the use of passive strategies adopted in the early stages of design.

In an attempt to solve the housing deficit in the country, the program *Minha Casa Minha Vida* (My House My Life) was created, which is a governmental effort set to build low-cost houses in a mass production manner. However, the projects display very low quality, perpetuating the same problems found in previous programs of the same kind established by earlier administrations. According to Amore, Shimbo and Rufino (2015), when considering thermal and acoustic comfort, the houses are inadequate, evidencing the little attention given to design quality and employment of passive strategies for a more comfortable environment. The implementation of shading devices in low-cost houses is very uncommon, since they are not a concern during the design process of such buildings. This situation highlights the importance of the meta-model being proposed, once it is presented as a contribution to faster evaluations during the design process.

The model intends to aid architects and engineers when designing low-cost houses, making it possible for them to investigate and compare different design options, and allowing them to make informed decisions that will result in thermally comfortable residences. The model also accounts for the importance of shading devices, since it is capable of quantifying the impact that a given element can have on a building's overall performance.

1.1 Objectives

1.1.1 Main Objective

The main objective of this research is to develop regression models that allow the fast evaluation of a building's thermal performance while in the early stages of design. It will be used to assess the performance of low-cost houses in at least three Brazilian bioclimatic zones.

1.1.2 Specific objectives

- Assessment of a low-cost house's features related to the building's sun exposure and shading, by using the model.
- Development of a method to aid in the creation of regression models for naturally ventilated Brazilian LCH.

1.2 General Structure

This work is divided into six chapters, with the first one being an Introduction, which includes the objectives aimed in the research. The second chapter is the Literature Review with topics about shading devices, statistical methods and simplified models for early design. The third chapter describes the Methodology adopted for the work developed. The fourth chapter shows all the Results for the meta-models created for each studied climate. The fifth chapter presents the Conclusions drawn from the research, and suggests further work that can be developed. The sixth chapter brings all the References used in this research.

2 Literature Review

2.1 Introduction

Architecture must serve mankind and provide all types of comfort, especially thermal comfort. Human beings can have a better life and health when their bodies are able to function without being submitted to stress or fatigue. Therefore, architecture must offer compatible thermal conditions to people inside buildings, regardless of the weather conditions on the outside (FROTA; SCHIFFER, 2001).

The beginning of all processes to reach comfort in an environment lays in the design. It should meet the cultural, physiological and environmental needs of where it will be built. A poor design can cause health damages, as well as result in high energy consumption (ATEM, 2003). The human body can either gain or loose heat and has certain demands, which are directly related to how the organism works. When the heat exchanges between the human body and the environment occur with little effort, the sensation is of comfort, which increases one's capacity to perform tasks.

The building is the most important instrument that allows people to meet their desired comfort needs, since it accepts changes to its surroundings and brings people closer to optimal living conditions (OLGYAY, 1998). Some architectural elements aid and contribute to a better indoor environment. Passive strategies have been applied for years, resulting in lower energy consumption, as well as improving thermal comfort. Shading devices are important elements to be considered when designing, since they improve the overall quality in an environment, by blocking undesired sunlight, while still letting through a necessary amount of daylight when properly dimensioned.

2.2 Basic Insolation Concepts

2.2.1 Solar Radiation

Solar radiation is an electromagnetic energy of short waves, which reaches Earth after being partially absorbed by the atmosphere. The radiation that crosses the atmosphere disperses, especially due to particles suspended in the air and air molecules, as well as part of it being diffusely reflected by clouds. Until it reaches the ground, radiation loses its intensity; it is absorbed by atmospheric constituents, carbon dioxide, vapor and even ozone (OLGYAY, 1998). The energy transmitted may vary, with moments of higher and lower intensity, for example, at noon and the last hour of the afternoon, respectively.

The amount of energy that effectively reaches the Earth depends, among other factors, on the sky's clarity, regarding clouds, and to the air purity in relation to dust, carbon dioxide and vapor (GIVONI, 1976). The annual and daily solar energy incidence patterns in a given region on the terrestrial surface depend on the solar radiation's intensity and duration.

The greatest influence of solar radiation is in temperature distribution on the globe. The amounts of radiation on Earth vary according to the time of the year and latitude. The phenomena can be better understood when analyzing the sun's apparent movement in relation to the earth (LECHNER, 2009). It is one of the most important natural means that favor a room's heating. However, architects must know how to calculate the desired intensity of such radiation, so there is no discomfort.

2.2.2 Apparent Motion of the Sun

The sun travels a plane circular trajectory, on a varying plane each day. The apparent trajectory plane has a constant inclination, indicated by the same angle as the latitude[2] of the place in question. The plane where the solar trajectory takes place reaches the equinoxes twice a year, established on March 21 and September 21, when the sun rises exactly from the East and sets on the West. After September 21, the plane shifts daily towards South. On December 21, the summer solstice, it reaches the maximum displacement point, and from there on, it starts shifting towards North. It reaches the

[2] Measured from the Equator line, may vary from 0° to 90°. If above the Equator, it is North, and below, South.

extreme north point on June 21, when it begins to shift again towards South, restarting its annual cycle (YANNAS; CORBELLA, 2003).

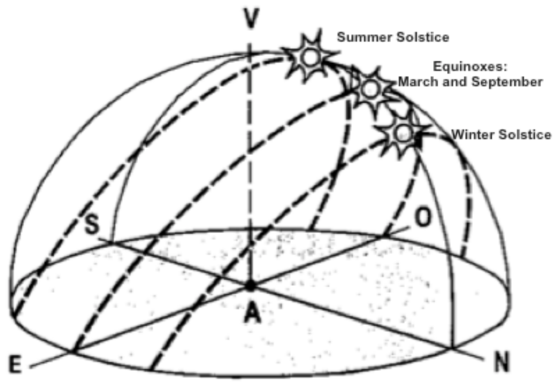

Figure 1 - Sun's trajectory and position at noon. Source: YANNAS; CORBELLA, 2003.

Figure 1 represents a simplified perspective of the above-mentioned trajectories, where it is possible to observe that the summer trajectories are longer than the winter ones. This depicts the fact that summer days are longer than winter days; consequently, the sun exposure during this season is more intense and prolonged.

It is important to understand the apparent motion of the sun, so designers can gather the necessary information to understand how to use the physical form of a building to better control and use the sun's energy to provide a healthy and comfortable environment.

2.2.3 Solar Chart

Solar charts are used to determine the sun's angle of incidence on a given surface. They consist in the graphic representation of the sun's apparent motion, being projected on a plane on the observer's horizon for each given latitude (LECHNER, 2009). When the trajectories are represented by several days of the year for the same latitude, there is a solar chart. The charts contain, for that latitude, the same information provided by expressions, thus being useful in solving insolation and shading problems, given their simplicity. The charts represent the Azimuth[3], varying from 0˚ to 360˚, the solar height[4] from 0˚ to 90˚, and the apparent solar trajectories of some days of the year during a whole day (LECHNER, 2009).

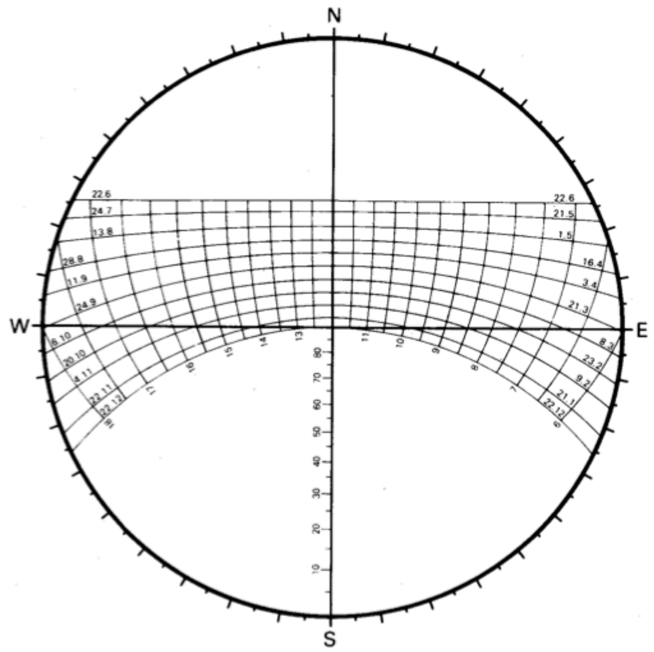

Figure 2 - Solar Chart for Latitude 24˚ South. Source: FROTA; SCHIFFER, 2001.

By directly analyzing the solar chart (Figure 2), it is possible to make important conclusions that can greatly influence a buildings design concerning its orientation and possible shading devices.

2.3 Shading Devices

There is a variety of shading devices, which can be adjustable, fixed or retractable, with different shapes and geometric configurations. These elements perform several functions, such as eliminating the sun in periods of intense heat, allowing it only in colder periods, and they can affect the sunlight and ventilation as well. The importance of such elements can vary according to the different weather conditions where they are applied, that is;

---

3 Horizontal angle, measured from south on a north-south line.

4 It is related to the hour of the day. When the sun rises, its height is zero, and the value increases until it reaches its maximum value at noon. After noon, the value starts to decrease until it reaches zero again, at sun down.

in a residence, direct sunlight can be appreciated during the winter and avoided during summer. In a classroom, direct sunlight can disturb the users regardless of the external conditions (GIVONI, 1976).

Shading devices are important to control sunlight exposure in a room, and they should be designed as part of the architectural project. Such elements can be applied to walls, be they transparent or not. They can be internal or external to windows, or even an element that composes the building's façade and provides thermal comfort to its users.

In order to use glass and still maintain adequate levels of comfort in the environment, it is necessary to intercept the energy before it enters the building. In other words, the solar radiation must be reflected and dissipated when it is still on the outdoor, so the internal temperature can be pleasant. According to Lechner (2009), the devices applied to the exterior are more efficient, since they block the solar radiation before it enters the room. One can argue that adjustable mechanisms show greater results, once they can be adapted according to the sun's trajectory, which varies during the year. However, because each device is designed according to the building's use, location and other factors, it all varies, and sometimes, an internal, or an external fixed device can be the most appropriate solution.

Providing shading elements for glazed surfaces can reduce the heat impact up to one-third (OLGYAY, 1998). The location, latitude and orientation of such elements contribute to defining the most efficient mechanism. The reasons to design such elements may vary, but ultimately, they will be based on regional models defined by the sun's intensity and angles of incidence.

During specific seasons, sunlight can be excessive, which is why it is important to design and dimension the shading devices accordingly. Preferably, they should block the excessive solar radiation of a given surface during months of intense heat, but allow sunlight to enter the room in the colder seasons, as illustrated by Figure 3. The functional demands for shading devices differ according to the climate and, within each specific region, to the climactic variations of each season.

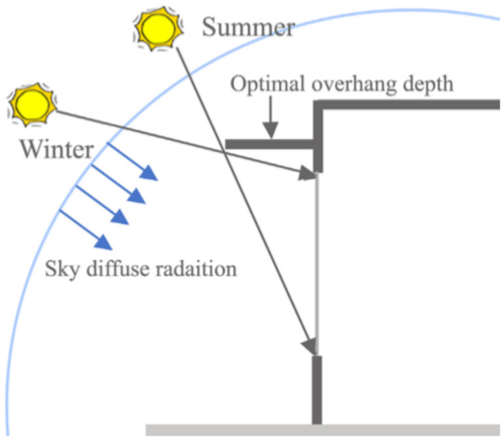

Figure 3 – Optimal overhang depth Source: Yao, 2014

The level of efficiency of the shading devices has a great significance to the comfort of naturally ventilated spaces, and contributes to the configuration of the internal air temperature. If a shading device is not adequately designed, solar radiation enters the room and heats it up, showing that the temperature is related to the window's orientation on a building. The use of shading devices affects the amount of incident radiation, and thus alters the heat flow to the interior as well as the internal temperatures.

2.4 Solar Incidence Control Studies and the use of Shading Devices by Measuring and Simulation

Several authors performed studies to verify the efficiency of shading devices, internal and external. It is important to highlight that windows also play an important role on a building's thermal performance, because they allow transmittance, solar energy enters the room through the glass and the heat generated is trapped in the room, a phenomena known as the greenhouse effect (GIVONI, 1976). As a means to improve thermal comfort and avoid the greenhouse effect in buildings, shading devices are presented as a solution.

In a study performed in China (YAO, 2014), by the means of measuring, the objective was to investigate the impact of articulated shading devices in relation to energy consumption in a residential building. It was observed that the windows with shading devices that received the most solar incidence not only presented a decrease of up to 30.87% in energy consumption, but also improved the thermal comfort in the environment by 21% during the summer. The elements reduced the risks of discomfort by approximately 80%, and improved the conditions for visual comfort in almost 20%.

Since simulation is an important tool and aid in the process of decision making during the early design stages, and contribute to a building's better thermal performance, several studies using different software have been conducted to verify the advantages of using shading devices and their relation to energy use and a buildings thermal performance.

Tian; Sun; Zhou[5] (2009, *apud* YAO, 2014) used DOE-2 to simulate the performance of non-fixed elements in residential buildings in different cities, which presented a very warm summer and very cold winter. The results showed a significant reduction in energy use, varying from 17.29% to 22.68%. Other similar studies performed by the same authors used simulation programs and varied the types of shading elements. Zhang *et al*[6], (2010, *apud* YAO, 2014) using CFD (Computational Fluid Dynamic) concluded that blinds and shades increase the indoor thermal performance. However, these elements present a negative impact on natural ventilation, in regards to the blinds.

Bellia et al. (2013) used EnergyPlus to verify the influence of external shading devices in relation to energy consumption in office buildings. The study focused on three specific locations in Italy, each representing a different type of climate; hot, mild and cold. The simulations were performed varying the depth of the elements from 0.5m, 1.0m and 1.5m, all fixed and horizontal. In general, the results presented a decrease in energy use where the elements were applied. The most significant results were from those with

---

[5] TIAN, H. F.; SUN, D. M.; ZHOU, H. Z. The energy saving performance of movable sola shading for building energy saving by 65%. *Wall Mater Innovation Energy Saving Buildings*, 2009.

[6] ZHANG, H. X. *et al.* Influence of retractable external shading of buildings on indoor thermal environment in Nanjing. *Jiangsu Construction*, 2010.

the depth of 1.0m, showing a decrease of up to 20% in the total energy use (lighting, cooling and heating) for the hottest climate.

Ahmed (2012) also performed a study using simulation, and the software of choice was TAS (Thermal Analysis Software). The building simulated was a residence inserted in a hot climate with vertical shading elements with a depth of 0.38m, and presented a decrease of up to 2˚C in the shaded rooms.

Several other studies (DATTA, 2001; VAN MOESEKE; BRUYÈRE; DE HERDE, 2007; PALMERO-MARRERO; OLIVEIRA, 2010; HAMMAD; ABU-HIJLEH, 2010; LITTLEFAIR; ORTIZ; BHAUMIK, 2010; DA SILVA; LEAL; ANDERSEN, 2012) varied the types of shading devices in different locations and also concluded that when the devices are used, the result is a decrease in energy consumption and an increase in thermal comfort. Some studies state that the devices also improve visual comfort, by reducing glare.

The dimensions attributed to the openings can influence the amount of heat gain in the environment, as well as the conditions for natural ventilation and the thermal physical properties of the building's materials.

2.5 NBR 15 220, NBR 15 757 and RTQ-R: Building's Thermal Performance

There are three regulatory documents that discuss the thermal performance and energy efficiency of a building in Brazil, namely NBR 15 220 (ABNT, 2005), the RTQ-R (INMETRO, 2012) and NBR 15 575 (ABNT, 2013).

In NBR 15 220, which is specific to low-cost houses, thermal performance is characterized by the minimal thermal performance behavior expected for buildings and/or its components – windows, roof, envelope material – to provide better conditions for comfort and less energy consumption. Part 3 of this regulation – Brazilian bioclimatic zoning and construction guidelines for low-cost single-family houses (*Zoneamento bioclimático brasileiro e Diretrizes construtivas para habitações unifamiliares de interesse social*) (ABNT, 2005), identifies 8 different types of climate in the country. It specifies for each of them, passive strategies for thermal conditioning, considering the following parameters and conditions: (a) windows' size for natural ventilation; (b) shading devices; (c) external seals; and (d) passive strategies for thermal conditioning.

The Brazilian Energy Labeling Schemes for Residential Buildings (RTQ-R; INMETRO, 2012) assesses and classifies residencies based on their level of energy efficiency by using a regression model. Specifically regarding shading devices in the equation, the variable for their calculation (somb) defines the presence of such devices placed on the exterior. Different values mean different types of devices: a value of zero (somb=0) means there are no shading devices; a value of 1 (somb=1) means there are blinds covering 100% of the window when the blinds are closed; when $0<somb \leq 0.5$, it is related to rooms shaded by a porch, roof overhang or overhang; and when somb=0.2, also for rooms shaded by a porch, roof overhang or overhang, there are angle limitations for each orientation and latitude.

NBR 15 575 is specific to residential buildings and presents two methods to evaluate a building's thermal performance; the simplified method and simulation. In the simplified method, the residence is evaluated solely based on the thermo physical properties of its walls and roof, and the effective window opening area. When using simulation, if the building doesn't meet the necessary performance criteria, the use of shading devices is recommended as such; external or internal shading device with an element that reduces at least 50% of the direct solar radiation that enters through the windows (CHVATAL; RORIZ, 2015).

2.6 Low-cost Houses

The way projects are designed, and most important, how their program is defined, is key to a sustainable project and its planning. If a design doesn't include energy efficiency and thermal comfort as a requisite in its program, for example, it is very unlikely that the project will meet this demand once it is ready. Because designing is a process, changing the process will significantly alter the product (WILLIAMS, 2007).

Despite the importance of the design process in architecture and its adequate insertion in the urban context, there is not enough emphasis on it in Brazil for low-cost houses. The housing deficit is high in the country, and there isn't a proper concern given to the projects for low-cost houses. According to a research conducted by Fundação Getúlio Vargas (FGV), the Brazilian housing deficit was of 5.8 million families, which, at the time, represented 9,3% of families with no place to live or that lived under inadequate conditions (IBGE, 2009). In response to this situation, the government has created several social programs in an attempt to solve the housing deficit problem that has been aggravating for the past years. However, it is possible to observe that many of the residences being offered by the programs show very low quality and don't address important issues for this type of building (AMORE; SHIMBO; RUFINO, 2015).

As part of the solutions created for the housing deficit, the federal government can financially support the construction of residences, which are destined to be low-cost houses (Habitações de Interesse Social – HIS). This measure is taken the government is able to provide the access to properties, such as in lease (CTHAB, 2012). In March 2009, the Brazilian government sanctioned a document (Medida Provisória n°459) that instituted the program 'Minha Casa Minha Vida' (My House My Life) (PMCMV, 2009). The program consolidates a public policy to promote and motivate financing, aiming to build a million residential units.

However, as indicated by Faria et al. (2003), such programs, despite their magnitude, don't take into consideration extremely relevant facts to adequate the residences to climatic conditions or their surroundings. One can notice a standardized pattern in the designs, showing the same typology being applied in all regions across the country.

National regulations can contribute to the designs' quality improvement, such as RTQ-R, NBR 15 575 and NBR 15 220. The latter, recommends design strategies for single-family low-cost residences for each bioclimatic zone to be applied during the design stage (ABNT, 2005). NBR 15 575 (ABNT, 2013) explores the performance of residential buildings, with requirements in several fields. RTQ-R (INMETRO, 2012), which can also be applied during the design stages, refers to energy efficiency in residential buildings. Despite the existence of such methods available to be applied when designing, the tendency is for these methods and regulations to be used only when the projects are ready, to simply verify the impact of small changes, yet not significant. It would be more interesting for the regulations to be applied when designing, at the early stages, so better options can be created and thus avoid changes in post-construction.

It would be ideal that the problems related to thermal comfort found in low-cost houses to be solved during the early design stages. To make informed decisions regarding an architectural project requires managing a great amount of detailed information about the design options and a prediction of their performance (MARQUES; CHVATAL, 2011). Such decisions could also be aided by the use of simulation tools, which, according to Petersen and Svendsen (2010) are ideal for this process.

2.7 Computer Simulation

2.7.1 Introduction

The concept of computer simulation and its importance are intrinsically related to energy efficiency and thermal performance. This is shown more clearly in the 1970's, after the oils crisis, when several countries turned their resources and researches to the development of alternative sources of energy and more efficient systems. In the following decade, conventions take place and protocols are written to reduce the emission of harmful gases into the ozone layer. In the 1990's the highlights are the *Agenda 21*, which took place in Rio de Janeiro to discuss the main challenges involved with sustainable construction, and the Kyoto Protocol. Such events resurfaced the issues about gas emissions and renewable energy sources, making them a concern in the civil construction field (GOLDEMBERG; AGOPYAN; JOHN, 2011). In this context, building energy performance gained more attention, in the residential sector as well as in the commercial and public ones, since they were responsible for an important parcel of the produced energy. European countries and the United States, very dependent on oil to supply electric energy, started to finance initiatives that promoted the development of more efficient buildings, which included the ones already built and the ones still in the design stages (MENDES, 2005).

The concept of energy efficiency became the focus of several engineering and architecture offices, especially in the public sector, which had the need to promote the use of technologies that guaranteed the same performance using less energy. However, to assess energy consumption in a building is not a simple task, on the contrary, it involves a great quantity of interdependent variables and multidisciplinary concepts (MENDES, 2005).

According to Mendes (2005), when computers became more popular, it was crucial for the development of physical models that represented the thermal and energy behavior of buildings, allowing simulations of different scenarios and providing solution alternatives. Computer simulation software started to be developed in the 1960's, and became a topic of interest only in the following decade. Since then, several tools have been developed to aid designers in analyzing more efficient alternatives I, in the field of energy efficiency (WESTPHAL, 2007). Investments in this area were gradually reduced, until they gained a new motivation when personal computers became more usual in the 1980's.

From the 1990's on, there was a growing concern related to energy and the environment. Simulation software, previously restricted to the academia, became more popular amongst professionals in the area. Today, much more accessible and advertised, they are estimated around 300, allowing an analysis from the thermal performance of a constructive component, to the integrated simulation of the building's energy behavior and its systems (WESTPHAL, 2007). Simulation programs present advantages in the moment of design or even for posterior verifications, allowing an evaluation of several items still in the early stages of design.

2.7.2 Importance

The design process has migrated from an artesian approach to a process that involves advanced technologies and inherits innumerable difficulties. This can be seen with the idea that simulation must not be used only to confirm the final performance, but as an integrated element to the design process (MORBITZER *et al.*, 2001). As a design requisite, there is a growing demand for better energy efficiency in buildings, which leads to the development of technological strategies to meet such demands and enhance energy efficiency in buildings without compromising its comfort, cost, aesthetics an other performance considerations (PETERSEN; SVENDSEN, 2010).

Energy simulation programs are able to calculate complex interrelations between the building, its systems and the outdoors. They also allow the performance prediction of the building's envelope, HVAC systems or natural ventilation controls, cooling and heating loads and energy consumption. The calculations they perform are based on algorithms that model the energy balance and heat transfer between a building's surfaces (ZHAI; CHEN, 2005). In general, it is important that the user is able to quickly comprehend how the building's geometry and shape, glazing areas and rooms with specific functions, as well as the types of construction will affect the building's environmental performance (MORBITZER *et al.*, 2001).

Choosing the ideal combination within the available design options is a highly complex and costly task. To create a general overview of the possible design options and their respective performances is a critical task for engineers and architects. According to Petersen and Svendsen (2010), if the design process is ill informed, there is the distinct risk of a design opportunity that could lead to a better performance be unnoticed, as well as the chance of making a choice that can lead to undesirable effects. Making informed decisions requires managing a great quantity of information about the detailed properties of a building's options and its performance simulation. According to other authors, simulation tools are ideal for this. However, it is also pointed out that most of the available tools are developed for researchers and, therefore, very specific for this area, resulting in programs that are not easy to apply in daily tasks, since they require a high level of expertise. On the other hand, as performance issues, such as environmental comfort and energy efficiency become more important, the capacities for building simulations become more specific when required to provide information to better decision making in the design process.

The objective for computer simulation is to allow the user to make informed decisions based on the results. However, it is necessary to know how to interpret and evaluate the results based on previous experiences and/or regulations pertaining the implantation site for a given building. Interpreting the results and making the appropriate decisions requires professional experience and knowledge of the real world, so that the decisions made based on the results are coherent to the local reality and society where the building will be inserted, thus meeting the needs presented by the client (PETERSEN; SVENDSEN, 2010).

According to Brahme *et al.*, (2001), despite the aid and importance that simulation software present, they still face some conflicts. It is important that the designer has a response at the earliest stage during the design process. However, many aspects related to the building's performance are affected by the projects of technical systems, which are configured in detail on later stages. Several characteristics related to a building's performance are significantly affected by a building's sub-systems; therefore, providing a good feedback to engineers and architects at the earlier stages is very valuable. The challenge, nonetheless, is to find a method that allows the use of a detailed simulation tool still at the early stages of design, when the values for several variables are not yet available. Such method could aid in reducing the amount of input data, and thus simplify the use of the tool for the common user; that is, a primary designer instead of a specialist in energy systems.

2.7.3 Advantages

Simulation programs allow the assessment of the thermal and energetic behaviors of a building for different design alternatives, be they in drawing, constructive components, openings, and lighting or air conditioning systems. Computer simulation allows to estimate energy consumption, the costs for the given consumption and the environmental impact that can be caused by certain design choices even before the project is executed; thus proving itself to be a valuable tool to attain and maintain the concept of energy efficiency (MENDES, 2005).

It is a method that presents good cost benefit and efficiency, predicting the thermal performance of buildings given several architectural choices. Simulation can model heat transfer and radiation processes in seconds based on heat balance and CFD (computational fluid dynamics), which can predict reliable results for airflow for the interior and exterior (WANG; WONG, 2009). In general, simulation tools include two fundamental modules: thermal simulation and airflow. These modules are essential to solve heat and mass transfer and ventilation in a building's systems. Such tools aid in sustainable projects that aim to achieve energy efficiency, by providing results pertaining a building's thermal behavior and helping designers to better understand the consequences that each design choice might bring.

The parametric analysis allows professionals to expand the concepts in their designs to incorporate new technologies and innovate, thus creating opportunities to save more energy. It is possible to observe that simulation is one of the main technologies that contribute to more efficient constructions; and this alternative may be the key to improve the overall building's performance. Simulation programs can be used to investigate the technical and economic viability of passive design options, such as shading devices, natural ventilation and lighting. Detailed programs, such as EnergyPlus, performs hourly calculations based on the indicated thermal zones; therefore, the most desirable option and building operation can be achieved (HONG; CHOU; BONG, 2000).

Today, building simulation is not integrated to the design process. However, due to the complexity posed by the process and the advanced technologies that can be used in construction, this is a very desirable option. Integrating this process to the modeling stages would increase awareness about environmental issues and provide an adequate status to the decision made during a project (MORBITZER *et al.*, 2001).

2.7.4 Simulation use nowadays

Building energy consumption in Brazil corresponded to approximately 40% of the total electricity consumed in the country in the early 2000's, taking into consideration the residential, commercial and public sectors. It is possible to observe an increase in building energy consumption accompanied by an increase in the GDP during the same period. Therefore, a growth in economy, did not proportionally represent an increase in building energy efficiency (MENDES, 2005).

With the progress of computer resources, such as an increase on memory processing, more complex and modern software could be developed. However, because they encompass complex physical phenomena, computational tools that provide reliable results, such as EnergyPlus, Fluent, CFX and Phoenics, are used mostly in research centers, such as universities and institutes, keeping their use and technology transfer to the commercial sector very diminished (MENDES, 2005).

Even though there are several programs today, one of the main reasons that keep them from being applied is their usability. As presented by Hong, Chou and Bong (2000), Annex 30 of IEA-ECBS approaches the relevant difficulties and aims to create bridges to solve some important gaps between what scientists and engineers are offering regarding such software, and what is really used in everyday life. The authors also indicate the following steps to assess a program's usability; (a) learn to use; (b) prepare the input data; (c) run the program; and (d) interpret the results. Ideally, the programs should be easy to learn and user-friendly, as well as offering a good manual.

The programs should go beyond offering usability; they should also provide the capacity of data exchange and support to the database. Sometimes it might be challenging to work with such programs, given their communication with other programs and systems is impossible, restricting part of the input data that could be provided by another software. Therefore, simulation software should have a mechanism to import data from other bases, as well as exporting them.

2.7.5 Difficulties

Even though there are several simulation programs available today, they are still underused; mostly because of their high level of difficulty and elevated costs to their application (HONG; CHOU; BONG, 2000). The use of detailed computational tools to assess a building's thermal performance is very accepted in the academic community. However, the tools developed for such purposes usually require a large number of input data describing the construction in detail, its thermo physical properties, the building's geometry and control strategies, among others. The different approaches and the lack of a common language to describe the tools could be an obstacle when choosing the appropriate one for each situation.

Depending on the user's goal, more than one software may be required to fulfill the task. Usually, it is possible to identify several stages within the architectural project, such as: (a) pre-design stage, where general conception ideas are formulated; (b) early design stage; (c) scheme design stage; (d) conceptual design stage, where decisions about the construction are made; and (e) detailed design stage, to characterize the whole building construction (CARLOS; NEPOMUCENO, 2012).

Decisions made within each stage influence the building's overall performance. However, it is during the early design stages that the most significant solutions are established, since the building's envelope parameters and air change rates are very determining in its performance.

In general, the programs can be assessed based on their cost and performance. The cost, which usually presents itself as the major obstacle to the use of such tools in architecture and engineering offices, is twofold: (1) the software's cost; and (2) the cost for its use. Within the costs mentioned, it is pointed out by Hong, Chou, Bong (2000) three main items: (a) the software's cost itself, the license, services and update fees; (b) a cost with training, usually charged by the ones selling the product to train new users; and (c) the use, including the work and resources, such as computers that are necessary.

When analyzing these factors from the user's standpoint, and with those, the additional costs that can be generated when applying simulation tools, it is possible to comprehend why such tools are not frequently used in the common practice of architects and engineers.

2.7.6 EnergyPlus

EnergyPlus is cited as a milestone in the new era of computer programs, since it allows the integration of modules developed independently. It was developed by the US Department of Energy, and validated by ASHRAE-140 (ASHRAE, 2004). Its first version was launched in 2001, and it was created using BLAST and DOE-2, incorporating the main features of both. The program provides the development of interfaces for less experienced users, while maintaining a robust simulation code (WESTPHAL, 2007), and working with input and output files in text format. It presents as an alternative EP-Launch, which allows managing the simulation, and IDF-Editor, where one can create and alter parameters.

The program was developed to simulate thermal loads and perform energy analysis of buildings and their systems. It is able to generate a differentiated simulation, such as time-step[7] with the calculation of less than one hour, modular system, possibility of different air infiltration calculations for each thermal zone, thermal comfort indexes calculations and integration with other systems (LABEEE, 2009).

[7] The object time-step refers to moments of iteration in the simulation. For example, within one hour, if the value of 6 is attributed to the time-step, the iterations will occur every ten minutes.

The input files present all the simulation's parameters that can be created or altered in the IDF-Editor. These are automatically generated with the .idf extensions to be read in EnergyPlus, with the possibility of being altered in Microsoft Word, since it's in text format. When the user manages the simulation, the program allows selecting an *.idf* file and a climate file with the *.epw* (EnergyPlus Weather File) extension to run the simulation for a year of reference. The output data can be post-processed in spreadsheet software, which allows the data analysis, as well as the creation of graphs to better visualize the results.

2.8 Statistical Methods

2.8.1 Introduction

According to Saltelli (2001), models can be developed to approximate or mimic systems and processes of different types and of varied complexities. Many processes, such as simulation, are complex, time consuming and expensive. Mathematical models can aid in the exploration of systems and processes, once they are a series of equations, input factors, parameters and variables that aim to define the process in question.

Hygh et al. (2012) state that simulations can become more effective with the development of simplified methods or interfaces, allowing a decrease in the necessary input data, faster results (outputs), and turning the entire process more intuitive for designers. Other studies also applied such methods; Chung, Hui and Lam (2006) used multiple linear regression to develop an evaluation process for energy efficiency in commercial buildings. Eisenhower et al. (2012), also using regression techniques and the Monte Carlo method for the random sampling, developed a base-model, which was then optimized and used to evaluate the thermal comfort and annual energy consumption in a building.

According to Westphal (2007), the regression equations obtained from the simulation results of several models, allow an estimate of a building's performance in a faster way, as opposed to the complete simulation process.

It can also be used to guide architects and engineers during the early stages of design.

2.8.2 Monte Carlo

The basis for a Monte Carlo analysis lays in performing multiple model evaluations with randomly selected inputs for a model, and then using the results of such evaluations to establish the uncertainty in the predictions, as well as the input variables that might cause such uncertainties. For this type of analysis, it is usually not necessary to specify or consider details (HELTON, 1993).

The Monte Carlo analysis can be divided into five steps as follows (SALTELLI, 2001) (HELTON, 1993):

1) Definition of a range and distribution for each one of the selected parameters being considered.
2) Generation of a sample from the given ranges defined on the previous step. A sequence of sample elements will be the result, where there is a number of input variables and a sample size. There are different sampling procedures, such as random sampling, stratified sampling and quasi-random sampling.
3) Evaluation of the model for each sample element, creating a sequence of results. Each element is supplied to the model as input, thus creating a sequence of results that can be later studied in uncertainty and sensitivity analysis.
4) Uncertainty analysis. Uses the results as a basis for it.
5) Sensitivity analysis. Distributes the variation in the output to the different sources of variation in the system under consideration.

2.8.3 Regression Analysis

Due to several difficulties faced when simulating a building's thermal performance, studies have been conducted to develop statistical methods as an alternative to overcome the obstacles presented by software. Statistical relationships don't necessarily imply connecting relationships, but if there is a statistical relationship, it can be used as the beginning of additional research. Once there is confidence of the existence of such relationship, one can try to model it mathematically and use the model for prediction (SEBER; LEE, 2003). Regression analysis is a method that can answer questions about the dependence of a response variable on one or more predictors. This includes the prediction of future values of a response, discovering the predictors that are important, as well as estimating the impact of changing a predictor or a treatment on the value of the response (WEISBERG, 2005).

Regression is a mathematical method that allows predictions about the behavior of a given phenomena from reality, presenting a relationship of cause and effect. It is the study of dependence, a statistical analysis, and the goal is to summarize the observed data as simply and usefully as possible. The goal is to construct mathematical models that describe the relations that may exist between the given variables, the simplest case being when there are two variables. An important task is to find the existing relationships, if there are any, in a set of variables when at least one of them is random, which will be subject to random fluctuations and possible measurement error (SEBER; LEE, 2003).

The method relates the behavior between two variables, X and Y, with the function *f*. The X variable is the independent one, while Y is the one that depends on the variations of X. Typically, in regression problems, the variable Y is called the *response* or the *dependent*, while X is usually called *explanatory* or *regressor*, and also known as the independent variable primarily used to predict or explain behaviors of Y.

The relationship between X and Y expressed by a function *f*, as mentioned, would be

Equation 1

$$y \approx f(x_1, x_2, \dots x_n)$$

By using *f*, Y can be predicted for a given set of X's. Due to unexplained fluctuations or noise, and some degree of measurement error in the data, the relationships will never be exact (SEBER; LEE, 2003). Because the parameters usually have physical interpretations, the main objective is to estimate the parameters as precisely as possible. The relationship between variables can be linear or nonlinear. Such type of analysis allows four basic models; a) simple linear; b) multivariate linear; c) simple nonlinear; and d) multivariate nonlinear.

An essential step in regression analysis is to draw adequate graphs for the data. When the data are plotted, the information pairs present a 'cloud' of dots defined by the coordinates of each point. The cloud defines the axis or direction that will set the relationship pattern between the variables. This fundamental graphical tool is a two-dimensional scatterplot. Sometimes, scatterplots alone can completely reveal the relationships between the model input and the predictions. A scatterplot of the response versus the predictor is the first step for regression analysis (WEISBERG, 2005), and an examination of these plots can also be a good starting point for a sensitivity study.

If there are *n* pairs of observations (x_i, y_i) (i= 1, 2, … *n*), these points can be plotted on the graph and try to fit a line through the points in a way that they are as close as possible to that line. An exact fit cannot be expected, due to the abovementioned fluctuations and factors not under one's control (SEBER; LEE, 2003).

2.8.4 Stepwise Regression Analysis

Stepwise regression analysis offers an alternative to build the regression model with all the input variables (HELTON, 1993). A sequence of regression models is built using the following steps (SALTELLI, 2001):

a) The first regression model contains the single most influential input variable in relation to the output variable. This is the input variable that shows the largest correlation with the output variable *y*.

b) The second model presents the next most influential input variables, given the one from the previous step. It contains two input variables; the one from the first step plus whichever of the remaining variables has the largest impact on the uncertainty and was not accounted for by the first variable.

c) The third model presents a third variable, given the variables in the previous steps. It contains the three input variables with the largest impact on the output variable; the two variables from the second step plus whichever of the remaining variables has the largest impact on the uncertainty and was not accounted for by the first two variables.

Additional models are defined in the sequence, until it reaches a point where the subsequent models cannot significantly increase the amount of variation in the output variable. In each step of this process, it is possible for an already selected variable to be dropped out if it no longer has a significant impact on the amount of uncertainty in the output variable that can be accounted for by the regression model. This is only the case when there are correlations between the input variables (SALTELLI, 2001).

Various aspects of this type of analysis can provide insights on the importance of individual variables. One of the aspects is the order in which the variables are selected in the procedure, indicating their importance with the most important being the first and so on. Another aspect concerns the R^2 values at successive steps, which can also be regarded as the determination value, and the closer it is to 1, the more precise the equation is. It also provides a measure of the variable's importance indicating how much of the uncertainty in the dependent variable can be accounted for by all variables selected in each step (SALTELLI, 2001).

2.8.5 Studies Applying Statistical Methods

The following studies used regression analysis to create simplified models to aid designers during early design stages.

Hygh *et al.* (2012) developed a regression model for a rectangular office building for four different cities in the USA; Miami, Winston-Salem, Albuquerque and Minneapolis. The study used EnergyPlus to run the simulations in a Monte Carlo framework, and a multivariate regression model created was based on 27 parameters considered as the most relevant in early design stages. A total of 20,000 simulations were run for each location, from which 16,000 were used to build the model and the remaining 4,000 to validate it. The validation procedure consisted in taking the predictions made by the model and comparing them to those given by EnergyPlus considering the same input data. All locations, except for Miami, presented R^2 values exceeding 96%, which suggests that the model is an acceptable support tool for early design stages instead of energy simulation models.

AlGharably et al. (2015) reformulated the model developed by Hygh et al. (2012) and tested it with different geometries, with the intention of generalizing the geometric properties of non-rectangular buildings. The simulation data used to develop the original model were used to create a revised regression model, including five new parameters. Stepwise linear regression was applied for heating and cooling loads for each of the four climates (Miami, Fl; Winston-Salem, NC; Albuquerque, NM; and Minneapolis, MN). The simulation set consisted of 16,000 simulations randomly chosen from the existing 20,000. The simulations were run using EnergyPlus, and the validation method used the remaining 4,000 energy simulations to assess the model's ability to accurately predict the energy loads. The predictions made by the model were compared to those given by EnergyPlus considering the same input data. According to the authors, the model yielded a R^2 value between 0.765 and 0.965 for heating loads, and between 0.956 and 0.993 for cooling loads.

Asadi et al. (2014) considered seven different geometries for one climate; Houston, TX, and specified 17 design variables as key parameters to be varied and considered as inputs in the regression models. The model was designed to predict the energy consumption of office buildings. The simulation software used to run the simulations coupled with the Monte Carlo framework was DOE-2. The same software was used in validation procedure of the model, which was considered as a viable substitution for the simulation process, as it yielded a determination coefficient (R^2) varying from 0.94 to 0.95.

Another study varying the building's geometry was conducted by Ourghi et al. (2007), where a simplified analysis method was developed to predict the impact of the shape of an office building on its annual cooling and total energy use considering two locations; Tunis and Kuwait. Various shapes were modeled using the software DOE-2 and typical occupancy patterns and schedules. Several parameters were varied to predict the annual electricity use considering different building configurations and shapes, as well as their relative compactness. The study was able to establish a strong correlation between shape and energy consumption, with determination coefficient values of 0.98 for Tunis and 0.86 for Kuwait.

Lam et al. (2010) developed a regression model varying 12 parameters in an office building. The model was simulated for five climates in China; severe cold, cold, hot summer cold winter, mild, hot summer warm winter. The outcome for the annual simulations run on DOE-2 was the energy consumption in air-conditioned office spaces. The random designs for the regression models' evaluation were produced by a pseudo-number generator based on three simple multiplicative congruential generators. The difference between the predictions given by the regression and the simulation run on DOE-2 was within 10%, with a coefficient of determination (R^2) varying from 0.89 in the city of Harbin, to 0.97 in Kumming.

Catalina et al. (2008) developed and validated a regression model to predict energy consumption in single-family residences in 16 temperate climates in France. The simulation software adopted was TRNSYS, with an hourly time-step. The best fit between the simulation data and the model results was found using the quadratic polynomial model. The validation was performed using 270 scenarios, which included 3 different building shapes, thus creating three validation scenarios. The authors concluded that there is a strong relationship between the building's shape and energy consumption. The average error was of 2%, establishing that the equations can predict well.

The above-mentioned authors conducted another study to create a multiple regression model for the fast prediction of heating energy demand in Moscow, Bucharest and Nice (CATALINA et al., 2013). The well-known software TRNSYS was used to develop the energy prediction model, and 8748 simulations were run, creating an essential database to develop a correlation method. The model was developed to relate the heating energy consumption to three key parameters; the weather data, the building's global insulation and the south equivalent surface (SES). The latter being a concept introduced by Catalina (2012) as a representation of the glazing area and its distribution on different orientations. The model's validation was performed with data collected on site from 17 blocks of flats with different sizes, thermal properties and glazing surfaces or orientation. A comparison was made between the measured values, the European norm and the results yielded by prediction model. The authors concluded that the model presented a good accuracy, with a determination coefficient (R^2) of 0.9744, and 90% of the samples with a relative error inferior to 20%.

Wu and Sun (2012) developed a two-stage regression model to predict thermal comfort in office spaces with HVAC systems. The regression model is a representation of ASHRAE's empirical predicted mean vote model, and it incorporates as its predictors architectural parameters and control variables.

In Brazil, the Brazilian Energy Labeling Schemes for Residential Buildings (RTQ-R; INMETRO, 2012) presents a regression model that was developed to assess and classify the energetic efficiency in residencies. Such regulation establishes a rating range for the buildings, which varies from Level 'A' (most efficient) to 'E' (least efficient) (SCALCO *et al.*, 2012).

The evaluations are based on pre-requisites that must be met to maintain the achieved energy level. As described by Scalco et al. (2012), the regulation provides maximum transmittance as a function of thermal capacity level and solar absorptance of walls and roof, as well as a minimum percentage for openings for natural ventilation and lighting, as defined according to each of the eight bioclimatic zones in the country. The prescriptive method developed and proposed by the regulation is based on cooling degree hours as a means to indicate and analyze a building's energy efficiency. The operating temperature adopted was of 26˚C as a fixed temperature instead of an adaptive comfort temperature to allow the use of an HVAC system, if desired (SCALCO *et al.*, 2012). The method can be used to estimate the cooling loads for a whole year or shorter periods, if necessary.

Within the overall method proposed by the regulation, there are two types of methods that can be used to assess the building's energy efficiency: the prescriptive method and the simulation method. The prescriptive method consists of equations developed from multiple regression equations based on over 150.000 cases simulated using EnergyPlus (VERSAGE, 2011). The equations were generated with multiple linear regression, and allow the prediction of the sum of the cooling degree hours and the energy consumption for the heating and cooling of a given environment. Such predictions are used as an indicator for the building's thermal performance and energy efficiency. Multiple linear regression was used to predict an index of energy efficiency for a given set of parameters. Four main parameters were highlighted as the ones that most affect the thermal performance of an environment, as follows (SCALCO *et al.*, 2012):

1. Thermal variables: thermal transmittance (U-value), solar absorptance and heat capacity of the building's elements.
2. Geometric variables: ambient areas. Floor-to-ceiling height, volume, wall area, glazed areas and effective opening area for ventilation.
3. Construction variables: ground temperature, roof exposure, shading devices in glazed areas, glazed areas with double-glazing.
4. Combined variables: combination of thermal and geometric variables.

Mathematical methods and models can be used as a simplified tool to predict a building's behavior according to the variables being considered and the desired outputs; energy consumption, thermal performance, cooling and/or heating loads, for example. Such tools don't present the difficulties associated to the use of simplified physical models, once they present a good fit to the results they predict compared to the ones given by detailed simulation tools. It is a known fact that simplified tools present limitations, since they are restricted to climatic patterns, geometry, materiality and the uses associated to each type of building and its occupation. However, such restrictions do not make their use impossible, they only highlight the importance of the right choice to be made and the characterization of the parameters to be considered in the desired model, so that it satisfactorily meets the demands to its creation.

3 Methodology

3.1 General Overview

The method illustrated by Figure 4 and used in this research, consists in creating *meta-models* based on parametric simulations run on a *base model* using EnergyPlus. It encompasses a standard geometry to properly represent the type of building in question, as well as the parameters selected as most influential to the study. It is generically defined as the model of a model; a simplified model of an actual model, useful for modeling a predefined set of problems (GARITSELOV; MOHANTY; KOUGIANOS, 2012). In this research, it is the mathematical relation of inputs and outputs, given as equations obtained from the regression analysis performed.

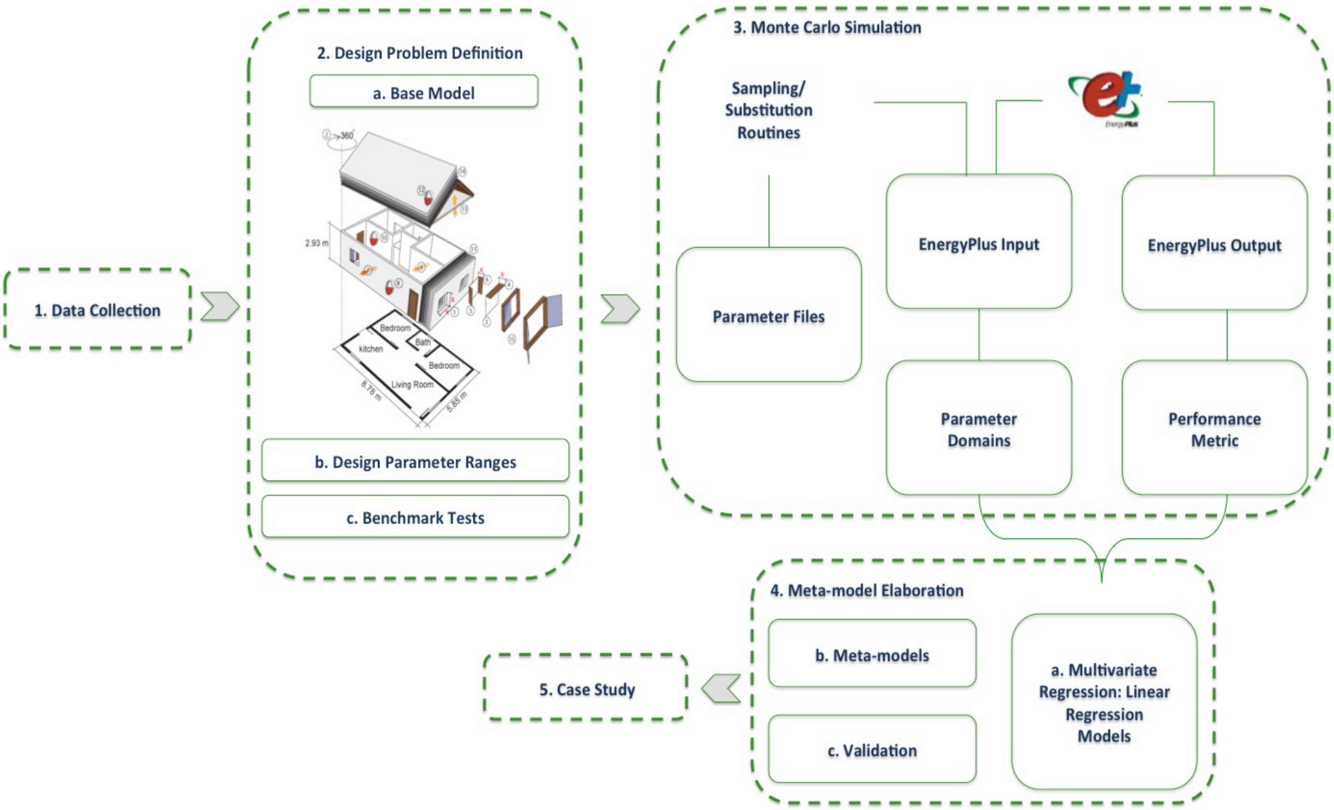

Figure 4 – Methodology's General Overview

The focus of this research was to analyze the aspects related to the building's insolation and shading: long-stay rooms' orientation in relation to the sun, window to wall ratio and shading devices.

In general, it was necessary to first gather the characteristics that define the type of building being studied (low-cost houses), which was part of the Data Collection. The next stage was the Design Problem Definition, where such characteristics were sorted in a way that determined the most relevant parameters in the early stages of design that influence the building's thermal comfort in a general manner, and more specifically, its insolation and shading. With this, the situations for the parametric simulations were defined: the geometric variation to be considered, the parameters to be varied and their ranges. Benchmark tests were performed at this stage to define the simplifications that could be made to the model without affecting the results provided by the software. The 3rd and 4th steps were the Monte Carlo simulation and the Regression Analysis, respectively. The Monte Carlo simulation used the defined ranges to run simulations with random combinations of parameters in EnergyPlus. The results were then used to build the regression models, which are equations that compose the meta-models, followed by their validation with reliability tests. The final step was a case study where the meta-models were applied to assess their accuracy and performance in regards to the impact of shading devices in thermal comfort.

3.2 Data Collection

The base model was extremely important for the present research, since all evaluations were conducted using it as a reference. It was designed based on an analysis of specific aspects of low-cost houses collected from different Brazilian cities. The projects were collected from cities that could represent distinct bioclimatic zones in the country, such as São Paulo (Zone 03), Curitiba (Zone 01) and Cuiabá (Zone 07), according to the bioclimatic zoning definition established by the Brazilian Regulation (NBR 15220; ABNT, 2005).

A database[8] was created by cataloguing designs that were seen as innovative, that is; designs that presented different materials and shapes from the ones usually observed in this type of construction. However, the search was not limited by such standard, and it included traditional designs as well. Architecture offices, construction companies, and city halls were the sources that provided part of the projects. Some older designs, but that also fit into the same category and presented a high architectural quality, were included.

The projects were classified and catalogued into three groups, as follows:

- Group A: Representative projects within the defined type of building (low-cost)
- Group B: Low-cost house projects with a high architectural quality
- Group C: Projects with constructive or material innovations

Once assigned to a group, each project was specified taking into consideration the most relevant aspects to build the base model. Three aspects were the main focus of all considerations, since they are the ones being studied in depth: shading devices and the building's insolation, natural ventilation and materials. Based on that, the following main areas were defined and assessed in each project: Windows, Geometry and Construction.

Within each main area defined, sub items were established to better detail each project, such as the existence of a roof overhang and its dimension, total building area, number of floors, among others. For this research, the most relevant items included in the categories are the roof overhangs and its specifications; dimension and material, other types of shading devices, as well as window distribution and dimension. Based on such categorization, it was possible to identify a regular pattern in the construction's dimensions, as well as their windows. The materials used are mostly ceramic or structural blocks for internal and external walls, and

---

[8] Excerpt of database in Appendix H-J

ceramic tiles for the roofs. The detailing and analysis of such categorized data was the basis to create the proposed base model.

3.3 Design Problem Definition

3.3.1 Base Model

3.3.1.1 Overview

Once the database is complete, it serves as a starting point to elaborate the base model. According to Hygh (2011), the base model must contain assumptions of all the necessary input data for a thermal comfort simulation with the intention of being implicit in the model. The author also states that there are two main categories that build a base model: geometry and thermal information. The thermal information includes data such as location, monthly values for ground temperature, internal gains and their schedules, material properties and other conditions that might be specific to the site. The base model, with a set of adopted values, serves as the basis for the Monte Carlo simulation.

3.3.1.2 Geometry

The geometry must be defined in the base model, and if it is not constant, it should be parametrically manipulated in the Monte Carlo analysis. The input data that characterize a model, as well as the thermal information and the coordinates to obtain the geometry, are all entered and manipulated in EnergyPlus. Since the goal is to apply the meta-model to similar designs, the base model must be sufficiently generic, while also being complex enough to portray a real design problem that is relevant in the design process. The long-stay rooms' distribution greatly influenced the design decisions made, since they are the focus of all evaluations. The windows have a fixed distribution, varying only their dimensions, as well as the shading devices attached to them.

3.3.1.3 Thermal Information

When analyzing the data from a thermal comfort standpoint, the following parameters were considered to be the most relevant and, therefore, used as guidelines to build the base model:

- Window to Wall Ratio (WWR)
- North axis direction
- Possibility of shading devices
- External walls' materials
- Roof's materials
- Types of windows

In regards to the distribution of Thermal Zones in the model, the geometry was divided into two sections; the attic and the floor plan, each of which defined as a thermal zone. The attic is a non-ventilated zone, not exchanging air with the remaining zone, nor with the outdoors. And the floor plan, consisting of the living room, bedrooms, kitchen and bathroom, composes another thermal zone, which allows air changes with the site outdoor and within itself. The simplification of the number of thermal zones adopted for the study is further detailed in the section Benchmark Tests.

3.3.2 Building Geometry

In order to generate the meta-model, it is necessary to first create a base model, where the parameters to be varied are defined, as well as the input and output data of the EnergyPlus input file (idf). The initial step was to develop a geometry model, which was based on an analysis of architectural projects collected (See Data Collection). By studying the low-cost house designs available, a geometry that would comprehend the main design concepts relevant to the research, and represent the patterns observed was created (Figure 5). Internal partitions were also based on the analyzed projects from the created database, taking into consideration the minimum area needed to fit standard furniture in each room and for circulation.

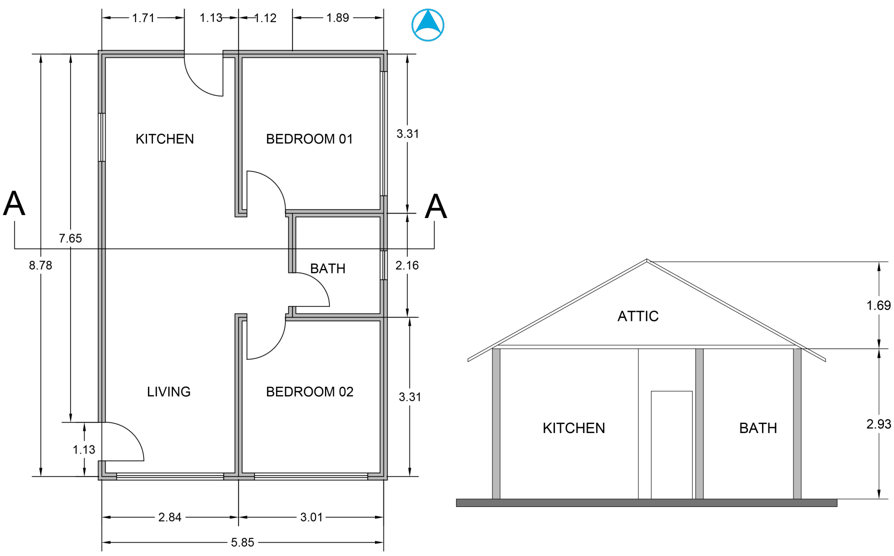

Figure 5 - Floor plan and Section A-A of base model in meters

The building geometry for the base model created is rectangular and does not vary. The windows' positioning on the wall and their distribution on the unit (Figure 6), one in each room, are also fixed as a way to further simplify the base model. Kitchen and bathroom windows have fixed sizes of 1m^2 and 0.36m^2, respectively. This shape was adopted for the study because LCH have small areas and therefore don't present the opportunity of designing with shapes differing from a rectangle or a square. The rectangle was the most commonly observed shape in the collected data, and thus also adopted to be representative of this type of building in this research. Even though the geometry was designed according to the ratios described below, the building remains representative of LCH in Brazil.

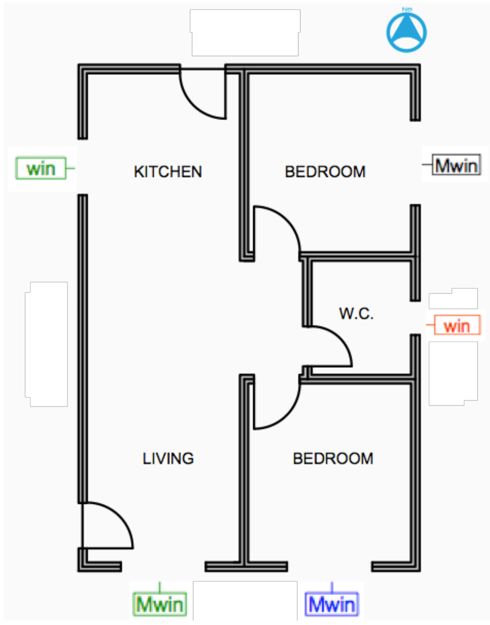

Figure 6 - Windows' distribution

Due to the rectangular shape adopted, the surface-average wind pressure coefficients from the EnergyPlus database were automatically adopted during the simulations. To enable a parallel investigation (ROSSI *et al.*, 2015) on the impact that such coefficients have when applied in simulations for thermal comfort instead of local wind pressure coefficients (from the Tokyo Polythecnic University Aerodynamic Database, post-processed by Catavento), the geometry proportions meet the following criteria: a ratio of 3/2 considering length/width, and a ratio of 2/4 regarding height/width. Based on such, the resulted geometry is a rectangular-shaped building of 8.78m x 5.85m, a floor-to-ceiling height of 2.93m and a total area of 47.56m^2.

3.3.3 Variable Parameters

Based on an analysis of all items selected as significant for detailing an architectural project, it is possible to identify basic parameters, that is, to parameterize the base model. Hygh (2011) specifies two criteria to determine the choice of parameters to be varied in the Monte Carlo simulation; (a) the parameter has an effect on thermal comfort; and (b) the parameter is architecturally relevant in the conceptual project.

Based on such criteria, key-parameters related to the building's thermal information, as specified in the previous item, can be identified. Once they are defined, ranges or sets of values are assigned to them so they are compatible to the options available in the design (Hygh, 2011). Base values must be established, as well as the output data to be analyzed and their impact regarding the focus of the research. The remaining input data that must be entered to run the simulations can be determined as default, taking into consideration the type of building and the model's components.

All parameters, as well as their ranges and status in the base model; either fixed or variable, are described and detailed in the following item.

3.4 General Input Data for Base Model

The following table (Table 1) shows the general input data with parameters and their values and/or specifications for the base model.

Table 1 - General input Data

	Parameter/Input	Variables: Range	Variables: Unit	Status: Fixed	Status: Variable
General building and climate information	Building geometry	47.56	m^2	x	
	North axis direction	0 to 359	Degrees		x
	Climate	São Paulo/SP Curitiba/PR Cuiabá/MT Manaus/MA	Climatic files (epw) from Roriz, 2012	x	
	Ground Temperature	Specific to each climate: monthly values	Degrees Celsius	x	
Shading Devices	Roof overhang	0.5	m	x	
	Window overhang position	on / off	-		x
	Windows overhang size	0.01 to 50	%		x
	Window fins position	on / off	-		x
	Windows fins size	0.01 to 50	%		x
	Kitchen and bathroom windows shading	Roof overhang only	-	x	
Window Properties	Window to wall ratio	10 to 90	%		x
	Glazing material	4 (clear glass)	mm	x	
	Effective window ventilation area: bedrooms and living room	50 or 100	%		x
	Effective window ventilation area: Kitchen	50	%	x	
	Effective window ventilation area: Bathroom	100	%	x	
	Kitchen window area	1	m^2	x	
	Bathroom window area	0.36	m^2	x	
Materials' Properties	External Walls' U-value	0.30 to 5.00	$m^2.K/W$		x
	External Walls' Heat capacity	40 to 445	Kg/m^3		x
	Internal Walls' U-value	0.30 to 5.00	$m^2.K/W$		x
	Internal walls' Heat capacity	40 to 445	Kg/m^3		x
	External Walls' absorptance	0.10 to 1.00	-		x
	Roof's Heat capacity	11 to 791	Kg/m^3		x
	Roof's U-Value	0.50 to 2.10	$m^2.K/W$		x
	Roof's absorptance	0.10 to 1.00	-		x
Natural Ventilation	Ventilation control	Schedule 01: 7a.m. to 10p.m.			x
	Ventilation set point temperature	Specific to each climate: daily values according to ASHRAE 55 (2013)	degrees	x	
Internal Gains	Occupation	4	people	x	
	Occupation pattern	As established by RTQ-R (INMETRO, 2012) with minor adaptations		x	
	Lighting pattern	As established by RTQ-R (INMETRO, 2012)		x	
	Metabolic rates for activities	As established by RTQ-R (INMETRO, 2012)		x	
	Equipment's internal loads	As established by RTQ-R (INMETRO, 2012)		x	

3.4.1 Building Orientation

The building's North Axis is specified according to the true North. Building orientation allows the rotation of the building to cover the full range of possibilities when considering sun and wind exposure, since these two factors contribute the most to heat gain in a building (Figure 7).

The consideration of different building orientations also helps explore the different possibilities for a building's implantation on site. The base model's long axis was aligned with the true North, and the following figure presents possible variations within the defined range of such parameter (0˚ to 359˚).

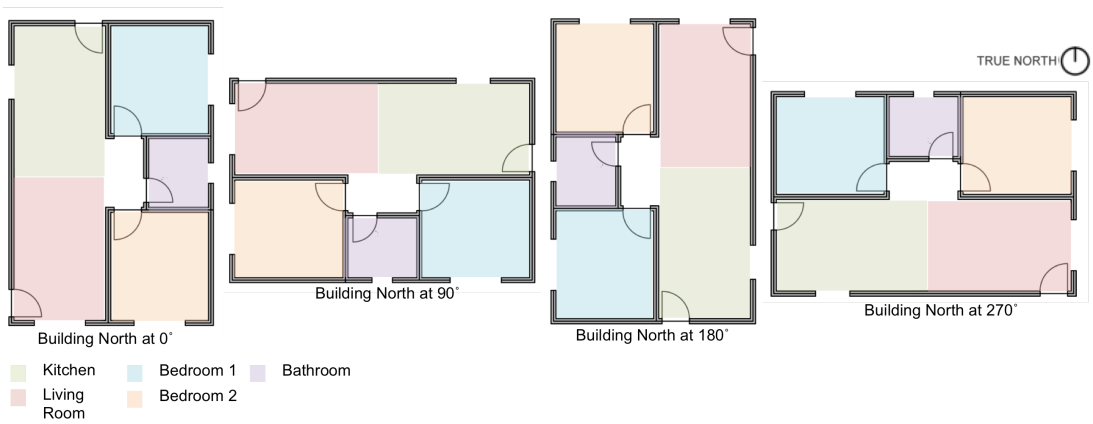

Figure 7 - Possible Building orientations – Building North Axis from 0˚ to 359˚

3.4.2 Weather Data

The climates specified in this section represent Brazil's weather diversity. They represent well the distinction between the coldest, intermediate and warmer climates in the country, making it possible to compare the output data from the simulation runs in relation to their specific characteristics. The differences between them imply in distinct constructive solutions and diverse designs to better adapt to each situation.

The bioclimatic zoning adopted is referenced in Part 3 of the Brazilian Regulation (NBR 15 220; ABNT, 2005), as follows:

- Curitiba, PR – Zone 01
- São Paulo, SP – Zone 03

- Manaus, AM – Zone 08

Figure 8 presents the national territory divided into the eight zones classified by the Brazilian Regulation. Table 2 indicates specific data for each of the selected cities.

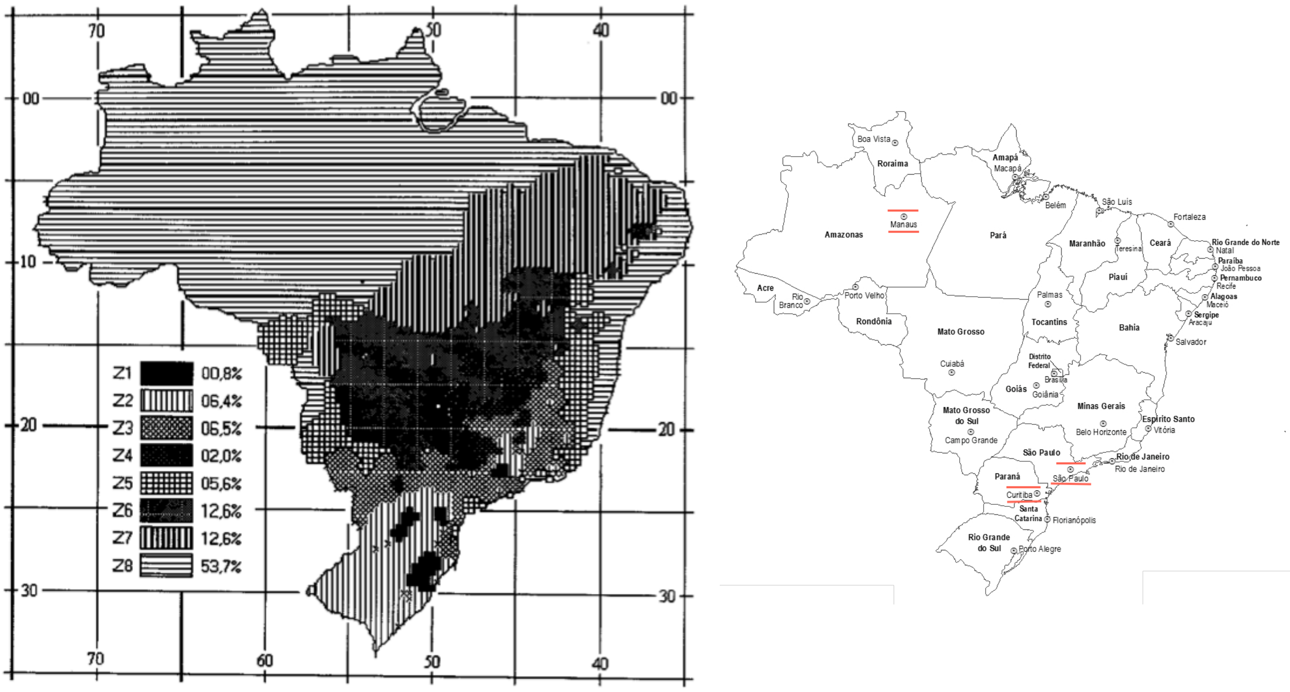

Figure 8 - Brazilian territory divided into bioclimatic zones. Source: NBR 15 220; ABNT, 2005.

Table 2 - Weather Data

State	City	Zone	Latitude	Annual Average Temperature (˚C)[1]	Heating Degree days: Base temperature of 18.33˚C (65˚F)[2]	Cooling Degree days: Base temperature of 10˚C (50˚F)[2]
Paraná	Curitiba	01	25.43° South	17	1,829	4,825
São Paulo	São Paulo	03	23.85° South	20	638	6,961
Amazonas	Manaus	08	3.1° South	27	0	10,795

[1] Temperatures calculated based on the epw from RORIZ (2012) for each city. [2] Fahrenheit-based 5-year average (2009-2013). Values calculated using temperature data from www.wunderground.com

The weather data files used for this research were developed by Roriz (2012) and are of a representative year with hourly data referring to the above-mentioned cities. With the data embedded in these files, it is possible to characterize the climates, which contributes to the study of a building's thermal performance, since weather is a key factor for such.

3.4.3 Ground Temperature

Ground temperature is an important parameter because it considerably influences the final simulation. It is especially significant in one-storey houses, since it influences the heat exchange between the ground and the floor.

In Brazil, for this type of building, there are no data or sources of information pertaining such parameter. For this reason, the usual values adopted in national articles and researches were also used for the present work, which are the same as the outdoor mean air temperature. In addition, the limits established for the ground temperature were from 15˚ to 25˚C, which correspond to the limits given by EnergyPlus. Because there are three distinguished climates being considered in this study, monthly ground temperatures were set for each of them in the base model. Table 3 through Table 5 present each climate and their respective monthly ground temperature and mean air temperature.

Table 3 - Ground Temperature - Manaus, AM

Manaus/AM		
Month	Mean Air Temperature (°C)[1]	Ground Temperature (°C) (Range: 15° - 25° C)
January	26.8	25
February	26.8	25
March	27.6	25
April	26.4	25
May	27.0	25
June	26.8	25
July	26.7	25
August	27.9	25
September	29.0	25
October	28.2	25
November	27.3	25
December	26.7	25

[1] Mean air temperature was taken from the city's epw file from Roriz (2012)

Table 4 - Ground Temperature - Curitiba, PR

Curitiba/PR		
Month	Mean Air Temperature (°C)[1]	Ground Temperature (°C) (Range: 15° - 25° C)
January	19.6	19.6
February	20.9	20.9
March	19.9	19.9
April	17.9	17.9
May	15.0	15.0
June	13.6	15.0
July	15.4	15.4
August	15.7	15.7
September	14.6	15.0
October	17.6	17.6
November	18.0	18
December	19.4	19.4

[1] Mean air temperature was taken from the city's epw file from Roriz (2012)

Table 5 - Ground Temperature - São Paulo, SP

São Paulo/SP		
Month	Mean Air Temperature (°C)[1]	Ground Temperature (°C) (Range: 15° - 25° C)
January	21.2	21.2
February	22.3	22.3
March	21.7	21.7
April	20.8	20.8
May	17.5	17.5
June	16.8	16.8
July	17.3	17.3
August	18.3	18.3
September	17.7	17.7
October	20.5	20.5
November	20.1	20.1
December	20.9	20.9

[1] Mean air temperature was taken from the city's epw file from Roriz (2012)

3.4.4 Shading Devices

3.4.4.1 Roof Overhang

One of the types of shading devices defined in the base model was a fixed one, which was the roof overhang of 0,50m on all eaves (

Figure 9). The main reasons for using this shading element is that it is commonly considered and used in the type of building in question, LCH; and it has been verified that such an element influences on a building's thermal performance (CHVATAL; MARQUES, 2015).

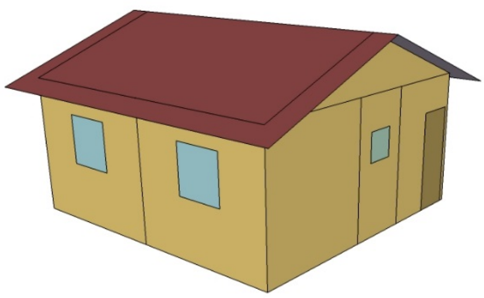

Figure 9 - Fixed Roof Overhang

3.4.4.2 *Overhangs and Fins*

Vertical and horizontal devices, the remaining two types of device included in the base model, were fins and overhangs, respectively (Figure 10). These types of shading devices were placed adjacent to the log-stay rooms' windows. Fixed elements were selected for this study due to the type of building in question: low-cost house projects. In order to combine adequate thermal performance while still offering low-maintenance design solutions, fixed fins and/or overhangs are presented as a solution that meets the criteria.

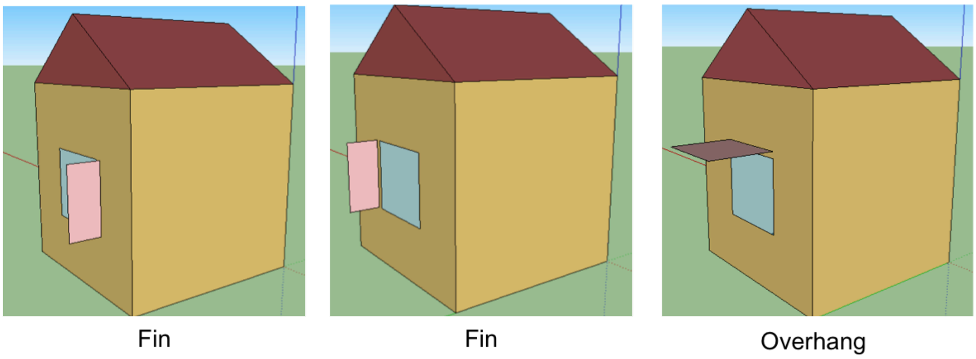

Figure 10 – Possible Shading Devices

Fins can be placed either to the left or right side of the window, while the overhangs can only be above it. The meta-model also provides the option of no shading devices, leaving only the roof overhang as a protection from sunlight.

The variable shading devices were modeled in EnergyPlus using the field *Shading:Overhang:Projection* and *Shading:Fin:Projection*, where the sizes of such devices can be altered, as well as several other properties as described in Table 6 with all the available fields in the software. The protections were set not to exceed their respective opening's width, the parameter that varies in the meta-model is the depth of each device, which is a factor of the window's height; therefore, they vary according to the Window to Wall Ratio (WWR), which, in turn, defines the window's size.

The range for the Depth Factor of the window's height considered in the Monte Carlo simulation was from 0.01 to 0.5. An exceedingly low value, such as 0.01, was the starting point for the range because EnergyPlus doesn't run a simulation with a depth factor of zero in this field for the objects Overhangs and Fins. The software requires a value for each object created as a shading device.

For this reason, when using the meta-model, the range to be adopted for a shading device is from 0.1 to 0.5, and if the option with no shading devices is desired, the value 0.01 is to be adopted instead of zero.

The tilt angle is fixed and set at 90˚ in relation to the window, thus considered flat by the software.

Table 6 - Overhangs and Fins specifications

Overhang		
Field	**Description**	**Value/Range**
Name	Object's name	-
Window or Door Name	Window or door where the device is placed	-
Height above Window or Door		0m
Tilt Angle from Window/Door		90˚
Left Extension from Window/Door width		0m
Right Extension from Window/Door width		0m
Depth as a Fraction of Window/Door Height		0.01-0.5
Fin		
Field	**Description**	**Value/Range**
Name	Object's name	-
Window or Door Name	Window or door where the device is placed	-
Left Fin Extension from Window/Door width		0m
Left Fin Distance Above Top of Window		0m
Left Fin Distance Below Bottom of Window		0m
Left Fin Tilt Angle from Window/Door		90˚
Left Fin Depth as a Fraction of Window/Door Height		0.01-0.5
Right Fin Extension from Window/Door width		0m
Right Fin Distance Above Top of Window		0m
Right Fin Distance Below Bottom of Window		0m
Right Fin Tilt Angle from Window/Door		90˚
Right Fin Depth as a Fraction of Window/Door Height		0.01-0.5

3.4.5 Window Properties

The windows' location on the geometry does not vary, always remaining in the same façade, as specified in Building Geometry. The windows were distributed according to each room; the bathroom and kitchen windows have fixed effective opening areas of 100% and 50%, respectively (Figure 11).

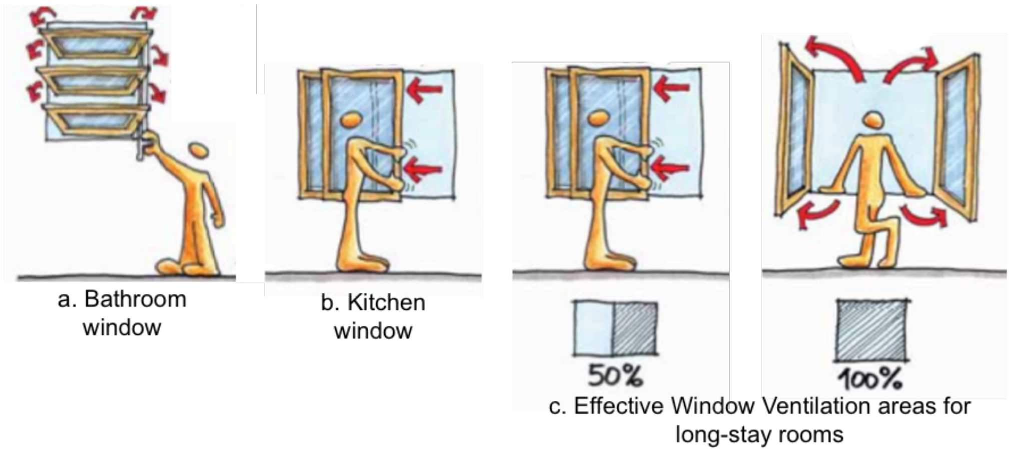

Figure 11 - Window types and Effective Window Ventilation Areas. Source: LAMBERTS; DUTRA; PEREIRA, 2014.

For each long-stay room there are two possibilities of effective window ventilation area (EWVA) as well, which results in two different types of window that can be considered. As illustrated in the figure above, there is the possibility of a sliding or casement window for the bedroom and/or living room, and their respective EWVA.

The windows' size is a variable parameter in the study for the bedroom and living room windows; bathroom and kitchen windows have fixed sizes (See Building Geometry). The windows' area is given according to the calculated WWR, which is calculated as a percentage in relation to that specific room's wall area where the window is located, and not the area for the entire façade; that is, each window's size is a ratio of its corresponding wall's area. The WWR can vary from 10% to 90%, thus creating exceedingly large, and perhaps unrealistic windows, as well as very small ones. The window's size range allows for unrealistic windows to portray very distinguished configurations and combinations in the meta-model. The long-stay rooms' windows are placed in the middle of their respective walls, and vary their sizes independently from one another.

3.4.6 Building Materials

EnergyPlus requires a set of high technical specifications to define the building materials and construction for a given model. Because the entry data required was complex, benchmark tests were performed to simplify the input data.

For the roof system, a four virtual layer construction was suggested, while for the internal and external walls, which vary independently in the meta-model, a three virtual layer construction (

Figure 12).

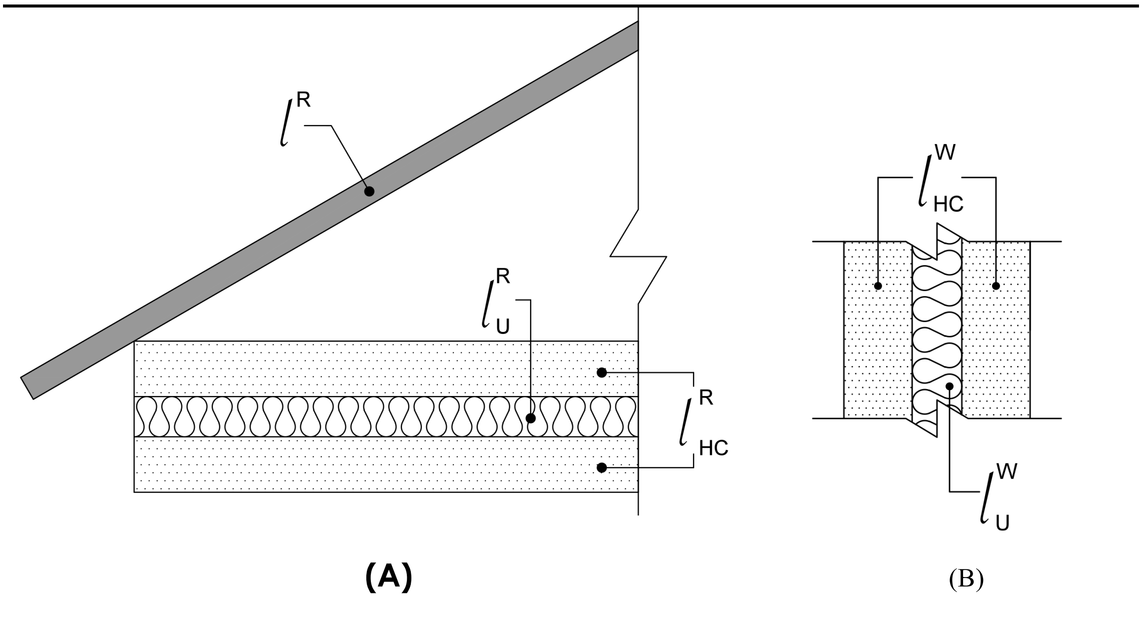

Figure 12 - Roof (A) and wall (B) virtual construction scheme. Source: Favretto, 2015.

In response to the difficulty to enter the data in the software, a series of benchmark tests was performed to create a more pertinent approach to the purpose of this work. The tests verified if, when maintaining the same U-value and Heat capacity (HC), the EnergyPlus model with virtual constructions could represent with accuracy similar models that used detailed construction input.

Table 7 specifies the fixed building materials or construction system, while Table 8 defines the virtual layer properties for the walls and the roof. The variable field data considered for the test are highlighted. This type of input data for the materials, allows the independent variation of their properties within the specified range, specifically of the Thermal Transmittance (U-value) and heat Capacity (HC) when the fields thermal resistance and material density are respectively altered (FAVRETTO; *et al.*, 2015).

Table 7 – Fixed Building Materials or Construction Systems

Building Material or Construction System	**Description**
Glass	Clear, 4mm
Door	Wood, 3.5cm
Floor	Ceramic floor tile (0.5 cm) + plaster (thickness = 2.5 cm) + concrete (e=8 cm) + gravel (e=3 cm)

Table 8 - Roof and wall virtual material properties. Source: Favretto, 2015.

	Layer	**EnergyPlus Input Group**	**Properties**			**Thermal Resistance [M2.K/W]**	**Heat Capacity [KJ/M2.K]**
ROOF	l^R	Material	Roughness	Medium		0.01	14
			Thickness [M]	0.01			
			Conductivity [W/(M2.K)]	1			
			Density [Kg/M3]	1400			
			Specific Heat [J/Kg.K]	1000			
			Solar Absorptance	0.7			
	l^R_{HC}	Material	Roughness	Medium		0.01	**Variable**
			Thickness [M]	0.05			
			Conductivity [W/(M2.K)]	5			
			Density [Kg/M³]	**Min**	**20**		
				Max	**5560**		
			Specific Heat [J/Kg.K]	1000			
	l^R_U	Material: No Mass	Roughness	Medium		**Variable**	-
			Thermal Resistance [M2.K/W]	**Max**	**1.55**		
				Min	**0.01**		
INTERNAL AND EXTERNAL WALLS	l^W_{HC}	Material	Roughness	Medium		**0.01**	**Variable**
			Thickness [M]	0.05			
			Conductivity [W/(M².K)]	5			
			Density [Kg/M³]	**Min**	**400**		
				Max	**4450**		
			Specific Heat [J/Kg.K]	1000			
			Solar Absorptance	0.7			
	l^W_U	Material: No Mass	Roughness	Medium		**Variable**	-
			Thermal Resistance [M².K/W]	**Max**	**3.07**		
				Min	**0.01**		

3.4.7 Natural Ventilation Control

Natural ventilation was modeled using the EnergyPlus group Natural Ventilation and Duct Leakage (Airflow Network). Average values given by EnergyPlus for wind pressure coefficients were adopted based on results of benchmark tests (ROSSI *et al.*, 2015). The building assumes a rectangular geometry, thus allowing the use of such values from the program's database.

The ventilation control was established based on temperature. The following requirements must be met to allow for natural ventilation in the building:

- Zone Temperature > Set point temperature
- Zone Temperature > Outdoor temperature
- Schedule allows ventilation from 7 a.m. to 10 p.m.

The set point temperatures were defined based on the comfort temperatures calculated for each climate according to the Adaptive Comfort Index ASHRAE-55 (ASHRAE, 2013) defined in the item *Adaptive Model – ASHRAE 55*.

Table 9 – Maximum and Minimum annual average temperatures

		Comfort Temperature (˚C)	**Months**
Curitiba, PR	Max	24.1	Jan and Mar
	Min	22.3	June
São Paulo, SP	Max	24.7	January
	Min	22.9	July
Manaus, AM	Max	26.7	Sep and Oct
	Min	26	Jan and April

3.4.8 Internal Gains

All loads related to human occupation, lights and electric equipment were based on the Brazilian Energy Labeling Schemes for Residential Buildings (INMETRO, 2012). This regulation specifies in its method for simulation the types (weekdays and time) of occupation, lighting and equipment use for a naturally ventilated residence that are to be adopted when running a simulation. The values given by the RTQ-R consider the occupation to be of two people per bedroom, with a total of four residents.

It is necessary to determine the metabolic rate for human occupation during a day in the model; the type of activity performed in each room helps establish such values. The regulation suggests values based on the ones given by ASHRAE Handbook of Fundamentals (ASHRAE, 2009) as follows (Table 10):

Table 10 - User's Activities - RTQ-R (INMETRO, 2012)

Room	**Activity**	**Heat (W/m^2)**	**Heat by skin area=1.80m^2 (W)**
Living room	Seated or watching TV	60	108
Bedrooms	Sleeping or resting	45	81

Occupation patterns are divided into weekdays and weekends. The regulation establishes times of day when the residence is occupied and specifies if the bedrooms or living room is in use. It also gives a fraction of the total of occupants that are in each room at each hour. The following table represents the occupation schedules used in this research with minor adaptations, so there is always at least one occupant in the building.

Table 11 - Occupation Pattern - RTQ-R (INMETRO, 2012)

Hour	**Bedrooms**		**Living Room**	
	Weekdays (%)	Weekends (%)	Weekdays (%)	Weekends (%)
1h	100	100	0	0
2h	100	100	0	0
3h	100	100	0	0
4h	100	100	0	0
5h	100	100	0	0
6h	100	100	0	0
7h	100	100	0	0
8h	0	100	25	0
9h	0	100	25	0
10h	0	0	25	0
11h	0	0	25	25
12h	0	0	25	75
13h	0	0	25	75
14h	0	0	25	75
15h	0	0	25	50
16h	0	0	25	50
17h	0	0	25	50
18h	0	0	25	25
19h	0	0	100	25
20h	0	0	50	50
21h	50	50	50	50
22h	100	100	0	0
23h	100	100	0	0
24h	100	100	0	0

Lighting patterns also present two types of use for bedrooms and living room: weekdays and weekends. When given the value of 100, it represents that lights are on, and when it is 0, they are off (Table 12).

Table 12 - Lighting Pattern - RTQ-R (INMETRO, 2012)

Hour	Bedrooms		Living Room	
	Weekdays (%)	Weekends (%)	Weekdays (%)	Weekends (%)
1h	0	0	0	0
2h	0	0	0	0
3h	0	0	0	0
4h	0	0	0	0
5h	0	0	0	0
6h	0	0	0	0
7h	100	0	0	0
8h	0	0	0	0
9h	0	100	0	0
10h	0	0	0	0
11h	0	0	0	100
12h	0	0	0	100
13h	0	0	0	0
14h	0	0	0	0
15h	0	0	0	0
16h	0	0	0	0
17h	0	0	0	100
18h	0	0	100	100
19h	0	0	100	100
20h	0	0	100	100
21h	100	100	100	100
22h	100	100	0	0
23h	0	0	0	0
24h	0	0	0	0

The following table represents the lighting power density according to each room.

Table 13 - Lighting power density - RTQ-R (INMETRO, 2012)

Room	Lighting power density (W/m²)
Bedrooms	5.0
Living room	6.0

For the electric equipment, the regulation sets values only for the living room, as follows.

Table 14 - Electric Equipment - RTQ-R (INMETRO, 2012)

Room	Period	Power (W/m²)
Living room	24h	1.5

3.4.9 Benchmark Tests

3.4.9.1 Types of Shading Devices

The shading devices to be included in the meta-model were selected, in part, based on tests described in this section, which simulated a simplified model with several different types of devices. The objective was to verify if the presence of shading elements presented an alteration on the room's temperature, which can consequently lead to an increase or decrease in thermal comfort. Eleven different types of shading devices and/or combinations were used, as shown in Figure 13 and detailed in Table 15.

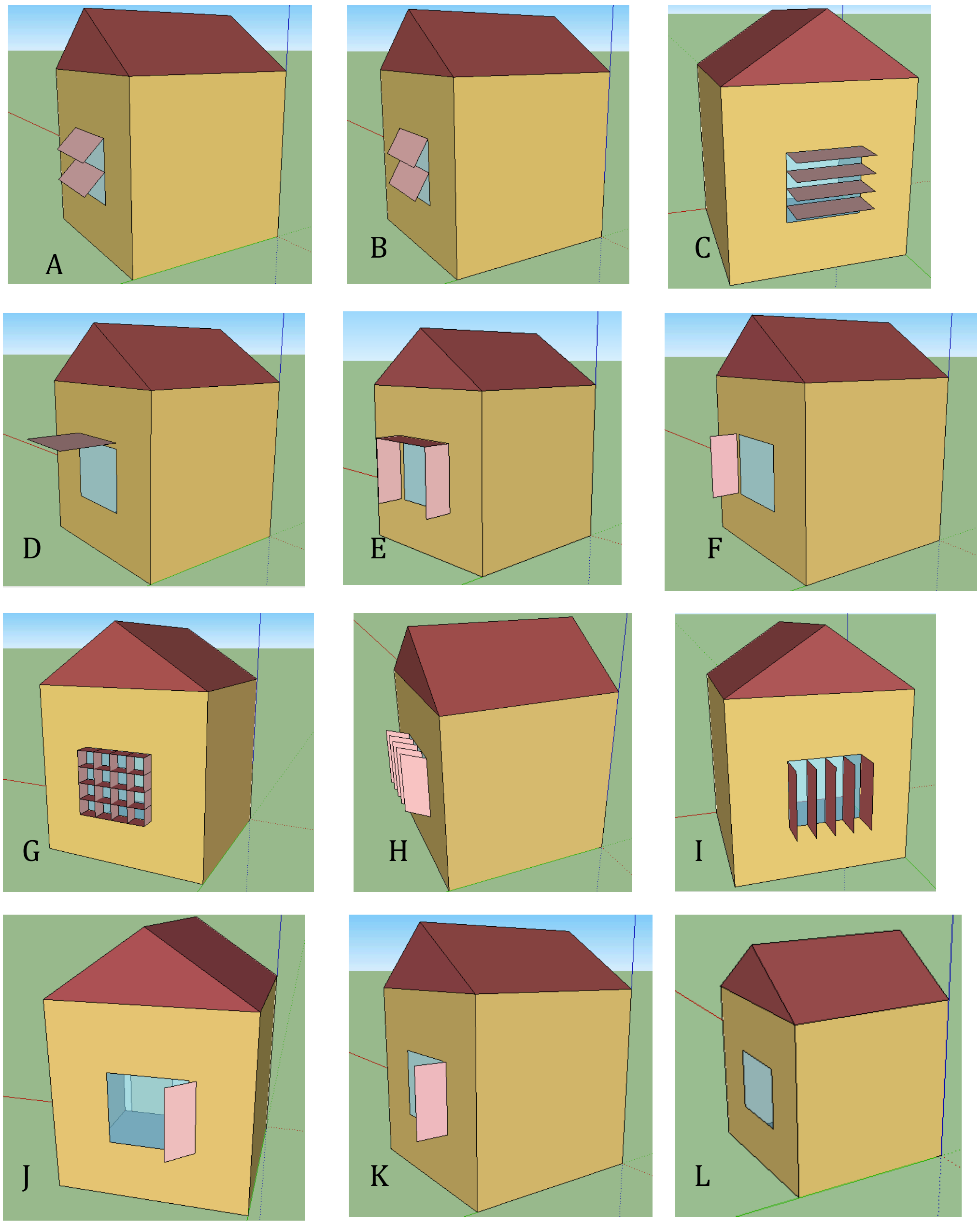

Figure 13 - Variations of Shading Devices analyzed

Table 15 - Shading Devices detailing

ID according to Figure 8	Depth (m)	Angle (˚)	Type/Specification/Position
A	0.5	30	Overhang
B	0.5	45	Overhang
C	0.5	90	Overhang
D	1	90	Overhang
E	0.5	90	Box: 2 fins and 1 overhang
F	0.5	90	Fin – Right
G	0.25	90	Eggcrate: 5 fins and 5 overhangs
H	0.5	45	Fin
I	0.5	90	Fin
J	0.5	45	Fin – Left
K	0.5	90	Fin – Left
L	0	0	No Shading

The basic model was 3mx3mx3m, with a gable roof and non-ventilated attic. The input data is specified in the following table.

Table 16 - General Input Data

Parameters	Variables
Climates	São Paulo and Manaus
Climatic files	*epw* files from Roriz, 2012
Orientation in relation to North	N=0˚
Constructive solution for external walls das (From the outermost layer to the innermost layer)	Plaster (2,5cm) + ceramic block with 8 wholes thickness=19cm + plaster (2,5cm) U=2,39W/m^2.K and HC=159KJ/m^2.K
Constructive solution of roof (From the outermost layer to the innermost layer)	Ceramic tile (1,0cm) + attic + ceiling PVC (2,0cm) U=1,73 W/m^2.K and HC=25 KJ/m^2.K
Floor	Crushed stone (3,0cm) + concrete (5,0cm) + plaster (2,5cm) + ceramic floor (0,4cm) U=3,08 W/m^2.K and HC=281 KJ/m^2.K
Window	1,2mx1,2m Clear glass: 4mm
Ventilation	05 ren/h
Infiltration rate	01 ren/h (constant)

There is one door and the window is always facing north. The climates chosen for the tests are within the climates used in the overall study. The cities of Manaus and São Paulo were chosen because they represent distinct climates in different bioclimatic zones. Manaus presents a very hot and humid climate, whereas São Paulo presents colder temperatures and less humidity.

The simulations were run hourly for an entire year, and the results present the average temperature for January and July, which are representative months for summer and winter, respectively.

The comparisons were performed by analyzing the operative temperature in model L, with no shading, to the resulting operative temperatures for each of the remaining cases. The outdoor temperature was also included for reference and to calculate the difference in percentage between the outdoor temperature and the varied shading situations. Comparisons in percentage were also made considering the No Shading situation.

Table 17 - Average Operative Temperatures for São Paulo, SP

Case	Operative Temperature (˚C)					
	January	**July**	**Difference in %[1]**			
Outdoor	22.5	16.0	January		July	
No shading	24.8	19.5				
Overhang one device (1m 90˚)	24.7	19.3	9.8	0.4	20.6	1
Overhang four devices (0.5m 90˚)	21.6	19.2	4	13	20	1.5
Overhang two devices (0,5m 45˚)	21.6	19.2	4	13	20	1.5
Overhang two devices (0.5m 30˚)	21.6	19.2	4	13	20	1.5
Fin one device (left – 0.5m 90˚)	21.7	19.5	3.6	12.5	21.9	0
Fin one device (right – 0.5m 90˚)	21.7	19.5	3.6	12.5	21.9	0
Fin five devices (0.5m 90˚)	21.6	19.3	4	13	20.6	1
Fin one device (left – 0.5m 45˚)	21.7	19.5	3.6	12.5	21.9	0
Fin five devices (0.5m 45˚)	21.6	19.2	4	13	20	1.5
Eggcrate (0.25m)	21.6	19.2	4	13	20	1.5
Box (0.5m)	21.7	19.3	3.6	12.5	20.6	1

1 Green column: Operative Temp of each shading device situation/ Outdoor | Red column: Operative Temp of each shading device situation/No Shading

Table 18 - Average Operative Temperatures for Manaus, AM

Case	Operative Temperature (˚C)					
	January	July	Difference in %[1]			
Outdoor	26.8	26.7	January		July	
No shading	25.3	26.5				
Overhang one device (1m 90˚)	25.3	26.2	5.6	0	1.8	1.1
Overhang four devices (0.5m 90˚)	25.4	26.1	5.2	0.4	2.2	1.5
Overhang two devices (0,5m 45˚)	25.4	26.1	5.2	0.4	2.2	1.5
Overhang two devices (0.5m 30˚)	25.4	26.1	5.2	0.4	2.2	1.5
Fin one device (left – 0.5m 90˚)	25.5	26.4	4.9	0.8	1.1	0.4
Fin one device (right – 0.5m 90˚)	25.5	26.4	4.9	0.8	1.1	0.4
Fin five devices (0.5m 90˚)	25.4	26.2	5.2	0.4	1.9	1.1
Fin one device (left – 0.5m 45˚)	25.5	26.4	4.9	0.8	1.1	0.4
Fin five devices (0.5m 45˚)	25.4	26.2	5.2	0.4	1.9	1.1
Eggcrate (0.25m)	25.4	26.1	5.2	0.4	2.2	1.5
Box (0.5m)	25.4	26.2	5.2	0.4	1.9	1.1

1 Green column: Operative Temp of each shading device situation/ Outdoor | Red column: Operative Temp of each shading device situation/No Shading

It was verified that shading devices have an impact on the thermal performance of an environment. A very small and limited model was used to demonstrate such impact, therefore there are limitations to the model, such as the fact that it is a single room, and the orientation is fixed. However, even with low values in the differences between each case, it is possible to infer that in a more complete and complex model, the results will show greater differences, meaning a greater impact of such devices.

The combinations made between elements was regarded as a good solution for the type of building in question; low-cost houses, since they keep the meta-model simple while still providing several different solution alternatives. Cases D, E and F are illustrations of possible combinations that can be created in the proposed meta-model that show an impact in thermal comfort. Cases such as A, B and C, for example, where the angle and number of devices are varied, also showed favorable results, but added complexity to the meta-model, therefore the types of variation illustrated by them were not included and were considered elements for further work.

3.4.9.2 Number of Thermal Zones

Benchmark tests to determine the amount of thermal zones modeled were performed considering the impact that different configurations had in thermal comfort predictions of a standard naturally ventilated residence within the three climates in this research. The model used for such tests and simulation was the same as the one developed for this work. All internal gain values and natural ventilation controls were maintained the same as the ones described in the sections above: Internal Gains and Natural Ventilation Controls, respectively.

As shown on Table 19, there were 9 analyzed cases. Iterations were performed by combining the climates to the building's different orientations. Wall and roof properties were not varied and shading devices were not included, except for the fixed roof overhang.

Table 19 - Overview of the analyzed cases

Case Number	1	2	3	4	5	6	7	8	9
Orientation	a	b	c	a	b	c	a	b	c
City	Curitiba			Manaus			São Paulo		
Wall properties	U=2.46 W/(m2.K) | HC=150 KJ/(m2.K) | α=0.4								
Roof properties	U=1.8 W/(m2.K) | HC=185 KJ/(m2.K) | α=0.7								
WWR	40%								

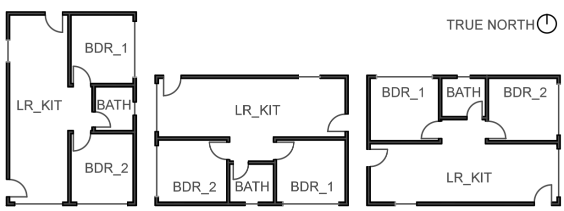

(a) (b) (c)

Figure 14 - Building orientations

The two configurations for the zone modeling were defined as Single Zone Model (SZM) and Multi Zone Model (MZM). The SZM considered one zone only, which was the building's entire floor plan, while the MZM considered each room a different thermal zone, resulting in a total of four zones. For both situations, the attic was a separate zone and defined as independent, since it is unconditioned and does not exchange air with the site outdoor or any of the interior zones (FAVRETTO; ROSSI; *et al.*, 2015).

The simulations run with these models aimed to predict the air and operative temperatures. The outputs studied were a) Zone Mean Air Temperature and b) Zone Operative Temperature.

The simulation results were used to compare the difference in prediction between the two types of modeling considering the long-stay rooms, which are the two bedrooms (BDR_1 and BDR_2) and living room and kitchen (LR_KIT) ($\Delta = SZM - MZM_{ROOM}$). A positive value indicated that the SZM temperature overestimated the value predicted by the MZM, while a negative value indicated the opposite. The following equations, Equation 2 and Equation 3, show the comparisons that considered the air and operative temperature differences between the two models, respectively:

Equation 2

$$\Delta Ta^{room} = \frac{\sum_{i=1}^{8760}(T_{a,i}^{S} - T_{a,i}^{M,room})}{8760}$$

Where,

ΔTa^{room} : Average difference in air temperature prediction between SZM and each long-stay room of MZM (°C).

$T_{a,i}^{S}$: SZM hourly air temperature (°C).

$T_{a,i}^{M,room}$: MZM hourly air temperature for each long-stay room (°C).

Equation 3

$$\Delta To^{room} = \frac{\sum_{i=1}^{8760}(T_{o,i}^{S} - T_{o,i}^{M,room})}{8760}$$

Where,

ΔTo^{room} : Average difference in operative temperature prediction between SZM and each long-stay room of MZM (°C).

$T_{o,i}^{S}$: SZM hourly operative temperature (°C).

$T_{o,i}^{M,room}$: MZM hourly operative temperature for each long-stay room (°C).

Thermal Comfort analysis was performed using ASHARE-55 Adaptive Comfort Index (ASHRAE, 2013), and the difference of comfort prediction in degree-hours was considered and compared according to the following equations (Equation 4 and Equation 5):

Equation 4

$$\Delta D_{c}^{room} = \frac{\sum_{i=1}^{8760}(D_{c,i}^{S} - D_{c,i}^{M,room})}{8760}$$

Where,

ΔDc^{room} : Average difference in discomfort by cold prediction between SZM and each long-stay room of MZM (°Ch).

$D_{c,i}^{S}$: SZM hourly discomfort by cold (°Ch).

$D_{c,i}^{M,room}$: MZM hourly discomfort by cold for each long-stay room (°Ch).

Equation 5

$$\Delta D_{h}^{room} = \frac{\sum_{i=1}^{8760}(D_{h,i}^{S} - D_{h,i}^{M,room})}{8760}$$

Where,

ΔDh^{room} : Average difference in discomfort by heat prediction between SZM and each long-stay room of MZM (°Ch).

$\mathrm{D}_{\mathrm{h,i}}^{\mathrm{S}}$: SZM hourly discomfort by heat (°Ch).

$D_{h,i}^{M,room}$: MZM hourly discomfort by heat for each long-stay room (°Ch).

Air Temperature

The ventilation control model is based on temperature; therefore air temperature is used to reach the defined set point, making it an important metric when modeling naturally ventilated buildings.

Figure 15 shows the average annual hourly difference in prediction between the two studied models regarding the analyzed cases.

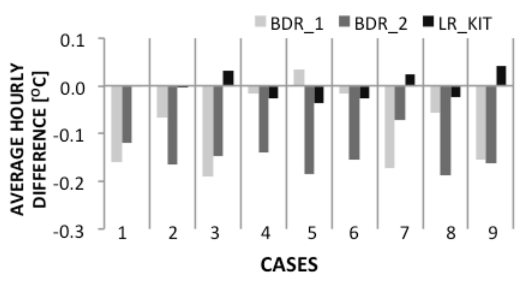

Figure 15 - Annual average hourly air temperature difference between SZM and each long-stay room of the MZM

The average annual hourly difference between the air temperatures predicted by the models shows very low values, the highest being -0.2˚C. In most of the cases, the annual hourly average of the SZM prediction underestimates the air temperature when compared to BDR_1 in the MZM. There are also overestimations, but these differences also remain in low values.

In all cases, when analyzing BDR_2, the hourly average air temperature is lower for the SZM, but still assuming very low values. In Manaus/AM – for cases 4, 5 and 6 – the SZM underestimates the LR_KIT of the MZM for all three building orientations. For the remaining climates, the underestimation occurred in cases 2 and 8, with building orientation "b".

The annual maximum differences in air temperature between the two models are shown in Table 20.

Table 20 - Maximum air temperature difference between SZM and MZM long-stay rooms for a year

CASE	BDR_1 [°C]	BDR_2 [°C]	LR_KIT [°C]
1	-1.33	-1.63	-1.61
2	-1.29	-1.56	-1.66
3	-1.45	-1.42	-1.42
4	+1.31	-1.56	-1.01
5	+1.10	-1.40	-0.91
6	+1.34	-1.88	-1.18
7	-1.72	-1.64	-1.52
8	-1.48	-2.04	-1.82
9	-1.28	-1.32	-1.43

Operative Temperature

The Operative Temperature is used as an output to evaluate the thermal comfort in ASHRAE 55 Adaptive Comfort Index (ASHARE, 2013).

Figure 16 illustrates the annual hourly operative temperature average differences between the SZM and the MZM long-stay rooms.

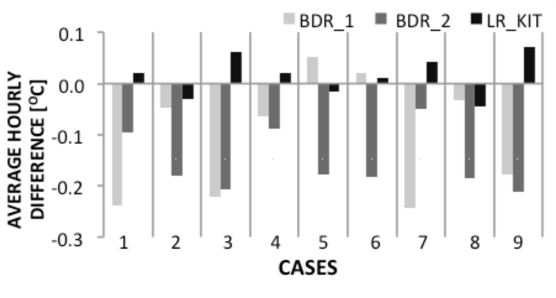

Figure 16 - Annual average hourly operative temperature difference between the SZM and each long-stay room of MZM

Very small differences, around -0.25˚C, were found between the SZM and the MZM annual hourly average predictions. In most of the cases, the SZM underestimated the operative temperature predicted by the MZM for BDR_1, which also occurred for all cases regarding BDR_2. Table 21 indicates the maximum operative difference between the models.

Table 21 - Maximum operative temperature difference between the SZM MZM long-stay rooms during a year

CASE	BDR_1 [°C]	BDR_2 [°C]	LR_KIT [°C]
1	-1.29	+0.84	-0.89
2	+1.02	-1.00	-0.87
3	-1.08	-1.31	+0.81
4	+0.99	-0.89	+0.65
5	+0.85	-0.89	+0.64
6	+0.96	-1.11	-0.71
7	-0.99	+0.87	-0.71
8	+0.93	-1.10	-1.05
9	+0.89	-1.02	+0.85

Considering all climates and building orientation, the lowest values were shown in the LR_KIT. Higher values were shown in BDR_1 and BDR_2 when building orientation is "b" and "c." Figure 17 is a summary of the distribution, over a year, of the differences predicted between the models showing very low values, with the largest share in the range of 0 to 0.30˚C.

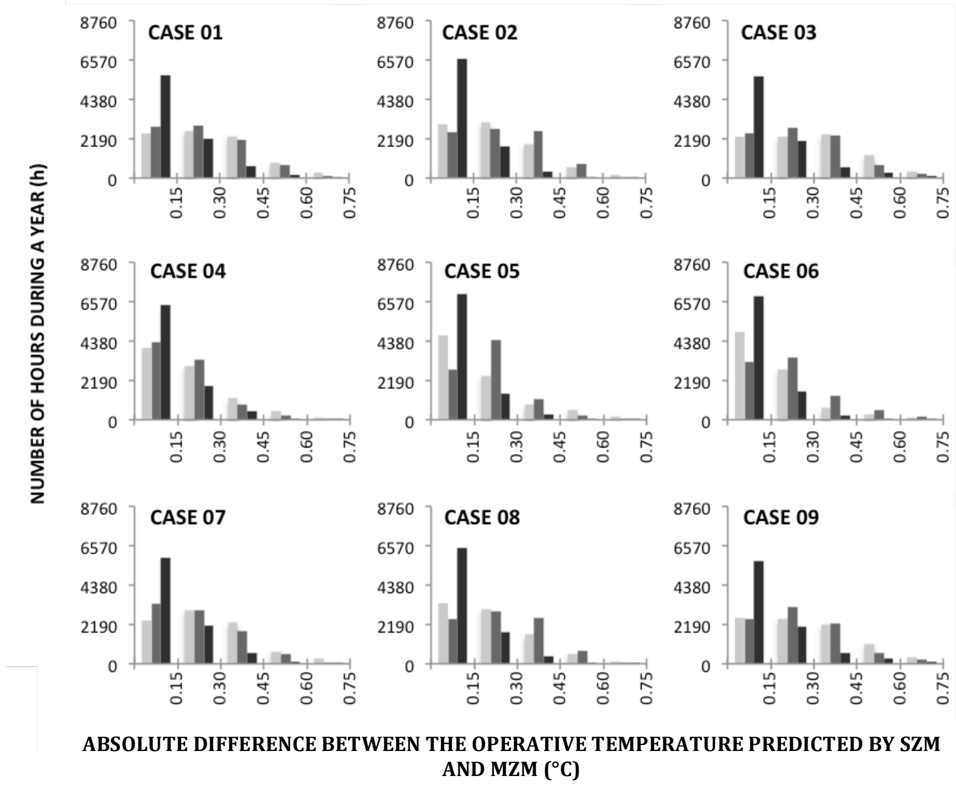

Figure 17 - Distribution of hourly absolute differences between the operative temperatures predicted by SZM and MZM over the course of a year

Degree-hours of discomfort by heat and cold

The same method applied to the research as a means to measure the discomfort in a building was applied to the thermal zone test. It considered the predictions from both models and defined a comfort range, from which the thermal discomfort was calculated.

To verify if the models showed similar results and achieved similar thermal comfort values, a comparison between the annual degree-hours by heat and cold was performed.

The difference between the annual average °Ch of discomfort by heat (A) and by cold (B) calculated based on predictions from SZM and MZM, which show very low values, can be seen in Figure 18. When analyzing by location, the warmest climate, cases 4-6, shows a greater difference in degree-hours of discomfort by heat. Mild and cold climates, cases 1–3 and 7–9, show the greater difference related to the difference of °Ch by cold.

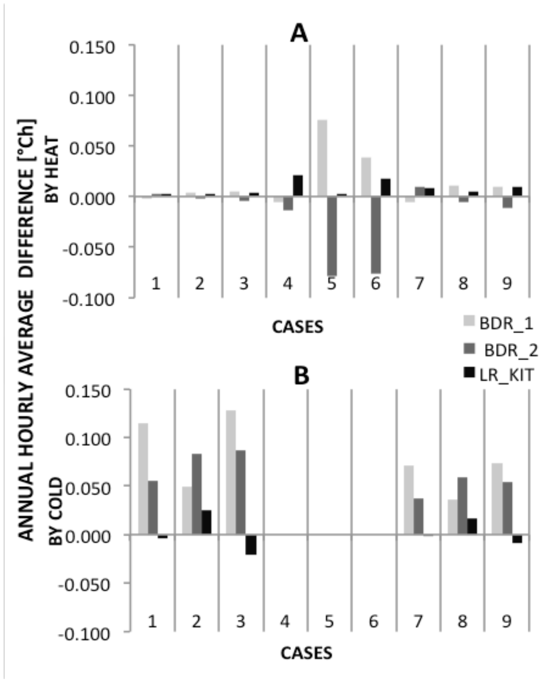

Figure 18 - Annual average difference between SZM and MZM in hourly discomfort by heat (A) and cold (B)

3.5 Adaptive Model – ASHRAE 55

ASHRAE 55-2013 “Thermal Environmental Conditions for Human Occupancy” (ASHRAE, 2013) describes the adaptive model, which determines the acceptable thermal conditions in naturally ventilated spaces. In order to apply the model, the space being considered has to meet the following criteria; (a) not have a mechanical system, such as air conditioning, (b) the metabolic rates for the representative occupants must range from 1.0 to 1.3 met[9], (c) the choice for clothing is free, and the representative occupants can adapt it to the indoor and/or outdoor thermal conditions within the range of 0.5 to 1.0 clo[10], and (d) the prevailing mean outdoor temperature has to be greater than 10˚C (50°F) and less than 33.5˚C (92.3°F).

---

[9] metabolic rate

[10] unit used to express the thermal insulation provided by garments and clothing ensembles, where 1 clo = 0.155 m2·°C/ W(0.88 ft2·h·°F/Btu)

The low-cost houses, as well as the three climates being studied in this research, meet the above-mentioned criteria.

The model relates the indoor design temperatures, or the acceptable temperature ranges, to outdoor meteorological parameters. The following equation accounts for effects such as, local thermal discomfort, clothing insulation, metabolic rate, humidity and air speed.

Equation 6

$$T_n = 17.8 + 0.31 \times T_{pma(out)}$$

Where:

T_n (˚C) is the ideal internal operative temperature, also known as neutral, which comprises a relation between the mean air and radiant temperatures. $T_{pma(out)}$ is the prevailing mean outdoor air temperature, which is based on the arithmetic average of the mean daily outdoor temperature over a given period of time. In this research, the mean outdoor air temperature was taken from the weather file from Roriz (2012), which provided the temperatures on an hourly basis. The values adopted were calculated based on the average over a period of fifteen days.

ASHRAE establishes an interval for comfortable temperatures, where the upper limit is given by T_n+ToleranceValue, and the lower limit by T_n-ToleranceValue. The allowable indoor operative temperatures are determined by the acceptability limit of 80%, where the Tolerance Value is 3.5˚C.

3.6 Degree-hours of discomfort

It is possible to account for the severity of the exceedance of thermal discomfort at any given time using the metric of degree-hours. The degree-hours of discomfort by heat or by cold is the sum of the difference between the hourly average operative temperature and the upper or lower comfort limits. When the temperature is above the upper comfort limit, it indicates the degree-hours (˚C · h) of discomfort by heat, and when below the lower limit, the ˚C · h of discomfort by cold (FAVRETTO *et al.*, 2015). The upper and lower limits vary according to each climate. Table 22 presents the degree-hours of discomfort for the studied climates considering the temperature for the site outdoor.

Table 22 – Annual Degree hours of Discomfort

	Annual Degree Hours of Discomfort for site outdoor[1]		
	By Heat	By Cold	Total
Curitiba	239	28209	28448
São Paulo	579	17918	18497
Manaus	2950	41	2991

[1] Calculated based on a period of 15 days

3.7 Monte Carlo Simulation

Monte Carlo simulation explores the building's design space associated to the range given to all the identified parameters and returns the annual thermal comfort with each building instance. An energy simulation tool is used to calculate the required outputs for each sample in the Monte Carlo simulation. EnergyPlus was the software of choice in this study, as specified in item Simulation: EnergyPlus.

The analysis starts by sampling each parameter and substituting the default value by one from the given range (See General Input Data for Base Model) in the base model for the specific parameter in question. Each parameter's value must be inserted in the appropriate location, so tags in the base model correspond to parametric objects. Once the software identifies that tag, it substitutes the value for that run in the parametric object.

For the present work random sampling was used, which statistically, has advantages since it generates unbiased estimates of the mean and the variance of *Y* (HELTON, 1993). The code was written in Python, and the EnergyPlus iterations were performed in a 21-node 656-core Linux cluster. A total of 10,000 simulations were run for the meta-model of each of the three climates, yielding 30,000 simulations.

3.8 Software

3.8.1 Simulation: EnergyPlus

Several authors (HOPFE; HENSEN; PLOKKER, 2007; STRUCK; HENSEN; KOTEK, 2009) indicate the use of simulation and its importance. They emphasize that it is a relevant detailed tool, aided by the increase of access to personal computers properly designed for such task. In this context, EnergyPlus was chosen as the simulation tool for the research. Some significant features are highlighted to support such choice; (a) it is validated by ASHRAE-140 (ASHRAE, 2004) and used by the Department of Energy of the United States, (b) uses input and output data in text format, making its an automated workflow easier, (c) it is not based on simple algorithms, (d) it is a free software, (e) includes an extensive documentation, and (f) it allows a limited visualization and modification of a model using OpenStudio (Hygh, 2011).

3.8.2 Meta-model Elaboration: Matlab

The software of choice to perform the regression analysis was Matlab. The functions *stepwisefit* and *stepwiselm* were used to build the regression models. *Stepwisefit* uses stepwise method to create a multilinear regression to rank the parameters according to their impact on the outputs, and generates a coefficient to each parameter that is defined as included. If a parameter is not included, the function does not allow for it to be reconsidered. The function also automatically includes a constant term in all models. *Stepwiselm* uses stepwise regression to add or remove predictors, that is, it uses forward and backward stepwise regression to create a final model. At each step, it searches for terms to be added or removed from the model based on the value established as the 'Criterion' argument.

The P-values demonstrate the potential a given term has to explain the predictable variable. Values were established as a criterion to add (*p-enter*) or remove (*p-remove*) a term from the regression model. If a term was included in the regression model (p-value <p-enter), it means that it will have a coefficient value assigned to it; if not included (p-value>p-remove), a value of zero will be determined for it.

3.9 Regression Analysis

Multivariate linear regression was performed on the results for discomfort by heat and cold for each studied climate regarding the variable parameters. The regression is an approximate equation to predict thermal comfort as a function of the key parameters. For each model, 10,000 simulations were run, of which, 6,000 were used to generate the regression equation and the remaining 4,000 to validate it by testing the model's accuracy in relation to the simulation results given by the software.

Each simulation run yielded a raw data set grouped by climate. The files from the data sets were treated and files containing only the relevant parameters for the regression analysis were kept, as well as the desired outputs.

The output for the regression analysis, to identify if a building is thermally comfort or not, is degree-hours of discomfort by heat and by cold. EnergyPlus doesn't provide this output for the simulations it runs, so this calculation was written in the code. It read the given outputs from EnergyPlus and calculated the degree-hours of discomfort by heat and by cold, providing only absolute values in separate columns; heat and cold. Since the software predicted no negative values, the lack of discomfort was always given by the value of zero.

Once the raw data sets were treated, *csv* files containing only the desired 24 parameters for the equation were created (Table 23). The parameters presented on the table are the *x* variables in the regression equation, and the *y* variable, what is predicted by the equation, is the annual discomfort by heat and by cold, as listed on Table 24.

Table 23 - x variables in regression equation

Design Parameters (x variables)	
Window Size (WWR) Bedroom 1	Overhang – Living Room
Window Size (WWR) Bedroom 2	Solar Absorptance - Roof
Window Size (WWR) Living Room	North Axis
Solar Absorptance – Exterior Wall	Effective Opening Area – Bedroom 1
Left Fin – Bedroom 1	Effective Opening Area – Bedroom 2
Left Fin – Bedroom 2	Effective Opening Area – Living Room
Left Fin – Living Room	U-Value – External Walls
Right Fin – Bedroom 1	U-Value – Internal Walls
Right Fin – Bedroom 2	U-Value – Roof
Right Fin – Living Room	Heat Capacity - External Walls
Overhang - Bedroom 1	Heat Capacity - Internal Walls
Overhang – Bedroom 2	Heat Capacity - Roof

Table 24 - *y* variables in regression equation

Final Equation Result (*y* variable)
Annual Discomfort by Heat Indoor
Annual Discomfort by Cold Indoor

The regression produces linear coefficients that are proportional to each parameter’s sensitivity to thermal comfort. The regression models’ accuracy can be improved by considering additional terms, such as derived or cross terms.

The first type of regression performed was *Stepwisefit*, to quantify, in a decreasing order, the importance of the parameters that were most influential in the output. This procedure indicated with the *P-values* which parameters were IN or OUT of the equation, given their influence on the results. The second type of stepwise regression used was the *stepwiselm*, which verified cross terms, allowing one term to be multiplied by another and thus improve the R^2 values. Different *P-values* were used in the above-mentioned regression methods with the respective values for p–enter and p-remove; 0.05 and 0.10. The established values determined if a term was included in or removed from the regression model. When p-value <0.05, the term was included (IN) and a coefficient value assigned to it, therefore indicating that the term was relevant and influential on the results, and thus should be part of the equation. If not included, p-value>0.10, then a value of zero was determined for such term. To verify the linearity of the variables, scatterplots were created during the process, by plotting variable vs. output.

3.10 Validation: Reliability Tests

The Monte Carlo simulation explores a building's thermal performance based on the given ranges of all specified parameters. A simulation tool, in this case EnergyPlus, calculates the performance of each given sample in the Monte Carlo. The output data generated by the latter, compose a set of definitions for the energy model, and are estimates that correspond to the degree-hours by heat and cold. According to Hygh (2011), a regression analysis of this data set provides an approximated equation of the degree-hours as a function of the key-parameters.

The reliability tests performed for such equation used the results independently generated by EnergyPlus with the input data generated in the Monte Carlo, in comparison to the ones yielded by the regression equation. The closer the equation results are to the software results, the more accurate the meta-model.

3.11 Case Study

The case study was to verify if the meta-model predicted the discomfort by heat and/or cold as expected in the studied locations. The meta-model was applied to a standard LCH, and the parameters for the shading devices were varied while the others remained fixed. Every time an alteration was made to the parameters in question, the results were analyzed.

4 Results

4.1 General

The results considered 24 varying parameters using random values as their input within a defined range. Table 25 lists such parameters and ranges, whereas the complete list of parameters used, fixed and varied, can be found in Methodology. A total of 10,000 simulations were run for each location, São Paulo, Curitiba and Manaus, from which 6,000 were used to create the meta-model and the remaining 4,000 to validate it by applying reliability tests. The meta-model predicts the degree hours of discomfort by heat and cold for the locations São Paulo, SP and Curitiba, PR. The meta-model developed for Manaus, AM only calculates the discomfort by heat, since there is no discomfort by cold in this location.

Distinct meta-models were created to calculate discomfort by heat and discomfort by cold separately due to the fact that each instance accounts for the parameters differently, and therefore it could not be one meta-model for both situations.

Table 25 – Parameter used in regression analysis and their ranges

#	Parameter Name	Range	#	Parameter Name	Range
1	Window Size (WWR) Bedroom 1	10-90%	13	Overhang – Living Room	0.01-0.5
2	Window Size (WWR) Bedroom 2		14	Solar Absorptance - Roof	0.10-1.00
3	Window Size (WWR) Living Room		15	North Axis	0°-359°
4	Solar Absorptance – Exterior Wall	0.10-1.00	16	Effective Opening Area – Bedroom 1	50 or 100
5	Left Fin – Bedroom 1	0.01-0.5	17	Effective Opening Area – Bedroom 2	
6	Left Fin – Bedroom 2		18	Effective Opening Area – Living Room	
7	Left Fin – Living Room		19	U-Value – External Walls	0.30-5.00 $m^2.K/W$
8	Right Fin – Bedroom 1		20	U-Value – Internal Walls	
9	Right Fin – Bedroom 2		21	U-Value – Roof	0.50-2.10 $m^2.K/W$
10	Right Fin – Living Room		22	Heat Capacity - External Walls	40-445 Kg/m^3
11	Overhang - Bedroom 1		23	Heat Capacity - Internal Walls	
12	Overhang – Bedroom 2		24	Heat Capacity - Roof	11-791 Kg/m^3

The regression analysis for the meta-model was run using Matlab with two types of stepwise analysis; *stepwisefit* and *stepwiselm*. *Stepwisefit* ranked the parameters from the ones showing the most influence in the results to the ones showing the least. This function yielded low R^2 values, since it only considered the raw parameters to generate coefficients and thus create the equation for the regression model. *Stepwiselm* allowed more flexibility in starting the model; it automatically verified cross terms in the process and showed a significant improvement in R^2 values. The P-values allowed for the stepwise functions were 0.05 for P-enter and 0.10 for P-remove.

4.2 Regression Models' Complexity and Accuracy

By increasing the regression models' complexity, their accuracy also increased. Therefore, the first step to increase the regression models' accuracy was to include cross terms, which allowed multiplying one term by the other. As expected, this resulted in an increase in the regression models' accuracy, since it recognized meaningful combinations of design parameters and their impact in the discomfort by heat or cold. The first regression models, with no interactions, presented between 9 to 20 terms, whereas the ones with interactions had between 38 to 72 terms.

To further increase the regression models' precision, a second step was taken; the inclusion of inverse terms. These are the inverse of each value from the design parameters used in the Monte Carlo simulation. This step expanded the dataset, which was used to build new regression models including the original design parameters and the inverse values. Another improvement in accuracy was observed, as well as an increase in the regression models' complexity, with 85 to 152 terms in each model.

One last step was to expand from interactions to quadratic, which allowed squared terms in the regression models. This last step presented the highest accuracy, although it didn't increase the models' complexity, with 101 to 171 terms. The greatest improvement was seen when inverse terms were added to the regression models.

The figure below (Figure 19) presents the models' accuracy for the discomfort by cold for São Paulo (SP) and Curitiba (CTB) as determined by the R^2 values, as well as their respective validation results. The meta-models presented good results, with high R^2 values for the values given by the simulation results used to build the meta-model, as well as for the validation results.

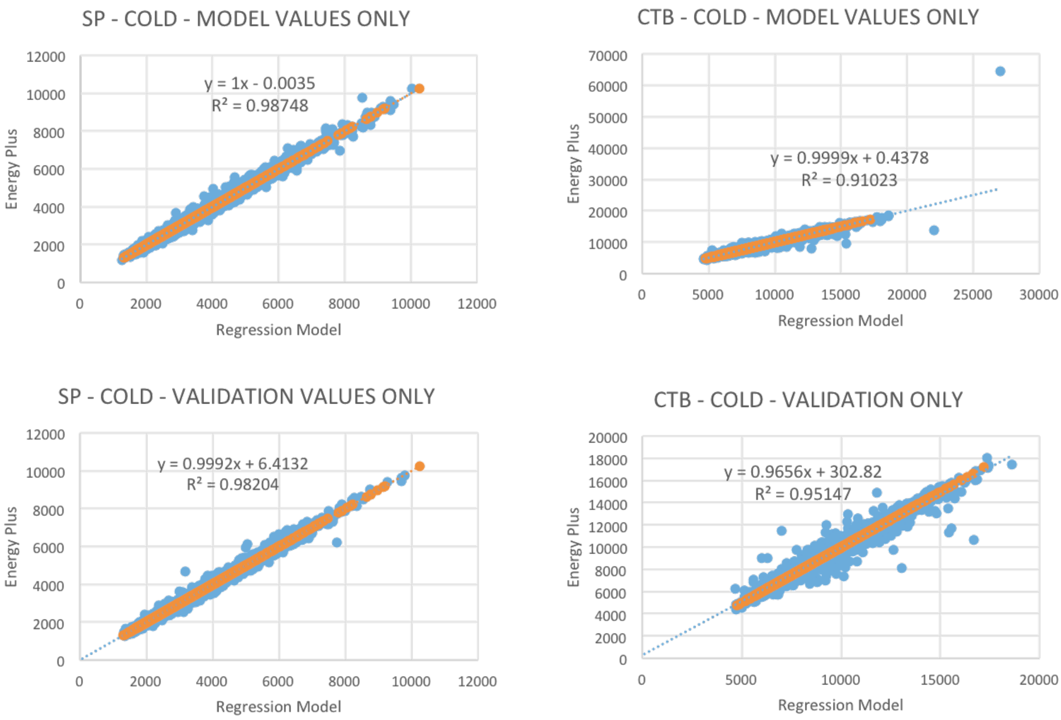

Figure 19 - Cold model values and validation for São Paulo and Curitiba

Table 26 presents the R^2 values for the regression models, as well as the average percentage error, which indicates a positive or negative bias. The highest R^2 values can be seen in Curitiba and São Paulo for cold, since the data used to build the regression models for these locations did not present a lot of zeroes, given they are cold and mild climates. Therefore, the discomfort by cold is greater, and situations of no discomfort, zero values as an output, were rare. The opposite happened to the regression model predicting the discomfort by heat for the same locations. For the same reason, for the milder climates, where very little discomfort by heat is registered, the results presented many zeroes as the output, causing the R^2 values to be lower. For Manaus, the R^2 value is high, since there is discomfort by heat all year long, presenting no zeroes as an output or a very small amount of such.

Table 26 - Error Analysis

		Curitiba	São Paulo	Manaus
Discomfort by Cold	RMSE	569.366	149.483	-
	CV(RMSE)	0.0651	0.0436	
	NMBE	1.31035^{-05}	4.2195^{-04}	
	Avg % Error	0.11%	0.11%	
	R^2	0.9515	0.982	
Discomfort by Heat	RMSE	13.459	30.118	167.092
	CV(RMSE)	4.241	1.7853	0.4098
	NMBE	-0.700	-0.363	-0.080
	Avg % Error	804.14%	2162.68%	5517.61%
	R^2	0.6107	0.7464	0.9505

The output from the EnergyPlus model was degree-hours of discomfort by heat and by cold, with no negative values in its predictions; meaning that when the result is zero, there is no discomfort. Other studies, such as Hygh et al (2012), were able to quantify the amount of heating and cooling loads necessary for each location studied. Due to the conditions of the present work, two points are highlighted; 1) negative values predicted by the regression model should be interpreted as zero, and 2) when the regression model tries to fit several datasets to the same output value (zero), the fit generated may not be accurate.

Further steps were taken to address the above-mentioned points. To address the first point, a post processing procedure was added to set all negative values predicted by the regression model to zero. Such action can be viewed as a "floor" on the regression values, mimicking the way EnergyPlus was unable to provide negative values as well. By adding the "floor", the R^2 values improved from 0.93 to 0.95 when analyzing model values only. Approximately the same improvement is seen in the validation numbers, indicating an increase in the regression models' accuracy (Figure 20).

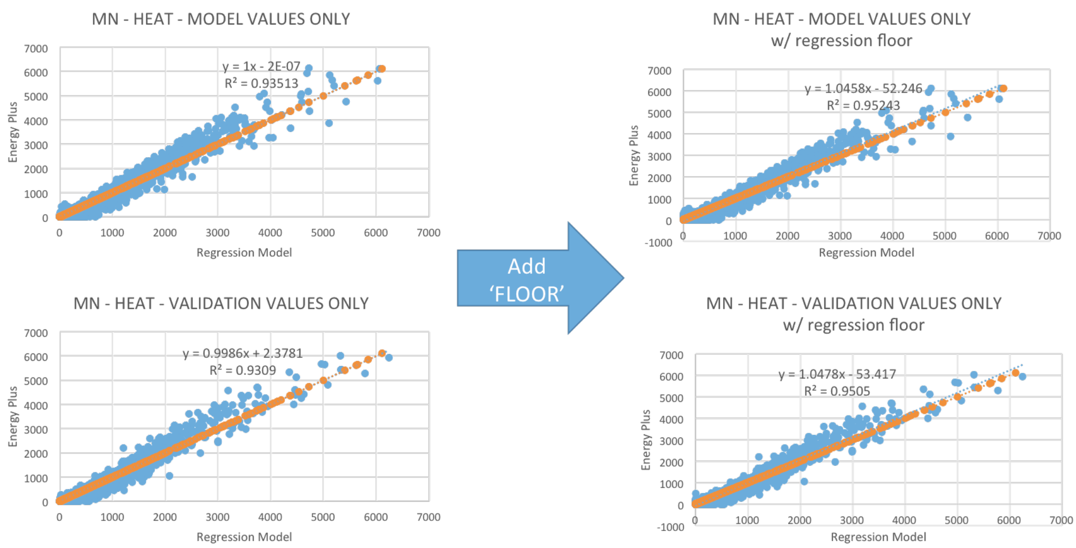

Figure 20 - Value for Manaus before and after adding "floor"

The second point refers to the preponderance of EnergyPlus zero values for the cities of São Paulo and Curitiba, in regards to the regression model calculating the discomfort by heat. There was no quantification of a lack of discomfort, since such situation results in an output of zero. Several combinations of input values resulted in an output of zero, indicating no discomfort, but the amount of this lack of discomfort is not calculated. Therefore, Curitiba had 81% of its dataset generated by zeroes, while São Paulo had 60% of zero values. Such a large amount of zero as an output meant that the regression models could not accurately predict the degree-hours of discomfort by heat using only standard regression methods. Such methods presented low R^2 values of 0.62 and 0.77, for Curitiba and São Paulo, respectively. In response to these poor values, an attempt to eliminate all zeroes from the dataset was made, which would train the model to use only non-zero (NZ) values to predict the discomfort. A new subset of data was created by eliminating all data sets containing zero as an EnergyPlus output. The regression models created using only NZ values presented better accuracy to predict the remaining NZ values, with an improved R^2 of 0.9 for São Paulo and 0.83 for Curitiba. However, such models did not show a good fit in the validation process (Figure 21 and Figure 22), and were, therefore, not employed for running further tests in the study.

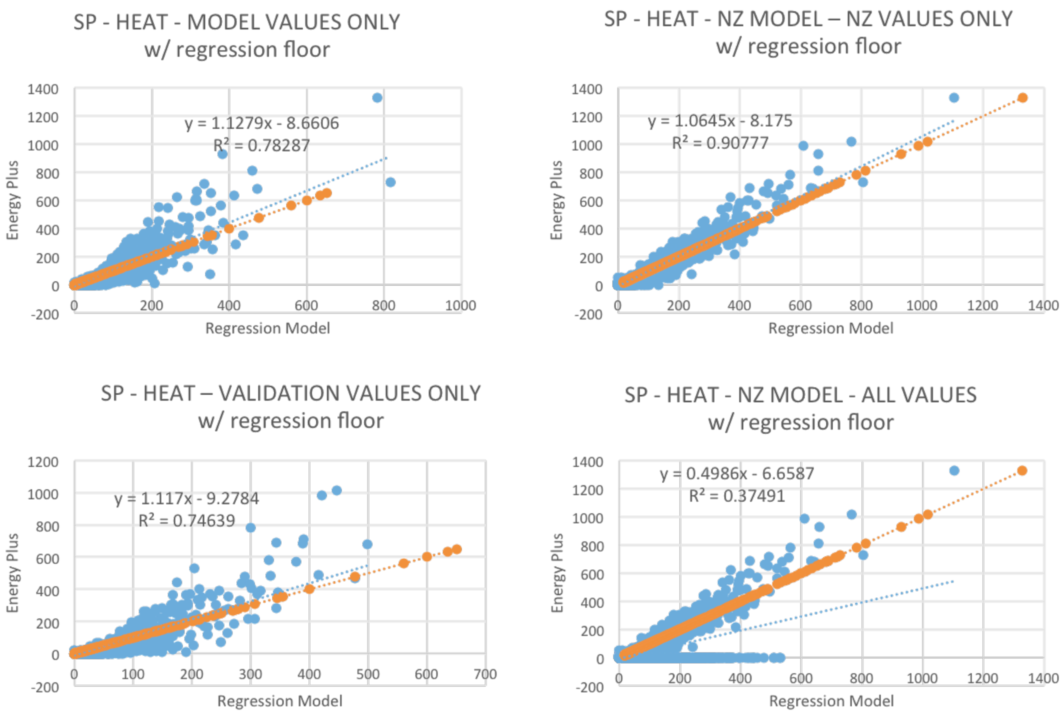

Figure 21 - Comparison between SP Heat Meta-Model with floor and NZ Model

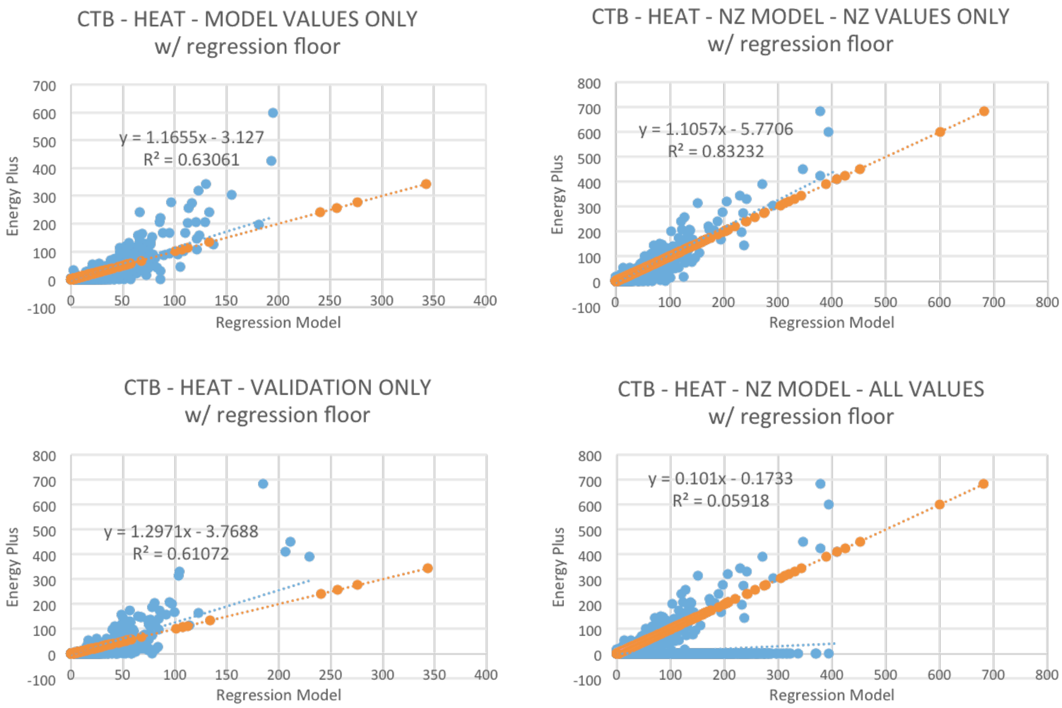

Figure 22 - Comparison between SP Heat Meta-Model with floor and NZ Model

4.3 Tests: Shading Devices

4.3.1 General Input Data

The meta-models for all three locations were tested to verify the impact of shading devices in each climate and assess if the meta-models perform as expected. Such tests were run using values for a standard LCH (Figure 23), with fixed window areas and constructive systems as proposed by Marques (2013), and presented on Table 27.

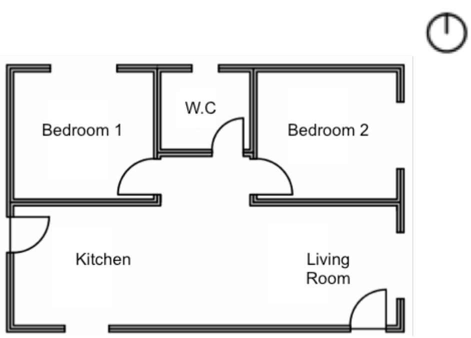

Figure 23 - Fixed geometry for meta-model at 270˚

Table 27 - Values adopted for a standard LCH

	Roof	External Walls	Internal Walls	Windows
Absorptance	0.75	0.4	N/A	N/A
U-Value	1.78 W/m2.K	2.76 W/m2.K	2.27 W/m2.K	
Heat Capacity	189 KJ/m2.K	266 KJ/m2.K	206 KJ/m2.K	
WWR Test 1	N/A	N/A	N/A	14%
WWR Test 2 (CTB only)				90%
EWVA				50%
Orientation	270˚			

The building was set at a fixed orientation of 270˚, and the tests were performed considering the North and East facing windows that corresponded to the long-stay rooms. In all tests the option 'No Shading' was included as a baseline to compare all the other combinations to, thus allowing the evaluation of a device's impact in each configuration established. Increments in size were made on each element, and in each step a new element was added to the same window and its impact verified.

Table 28 reports the values used and varied for the shading devices; it presents the depth in meters that were calculated based on the windows' height. All values in meters are rounded up and approximately the same because all WWR's are also of approximate values, since all facades have almost the same area, which results in shading devices of the same depth.

Elements were added to each façade individually, and then combined, having all windows shaded with all possible elements as the extreme opposite from the baseline.

Table 29 presents the increments and gradual combinations made for each test run showing Depth Factor values. The possible scenarios are No Shading, only Overhangs (a), only Fins (b – always left and right), and Box (c- Fins and Overhang) (Figure 24).

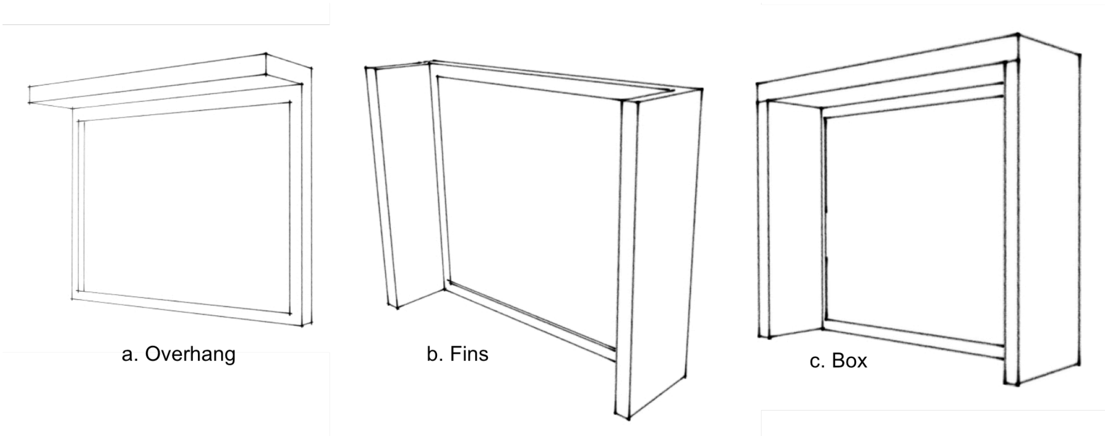

Figure 24 - Shading Devices Combinations considered in the tests

Table 28 - Shading Devices' Increments in meters

	WWR (%)	Depth (m)
		Bedroom 1, Bedroom 2 & Living Room
Overhang and Fins	14	0
		0.25
		0.35
		0.5
	90	0
		0.71
		1
		1.43

Table 29 - Combinations and increments established for the tests

				Overhang			Fins (Left and Right)		
		North window	East windows	0.25	0.35	0.5	0.25	0.35	0.5
	Set 1[1]	x	x						
Set 2	Set 2a	x							
	Set 2b	x							
	Set 2c[2]	x							
Set 3	Set 3a		x						
	Set 3b		x						
	Set 3c[2]		x						
Set 4	Set 4a	x	x						
	Set 4b	x	x						
	Set 4c[2]	x	x						

1: No Shading   2: Box

4.3.2 Manaus

All values given by the meta-model for Manaus were as expected; whenever a shading device is added to a window, the discomfort by heat decreases. The progressive improvements can be seen by the following figures (Figure 25, Figure 26 and Figure 27), illustrating that increments in size and quantity of the devices gradually contribute to a decrease in the discomfort by heat.

According to the values predicted by the meta-model, overhangs and fins present different performances according to their orientation. Overall, fins showed to be more efficient when applied to east-facing windows, while overhangs showed better performance when used facing north, even though the impact is smaller when compared to fins on east facades. The Box configuration showed the highest impact in all cases; however, it is highly dependent on the depth factor. This dependence can be seen in Figure 26, where fins with the highest depth factor present similar results to the box with the lowest depth factor tested. Therefore, depth factor is very relevant for the device to have a significant impact in the unit.

The differences in the values observed in the tests run with these configurations also show that the combination of the amount of devices, their size and the façade where they are placed have a significant impact in the thermal performance of the building. It can also be observed that for this location, with the proposed configurations in the tests, the solution with the most impact is the box in all long-stay rooms' windows, presenting a decrease of approximately 50% in degree-hours of discomfort by heat. It is important to highlight that these results can be applied to a standard LCH, with small windows, which is also a standard practice for this type of building. Therefore, it is possible to argue that if no other improvements were made to the LCH designs, expect for the addition of shading devices, the discomfort by heat in such units in Manaus would be half of what it is with what it is today.

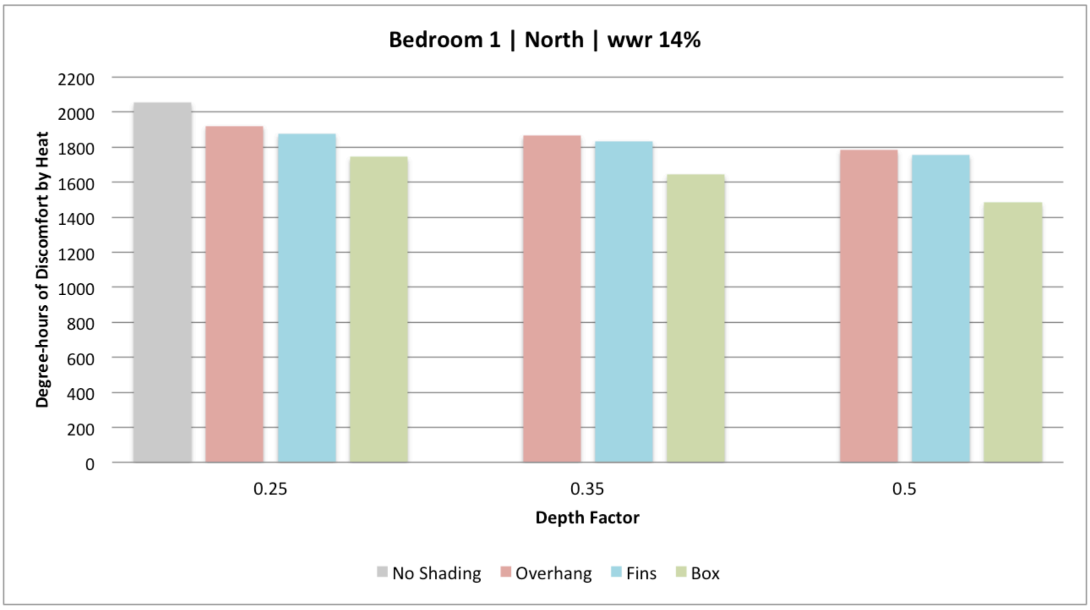

Figure 25 - Impact of Shading Devices when applied only to Bedroom 1 facing North

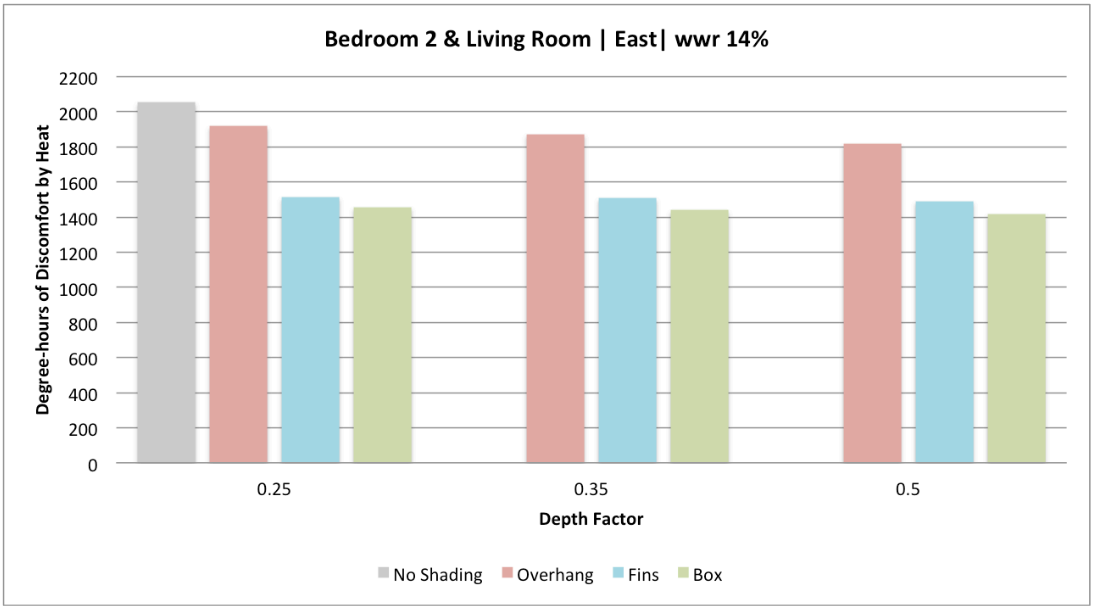

Figure 26 - Impact of Shading Devices when applied only to Bedroom 2 and Living Room facing East

Figure 27 - Impact of Shading Devices when applied all long-stay rooms

4.3.3 Curitiba and São Paulo

4.3.3.1 Discomfort by Heat

The values predicted by the meta-model for discomfort by heat for São Paulo and Curitiba reflect, in general, the expected behavior for such locations. As illustrated by the figures below (Figure 28, Figure 29 and Figure 30), when a shading device is applied to a window, the discomfort by heat decreases, as seen in most cases for these locations. When only fins are used only in the north façade in São Paulo there is no improvement, leaving only overhangs as an option to improve the overall comfort in the unit. As for Curitiba, no change was observed when any type of device was added only to Bedroom 1 (Figure 28), and there was a very small decrease in the degree-hours of discomfort by heat when using shading devices in more than one window. One can also observe that in Curitiba fins are not effective in any of the presented configurations, leaving only the overhang as a viable option. However, in São Paulo, when the box is used at its maximum depth in all windows, there is a greater decrease in the discomfort by heat.

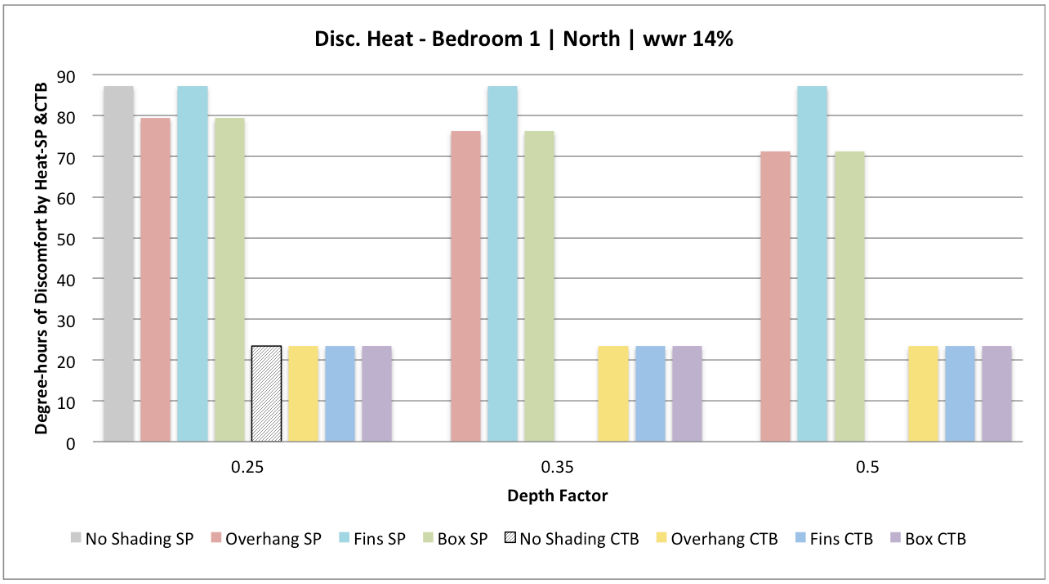

Figure 28 - Impact of Shading Devices when applied only to Bedroom 1 facing North-São Paulo and Curitiba

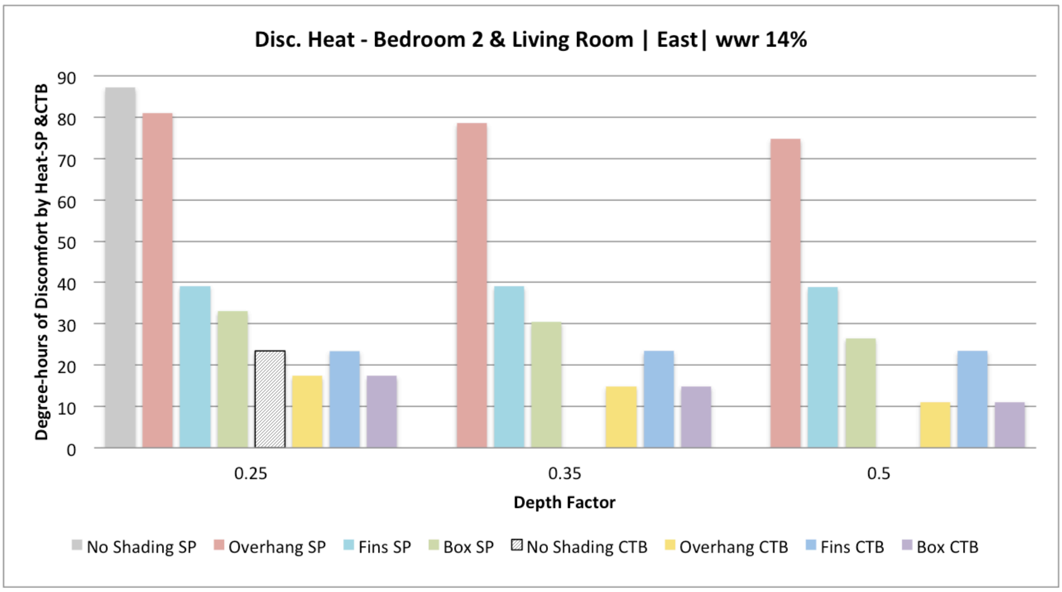

Figure 29 - Impact of Shading Devices when applied only to Bedroom 2 and Living Room facing East- São Paulo and Curitiba

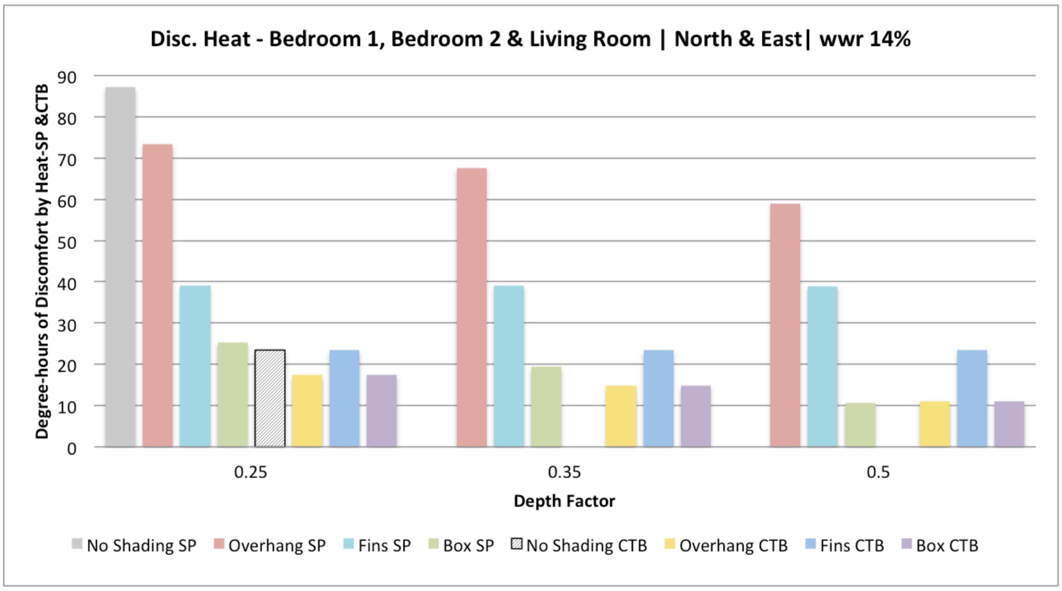

Figure 30 - Impact of Shading Devices when applied to all long-stay rooms-São Paulo and Curitiba

Such low values of decrease in discomfort for Curitiba, or the lack of it, can be accounted as noise in the meta-model. It can also be explained by the amount of zeroes in the data set used to create the regression model for this location. Curitiba is the coldest climate in this study; therefore numerous simulation runs had an output of zero, indicating no discomfort by heat with several parameters' combinations. Because of this, the meta-model might not predict well the impact of shading devices, since it might not be sensitive to such parameters. When the values are lower than 100, as is the case for the baseline in Curitiba and São Paulo, 23 and 87 respectively, the predictions are not accurate, failing to properly depict the impact of such devices.

4.3.3.2 Discomfort by Cold

The meta-model's predictions for the degree-hours of discomfort by cold in São Paulo and Curitiba presented some incongruences. The expected prediction was an increase in the discomfort when the devices were employed, and the meta-models provided values demonstrating a decrease in some cases. As illustrated in Figure 31, when there is an overhang in the north-facing window, there is less discomfort by cold, where there should be more. The opposite outcome was expected since the shading devices cover part of the window, allowing less solar heat gain in the room, causing it to be colder.

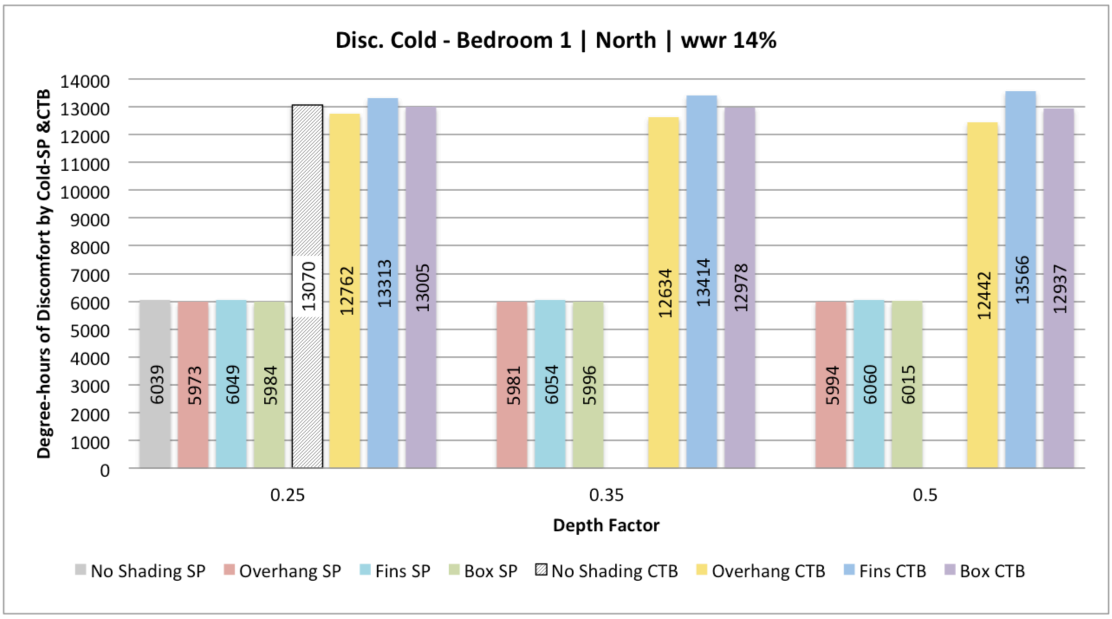

Figure 31 - Impact of Shading Devices in the Discomfort by Cold when applied only to Bedroom 1 facing North-São Paulo and Curitiba

The same effect can be observed when the east-facing windows are shaded, as well as when all of them are. Figure 32 shows the predictions for shading devices on Bedroom 2 and Living Room, presenting values very close to the baseline for both locations. In Curitiba a slight decrease in discomfort can be seen when the factor is at its maximum value (0.5), which is the opposite of the expected behavior. For São Paulo, values for these rooms are logical, but the differences are also very low to demonstrate a real impact.

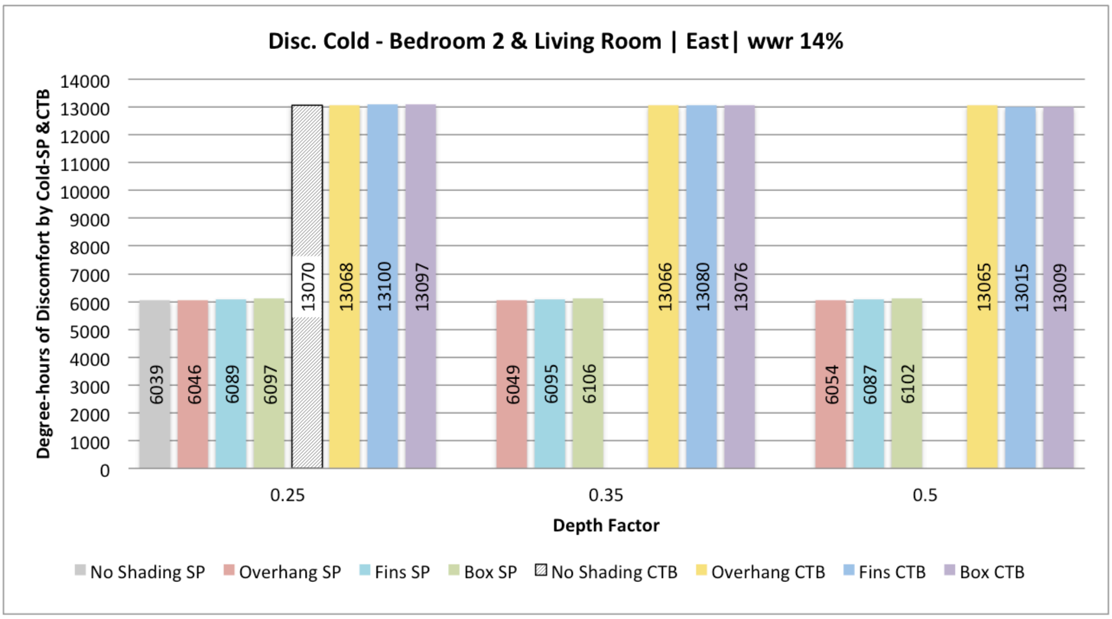

Figure 32 - Impact of Shading Devices in the Discomfort by Cold when applied only to Bedroom 2 and Living Room facing East-São Paulo and Curitiba

Figure 33 shows a slight increase in the discomfort by cold in both locations when only fins are used in all windows, which is consistent with the expected outcome. However, even with all the windows being shaded by overhangs or the box, the meta-model still predicts an unexplained improvement in the degree-hours of discomfort by cold.

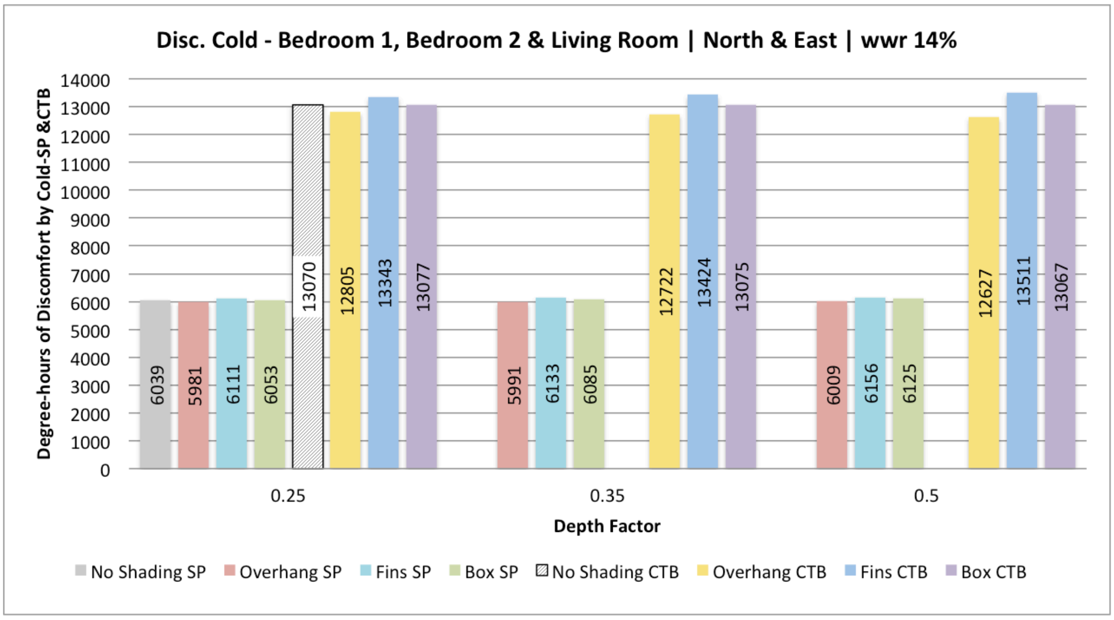

Figure 33 - Impact of Shading Devices in the Discomfort by Cold when applied to all long-stay rooms-São Paulo and Curitiba

A possible explanation for the incongruent values predicted by the model was the windows' size, since the WWR was very low in order to depict a standard LCH. Due to this fact, there was a possibility that the solar heat gain was not being properly accounted for in the meta-model and the impact caused by the devices was not being shown. Further tests were run using the maximum WWR value allowed by the meta-model. The figures below (Figure 34, Figure 35 and Figure 36) show a comparison between the WWR of 14% and 90% for Curitiba.

The same increments and situations were varied, altering only the WWR. As it was expected, the baseline 'No Shading' showed lower values, since the window area is larger, thus allowing more solar heat gain in the room. However, the previously observed pattern is repeated in Bedroom 1(Figure 34), with the only difference of a higher value of discomfort when using the box with the window set at a 90% WWR.

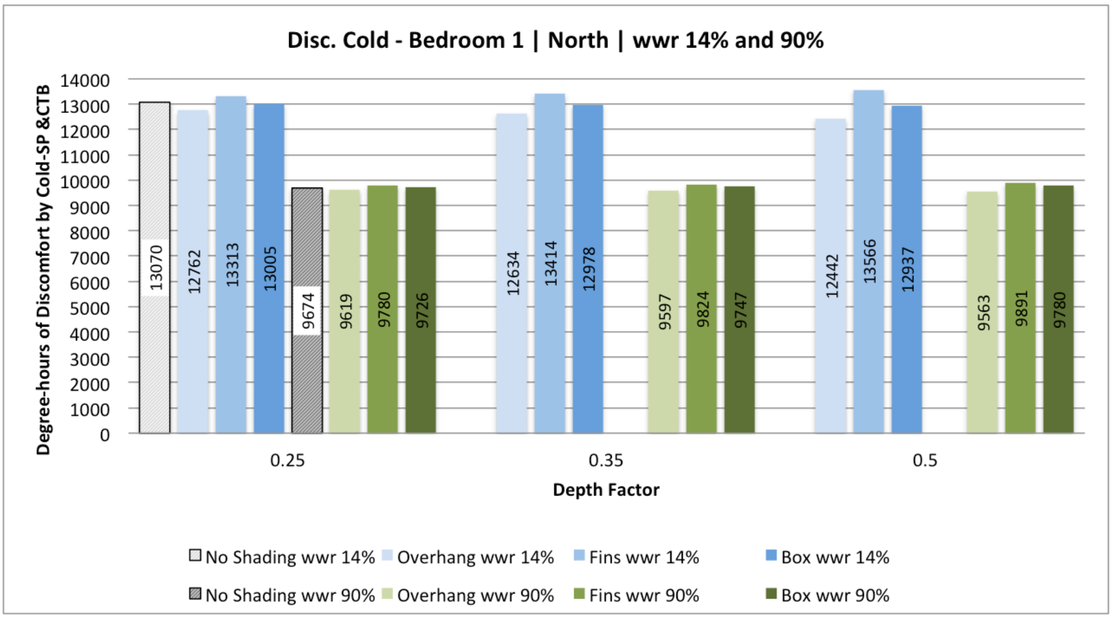

Figure 34 - Comparison of the Impact of Shading Devices with windows set with a WWR of 14% and 90% - Bedroom 1

For the remaining configurations, with shading devices in two long-stay rooms and in all long-stay rooms, the results are more consistent, in comparison to the baseline, when the WWR is set to its maximum; even though the differences are very low (Figure 35 and Figure 36). Such results suggest that further analysis of the original idf file used in the simulation may be necessary, once the values observed in these tests depict a discrepancy from the expected outcome.

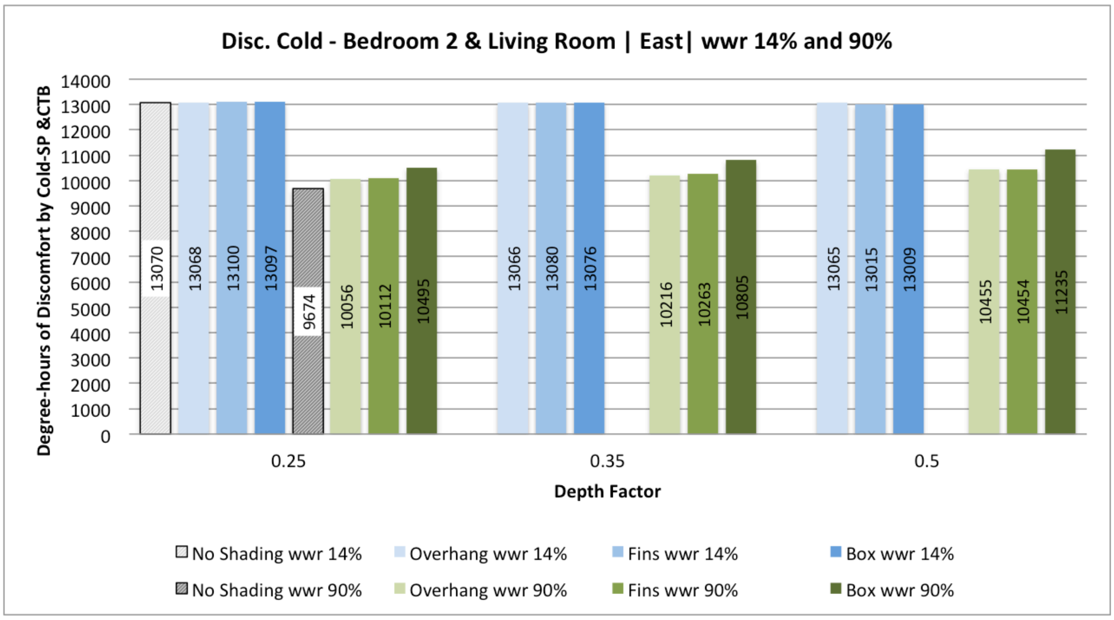

Figure 35 - Comparison of the Impact of Shading Devices with windows set with a WWR of 14% and 90% - Bedroom 2 and Living Room

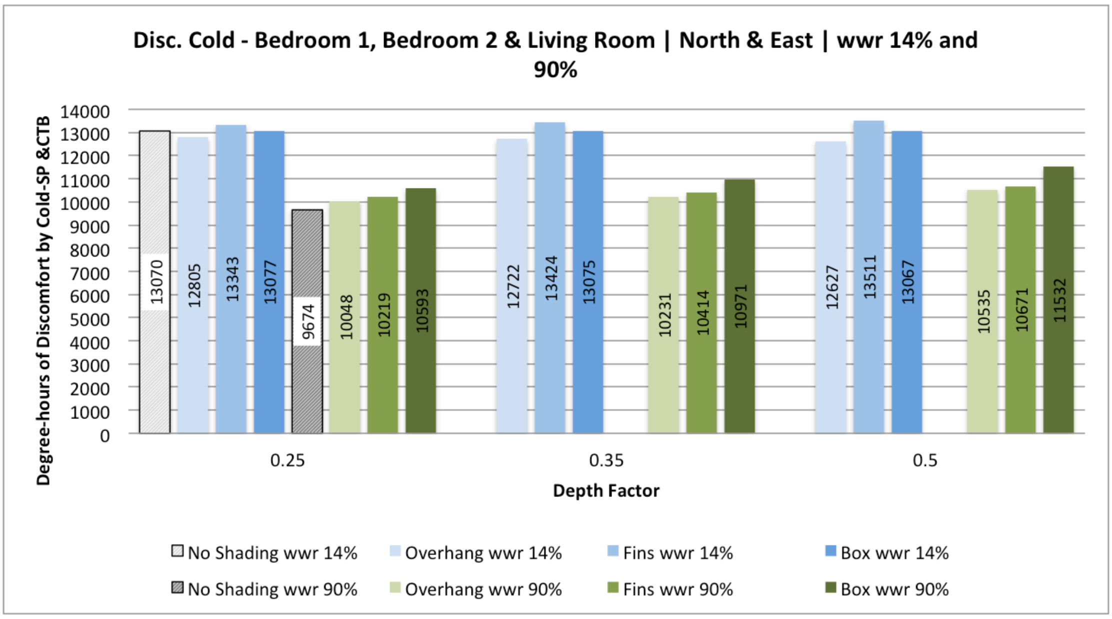

Figure 36 - Comparison of the Impact of Shading Devices with windows set with a WWR of 14% and 90% - All long-stay rooms

5 Conclusions

This research has created meta-models to aid in the assessment of the thermal performance of low-cost houses in Brazil while in the early stages of design. For each location selected in this study (Curitiba, PR, São Paulo, SP and Manaus, AM) a meta-model was created to predict the discomfort by heat and/or by cold given the selected parameters deemed most influential in thermal comfort.

A base model was developed to be representative of Brazilian LCH, with the key parameters identified and minimum and maximum values established for each of them, set as the range. Benchmark tests were conducted to assess which parameters could be simplified when running the simulations in EnergyPlus without compromising the outputs' accuracy. The following step in the procedure was the Monte Carlo simulation, which randomly assigned values to each key parameter and created diverse combinations to run the simulations in the software. With the simulations' results, the regression analysis was performed, as well as the validation for the meta-models created. The meta-models' accuracy was given by the R^2 values, which were all above 0.95, except for the meta-models for São Paulo and Curitiba for discomfort by heat. Another objective of this work was to use the meta-model to evaluate the impact of shading devices in thermal comfort for LCH. Standard values for a unit were used to run the tests, and in regards to shading devices, the main conclusions are that in Manaus, the warmer climate and where there is only discomfort by heat, the use of shading devices on windows for all orientations, presents a clear impact in the discomfort of almost 50%, significantly improving the thermal comfort in the unit. From this, it is possible to conclude that given the appropriate dimensions of the devices and their combinations, the use of shading devices in this location is highly recommended and the meta-model predicts as expected.

As for the cold and mild locations in the study, Curitiba and São Paulo, respectively, the meta-models for heat presented some unexpected predictions for Curitiba and consistent predictions for São Paulo. The meta-model for heat for São Paulo presented the expected behavior, indicating that the devices cause an impact in the unit's thermal comfort, although the values predicted were very low, indicating that the meta-model might not be sensitive to such parameters. The meta-model for heat for Curitiba predicted very small changes on the discomfort by heat when using overhangs. However, it didn't show any impact in some situations when the shading devices of any configuration were applied, either due to the large amount of zeroes in the data set used to create it or because the meta-model is not sensitive to such parameters. This leads to the conclusion that this specific model needs further investigation to identify the lack of change in some results, and in such cases a sensitivity analysis is proposed in the item *Suggestions for Future Work*.

The meta-models' predictions for discomfort by cold for these two locations differed from the expected behavior, presenting lower values of discomfort by cold when some configurations of shading devices were added to the windows. In other cases, when the WWR was varied, for example, slightly more consistent results were presented. However, all values varied very little from the established baseline value, which can indicate that there is no significant impact in the unit's discomfort by cold when shading devices are used. It is possible to conclude that for the meta-models predicting the discomfort by cold, a sensitivity analysis is also required to assess how sensitive the meta-model is to the parameters regarding the shading devices.

5.1 Suggestions for Future Work

For further work based on this research, the first point is the overall improvement of the base-model's modeling to create the meta-model. It is suggested a review of the Ground Temperatures, as well as of the Set-point Temperatures for ventilation, the latter being set too high. One of the options to mitigate this problem is to validate the data in question with real measured data. It is important to address such limitations in the meta-model in order to improve its accuracy in portraying real life effects. Even though the type of building is LCH and thus very simple, it still presents some difficulties during the modeling process that consequently lead to limitations in the meta-model.

Improvements can also be made to generalize the meta-model. This research was based on a fixed geometry, with windows fixed on the center of their respective walls, and with fixed internal partitions and only one option for a roof. In an effort to improve this work and make it more viable to professionals, it is important to address such points. It is extremely significant to have a flexible, or multiple, geometries, so the meta-model can better depict reality and provide more design options to professionals. For the same reason, improvements to the window location, internal partitions and roof should be considered.

Specifically regarding the focus of this research, some enhancements can be made to the meta-model concerning the shading devices. It is suggested the inclusion of a variation to the way the windows increase their size; instead of all coordinates varying in an offset manner, the coordinates could vary in different proportions, allowing different window heights (A and B), which would allow different depths for the shading devices for the same

WWR, since the shading device is a function of the window's height (Figure 37).

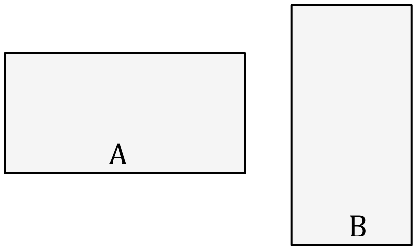

Figure 37 - Suggested variation of window height

In regards to the results, it is important to highlight that the meta-models calculate the discomfort by heat and/or by cold based on the Adaptive Model from ASHRAE-55 (ASHRAE, 2013), which does not establish limits for humidity in its equation, only for temperature. Given the influence that relative humidity has in thermal sensation, and therefore, in thermal comfort, one can infer that the meta-models could be more accurate if they were to include such element, or limits to it, when predicting thermal comfort.

Another interesting point to be further investigated is the incongruent values predicted by the meta-models for discomfort by cold for São Paulo and Curitiba. A first step in addressing this issue would be to analyze the original idf files within the 10,000 that were generated by the Monte Carlo simulation, to search cases that are very close or match the ones used for the tests in Results and verify the total annual heat gain to see how much difference there is from the tested examples. If the results are similar, then the meta-models are not sensitive to such parameters. Another point to be observed is that the heat gain occurs only during the day, and yet the schedule in the meta-model is set to measure all 24 hours, which could also influence in the results. In relation to the parameters' sensitivity, one last step is suggested to improve the meta-models' prediction of the impact of shading devices on LCH, which is a sensitivity analysis to verify if the meta-models for

São Paulo and Curitiba are, in fact, sensitive or not to shading device parameters.

6 References

ABNT. *ASSOCIAÇÃO BRASILEIRA DE NORMAS TÉCNICAS. NBR 15220: Desempenho Térmico de edificações*. Rio de Janeiro: [s.n.], 2005.

ABNT. *ASSOCIAÇÃO BRASILEIRA DE NORMAS TÉCNICAS. NBR 15575: Edificações habitacionais – Desempenho*. Rio de Janeiro: [s.n.], 2013.

AL GHARABLY, M.; DECAROLIS, J. F.; RANJITHAN, S. R. An enhanced linear regression-based building energy model (LRBEM+) for early design. *Journal of Building Performance Simulation*, n. NREL 2014, p. 1–19, 2015. Disponível em: <http://www.tandfonline.com/doi/abs/10.1080/19401493.2015.1004108>.

ALI AHMED, A. A. E.-M. M. Using simulation for studying the influence of vertical shading devices on the thermal performance of residential buildings (Case study: New Assiut City). *Ain Shams Engineering Journal*, v. 3, n. 2, p. 163–174, jun. 2012. Disponível em: <http://www.sciencedirect.com/science/article/pii/S2090447912000123>. Acesso em: 25 set. 2015.

AMORE, C. S.; SHIMBO, L. Z.; RUFINO, M. B. *Minha CAsa...e a Cidade? Avaliação do programa Minha Casa Minha Vida em seis estados brasileiros*. [S.l.]: Letra Capital, 2015.

ASADI, S.; AMIRI, S. S.; MOTTAHEDI, M. On the development of multi-linear regression analysis to assess energy consumption in the early stages of building design. *Energy and Buildings*, v. 85, p. 246–255, 2014. Disponível em: <http://dx.doi.org/10.1016/j.enbuild.2014.07.096>.

ASHRAE. AMERICAN SOCIETY OF HEATING, REFRIGERATING AND AIR-CONDITIONING ENGINEERS. *ASHRAE Handbook of Fundamentals*, 2009.

ASHRAE-140. AMERICAN SOCIETY OF HEATING, REFRIGERATING AND AIR-CONDITIONING ENGINEERS. *ANSI/ASHRAE Standard 140: Standard method of test for the evaluation of building energy analysis computer programs*, 2004.

ASHRAE-55. *American Society of Heating, Refrigerating and Air-Conditioning Engineers. Ansi/ASHRAE Standard 55: Thermal Environmental Conditions for Human Occupancy*. Atlanta: [s.n.], 2013.

ATEM, C. G. *Apropriação e eficiência de dispositivos de proteção solar utilizados na arquitetura moderna: o caso de Londrina*. 2003. Universidade de São Paulo, 2003.

BELLIA, L.; DE FALCO, F.; MINICHIELLO, F. Effects of solar shading devices on energy requirements of standalone office buildings for Italian climates. *Applied Thermal Engineering*, v. 54, n. 1, p. 190–201, maio 2013. Disponível em: <http://linkinghub.elsevier.com/retrieve/pii/S1359431113000835>. Acesso em: 21 fev. 2014.

BRAHME, R. *et al.* COMPLEX BUILDING PERFORMANCE ANALYSIS IN EARLY STAGES OF DESIGN : A solution based on differential modeling , homology-based mapping , and generative design agents School of Architecture , Carnegie Mellon University , Pittsburgh , PA 15213 , USA School of. v. 2, n. Mahdavi 1999, p. 661–668, 2001.

CARLOS, J. S.; NEPOMUCENO, M. C. S. A simple methodology to predict heating load at an early design stage of dwellings. *Energy and Buildings*, v. 55, p. 198–207, dez. 2012. Disponível em: <http://linkinghub.elsevier.com/retrieve/pii/S0378778812004938>. Acesso em: 18 fev. 2014.

CATALINA, T.; IORDACHE, V.; CARACALEANU, B. Multiple regression model for fast prediction of the heating energy demand. *Energy and Buildings*, v. 57, p. 302–312, 2013. Disponível em: <http://dx.doi.org/10.1016/j.enbuild.2012.11.010>.

CATALINA, T.; VIRGONE, J.; BLANCO, E. Development and validation of regression models to predict monthly heating demand for residential buildings. *Energy and Buildings*, v. 40, n. 10, p. 1825–1832, 2008.

CHUNG, W.; HUI, Y. V.; LAM, Y. M. Benchmarking the energy efficiency of commercial buildings. *Applied Energy*, v. 83, n. 1, p. 1–14, jan. 2006. Disponível em: <http://www.sciencedirect.com/science/article/pii/S0306261904002028>. Acesso em: 15 set. 2015.

CHVATAL, K. M. S.; MARQUES, T. Avaliação de diferentes alternativas de modelagem de habitação de interesse social no programa de simulação de desempenho térmico EnergyPlus. *Revista tecnológia*, 2015. Disponível em: <http://periodicos.uem.br/ojs/index.php/RevTecnol>.

CHVATAL, K. M. S.; RORIZ, V. Avaliação do desempenho térmico de habitações segundo a ABNT NBR 15575. Avaliação de Desempenho de Tecnologias Construtivas. *ANTAC*, n. 1ed, p. 41–54, 2015.

CTHAB. Inovação e Responsabilidade. *IV Congresso Brasileiro e III Congresso Ibero-Americano Habitação Social: Ciência e Tecnologia*, 2012. Disponível em: <http://www.cthab.ufsc.br/downloads/Programa.pdf>.

DA SILVA, P. C.; LEAL, V.; ANDERSEN, M. Influence of shading control patterns on the energy assessment of office spaces. *Energy and Buildings*, v. 50, p. 35–48, jul. 2012. Disponível em: <http://www.sciencedirect.com/science/article/pii/S0378778812001673>. Acesso em: 16 nov. 2015.

DATTA, G. Effect of fixed horizontal louver shading devices on thermal perfomance of building by TRNSYS simulation. *Renewable Energy*, v. 23, n. 3-4, p. 497–507, jul. 2001. Disponível em: <http://linkinghub.elsevier.com/retrieve/pii/S0960148100001312>.

EERE - DEPARTMENT OF ENERGY EFFICIENCY AND RENEWABLE ENERGY. 2014a. EnergyPlus. V ersion 8.1.0.009 US: Department of Energy Efficiency and Renewable Energy, Office of Building Technologies. Available in: <http://apps1.eere.energy.gov/buildings/Energy Plus/>. Accessed: 22 March 2014

EISENHOWER, B. *et al.* A methodology for meta-model based optimization in building energy models. *Energy and Buildings*, v. 47, p. 292–301, abr. 2012. Disponível em: <http://linkinghub.elsevier.com/retrieve/pii/S0378778811005962>. Acesso em: 8 nov. 2013.

FARIA, F. M.; UMETSU, C. M.; FROTA, A. B. O CONFORTO TÉRMICO NAS HABITAÇÕES POPULARES DA CIDADE DE SÃO PAULO. *Encontro Nacional de Conforto no Ambiente Construído*, n. 1, p. 98–104, 2003.

FAVRETTO, A. P. O.; ROSSI, M. M.; *et al.* ASSESSING THE IMPACT OF ZONING ON THE THERMAL COMFORT ANALYSIS OF A NATURALLY VENTILATED HOUSE DURING EARLY DESIGN Institute of Architecture and Urbanism , University of São Paulo , São Carlos , SP , Brazil School of Architecture , North Carolina State Un. *14th International Conference of the International Building Performance Association - no prelo*, 2015.

FAVRETTO, A. P. O.; *et al.* Material and Construction modeling simplification approach for EnergyPlus to promote building performance simulation during the early design stage. *em elaboração*, 2015.

FROTA, A.; SCHIFFER, S. *Manual de Conforto Térmico*. São Paulo: Studio Nobel, 2001.

GARITSELOV, O.; MOHANTY, S. P.; KOUGIANOS, E. A Comparative Study of Metamodels for Fast and Accurate Simulation of Nano-CMOS Circuits. *IEEE Transactions on Semiconductor Manufacturing*, v. 25, n. 1, p. 26–36, 2012.

GIVONI, B. *Man, Climate and Architecture*. 2nd. ed. London: Applied

Science, 1976.

GOLDEMBERG, J.; AGOPYAN, V.; JOHN, V. *O Desafio da Sustentabilidade na Construção Civil*. São Paulo: Edgard Blucher Ltda., 2011.

HAMMAD, F.; ABU-HIJLEH, B. The energy savings potential of using dynamic external louvers in an office building. *Energy and Buildings*, v. 42, n. 10, p. 1888–1895, out. 2010. Disponível em: <http://www.sciencedirect.com/science/article/pii/S0378778810001866>. Acesso em: 16 nov. 2015.

HELTON, J. C. Uncertainty and sensitivity analysis techniques for use in performance assessment for radioactive waste disposal. *Reliability Engineering & System Safety*, v. 42, n. 2-3, p. 327–367, jan. 1993. Disponível em: <http://www.sciencedirect.com/science/article/pii/095183209390097I>. Acesso em: 25 set. 2015.

HONG, T.; CHOU, S. .; BONG, T. . Building simulation: an overview of developments and information sources. *Building and Environment*, v. 35, n. 4, p. 347–361, maio 2000. Disponível em: <http://linkinghub.elsevier.com/retrieve/pii/S0360132399000232>.

HOPFE, C.; HENSEN, J.; PLOKKER, W. UNCERTAINTY AND SENSITIVITY ANALYSIS FOR DETAILED DESIGN SUPPORT. *Proceedings of the 10th IBPSA Building Simulation Conference*, p. 1799–1804, 2007.

HYGH, J. S. *Implementing Energy Simulation as a Design tool in Conceptual Building Design with Regression Analysis*. 2011. North Carolina State University, 2011.

HYGH, J. S. *et al.* Multivariate regression as an energy assessment tool in early building design. *Building and Environment*, v. 57, p. 165–175, nov. 2012a. Disponível em: <http://linkinghub.elsevier.com/retrieve/pii/S0360132312001400>. Acesso em: 17 jun. 2013.

HYGH, J. S. *et al.* Multivariate regression as an energy assessment tool in early building design. *Building and Environment*, v. 57, p. 165–175, nov. 2012b. Disponível em: <http://linkinghub.elsevier.com/retrieve/pii/S0360132312001400>.

IBGE. INSTITUTO BRASILEIRO DE GEOGRAFIA E ESTATÍSTICA. PNAD – Pesquisa Nacional por Amostra de Domicílios. 2009.

INMETRO. *INSTITUTO NACIONAL DE METROLOGIA, NORMALIZAÇÃO E*

QUALIDADE INDUSTRIAL. RTQ-R - Regulamento técnico da qualidade para o nível de eficiência energética em edificações residenciais. Rio de Janeiro: [s.n.], 2012.

LABEEE. *LabEEE-Apostila do Curso Básico do Programa EnergyPlus*. . [S.l: s.n.]. , 2009

LAM, J. C. *et al.* Multiple regression models for energy use in air-conditioned office buildings in different climates. *Energy Conversion and Management*, v. 51, n. 12, p. 2692–2697, dez. 2010. Disponível em: <http://linkinghub.elsevier.com/retrieve/pii/S0196890410002141>. Acesso em: 8 nov. 2013.

LAMBERTS, R.; DUTRA, L.; PEREIRA, F. O. R. Eficiência Energética na Arquitetura. p. 382, 2014.

LECHNER, N. *Heating, cooling, lighting*. New Jersey: John Wiley & Sons, 2009.

LITTLEFAIR, P.; ORTIZ, J.; BHAUMIK, C. D. A simulation of solar shading control on UK office energy use. *Building Research & Information*, 2010.

MARQUES, T. *Influência das propriedades térmicas da envolvente opaca no desempenho de habitações de interesse social em São Carlos , SP*. 2013. Universidade de São Paulo, 2013.

MARQUES, T.; CHVATAL, K. DESEMPENHO TÉRMICO NO PROJETO DE EDIFICAÇÕES. *VII Encontro Tecnológico da Engenharia Civil e Arquitetura*, p. 1–11, 2011.

MATHWORKS. Matlab, R2015b.

MENDES, N. Uso de instrumentos computacionais para análise do desempenho térmico e energético de edificações no Brasil. p. 47–68, 2005.

MORBITZER, C. *et al.* INTEGRATION OF BUILDING SIMULATION INTO THE DESIGN PROCESS OF AN ARCHITECTURE. p. 697–704, 2001.

OLGYAY, V. *Arquitectura y Clima*. Barcelona: Gustavo Gili, 1998.

OURGHI, R.; AL-ANZI, A.; KRARTI, M. A simplified analysis method to predict the impact of shape on annual energy use for office buildings. *Energy Conversion and Management*, v. 48, n. 1, p. 300–305, 2007.

PETERSEN, S.; SVENDSEN, S. Method and simulation program informed decisions in the early stages of building design. *Energy and Buildings*, v. 42, n. 7, p. 1113–1119, jul. 2010. Disponível em: <http://www.sciencedirect.com/science/article/pii/S0378778810000332>.

Acesso em: 23 fev. 2015.

PMCMV. *Brasil, Governo Federal–Medida Provisória n˚ 459*. . [S.l: s.n.]. , 2009

RORIZ, M. Arquivos Climáticos de Municípios Brasileiros. *ANTAC – Associação Nacional de Tecnologia do Ambiente Construído. Grupo de Trabalho sobre Conforto e Eficiência Energética de Edificações*, 2012.

ROSSI, M. M. *et al.* Impact of using surface-average instead of local wind pressure coefficints in thermal comfort analysis of a naturally ventilated Brazilian low-cost house. *em elaboração*, 2015.

SALTELLI, A. *Mathematical and Statistical Methods: Sensitivity Analysis*. England: John Wiley & Sons, 2001.

SCALCO, V. A. *et al.* Innovations in the Brazilian regulations for energy efficiency of residential buildings. *Architectural Science Review*, v. 55, n. 1, p. 71–81, 2012. Disponível em: <http://www.tandfonline.com/doi/abs/10.1080/00038628.2011.641731>.

SEBER, G.; LEE, A. *Linear Regression Analysis*. New Jersey: John Wiley & Sons, 2003.

STRUCK, C.; HENSEN, J. ON SUPPORTING DESIGN DECISIONS IN CONCEPTUAL DESIGN ADDRESSING SPECIFICATION UNCERTAINTIES USING PERFORMANCE SIMULATION. *Proceedings of the 10th IBPSA Building Simulation Conference*, p. 1434–1439, 2007.

STRUCK, C.; HENSEN, J.; KOTEK, P. On the application of uncertainty and sensitivity analysis with abstract building performance simulation tools. *Journal of Building Physics*, v. 33, p. 5–27, 2009.

TIAN, H. F.; SUN, D. M.; ZHOU, H. Z. The energy saving performance of movable sola shading for building energy saving by 65%. *Wall Mater Innovation Energy Saving Buildings*, 2009.

Tokyo Polythecnic University.

VAN MOESEKE, G.; BRUYÈRE, I.; DE HERDE, A. Impact of control rules on the efficiency of shading devices and free cooling for office buildings. *Building and Environment*, v. 42, n. 2, p. 784–793, fev. 2007. Disponível em: <http://www.sciencedirect.com/science/article/pii/S0360132305003975>. Acesso em: 16 nov. 2015.

VERSAGE, R. *Equações prescritivas para o regulamento de etiquetagem de eficiência energética de edificações residenciais*. . [S.l: s.n.], 2011.

WANG, L.; WONG, N. H. Coupled simulations for naturally ventilated rooms between building simulation (BS) and computational fluid dynamics (CFD) for better prediction of indoor thermal environment. *Building and Environment*, v. 44, n. 1, p. 95–112, jan. 2009. Disponível em: <http://linkinghub.elsevier.com/retrieve/pii/S0360132308000231>. Acesso em: 3 jun. 2013.

WEISBERG, S. *Applied Linear Regression*. 3rd. ed. New Jersey: John Wiley & Sons, 2005.

WESTPHAL, F. S. Fernando simon westphal análise de incertezas e de sensibilidade aplicadas à simulação de desempenho energético de edificações comerciais. 2007.

WILLIAMS, E. D. *Sustainable Design: Ecology, Architecture and Planning*. New Jersey: John Wiley & Sons, 2007.

WU, S.; SUN, J.-Q. Two-stage regression model of thermal comfort in office buildings. *Building and Environment*, v. 57, p. 88–96, 2012. Disponível em: <http://dx.doi.org/10.1016/j.buildenv.2012.04.014>.

YANNAS, S.; CORBELLA, O. *Em busca de uma arquitetura sustentável para os trópicos: conforto ambiental*. Rio de Janeiro: Revan, 2003.

YAO, J. An investigation into the impact of movable solar shades on energy, indoor thermal and visual comfort improvements. *Building and Environment*, v. 71, p. 24–32, jan. 2014. Disponível em: <http://linkinghub.elsevier.com/retrieve/pii/S0360132313002758>. Acesso em: 20 fev. 2014.

ZHAI, Z. J.; CHEN, Q. Y. Performance of coupled building energy and CFD simulations. *Energy and Buildings*, v. 37, n. 4, p. 333–344, abr. 2005. Disponível em: <http://linkinghub.elsevier.com/retrieve/pii/S0378778804002130>. Acesso em: 21 fev. 2014.

ZHANG, H. X. *et al.* Influence of retractable external shading of buildings on indoor thermal environment in Nanjing. *Jiangsu Construction*, 2010.

7 Appendix

7.1 Appendix A - Curitiba/PR Meta-model coefficients – Degree-hours of Discomfort by Cold

Table 30 - Standard approach with regression 'floor'

Coefficient	Parameter Identification	value	p-value
INTERCEPT	INTERCEPT	18385,64	3,6E-116
x4	External Walls' Solar Absorptance	-2756,91	1,13E-28
x5	Bedroom_1 Left Fin size	494,6549	5,78E-06
x6	Bedroom_2 Left Fin size	3175,784	1,3E-09
x7	Living room Left Fin size	3386,239	3,22E-07
x8	Bedroom_1 Right Fin size	-327,328	0,067332
x9	Bedroom_2 Right Fin size	-3608,49	2,48E-07
x10	Living room Right Fin size	226,1234	0,293776
x11	Bedroom_1 Overhang size	3096,869	1,68E-05
x12	Bedroom_2 Overhang size	2787,848	4,28E-09
x13	Living room Overhang size	-2377,56	1,85E-07
x14	Roof's Solar Absorptance	-4334,19	1,33E-44
x15	North Axis/ Orientation in the terrain	-20,7409	8,66E-76
x16	Bedroom_1 Window to Wall Ratio (WWR)	-961,52	0,001007
x17	Bedroom_2 Window to Wall Ratio (WWR)	-7686,31	2,33E-17
x18	Living room Window to Wall Ratio (WWR)	-1599,12	3,21E-09
x19	External Walls' U-value	2666,385	2,5E-258
x21	Roof's U-Value	2865,937	6,31E-30
x22	External Walls' Heat Capacity	-6,96385	5,64E-14
x23	Internal Walls' Heat Capacity	-11,8464	2,61E-15
x24	Roof's Heat Capacity	-6,50643	1,52E-10
x39	inverse of North Axis/ Orientation in the terrain	-1301,22	0,005534
x41	inverse of Bedroom_2 Window to Wall Ratio (WWR)	-1007,71	1,96E-20
x47	inverse of Internal Walls' Heat Capacity	-443728	9,36E-29
x48	inverse of Roof's Heat Capacity	-230452	1,49E-35
x4:x14	External Walls' Solar Absorptance x Roof's Solar Absorptance	723,4714	1,54E-08
x4:x16	External Walls' Solar Absorptance x Bedroom_1 Window to Wall Ratio (WWR)	757,6435	0,000148
x4:x17	External Walls' Solar Absorptance x Bedroom_2 Window to Wall Ratio (WWR)	707,6947	0,000482
x4:x18	External Walls' Solar Absorptance x Living room Window to Wall Ratio (WWR)	690,4265	0,000597
x4:x19	External Walls' Solar Absorptance x External Walls' U-value	-1583,65	0

x4:x22	External Walls' Solar Absorptance x External Walls' Heat Capacity	-1,39113	8,01E-07
x5:x39	Bedroom_1 Left Fin size x inverse of North Axis/ Orientation in the terrain	-1563,43	0,001514
x5:x47	Bedroom_1 Left Fin size x inverse of Internal Walls' Heat Capacity	-31719,7	0,014659
x5:x48	Bedroom_1 Left Fin size x inverse of Roof's Heat Capacity	-16085,7	0,029741
x6:x21	Bedroom_2 Left Fin size x Roof's U-Value	-303,979	0,035609
x6:x22	Bedroom_2 Left Fin size x External Walls' Heat Capacity	-0,99393	0,047843
x6:x23	Bedroom_2 Left Fin size x Internal Walls' Heat Capacity	-2,11604	0,021566
x6:x24	Bedroom_2 Left Fin size x Roof's Heat Capacity	-1,34206	0,007808
x6:x41	Bedroom_2 Left Fin size x inverse of Bedroom_2 Window to Wall Ratio (WWR)	-144,855	0,000942
x6:x47	Bedroom_2 Left Fin size x inverse of Internal Walls' Heat Capacity	-80661,8	0,000824
x6:x48	Bedroom_2 Left Fin size x inverse of Roof's Heat Capacity	-35746,7	0,000284
x7:x15	Living room Left Fin size x North Axis/ Orientation in the terrain	-1,28118	0,02376
x7:x17	Living room Left Fin size x Bedroom_2 Window to Wall Ratio (WWR)	-1550,29	0,037601
x7:x23	Living room Left Fin size x Internal Walls' Heat Capacity	-2,85755	0,001871
x7:x41	Living room Left Fin size x inverse of Bedroom_2 Window to Wall Ratio (WWR)	-275,727	0,001711
x7:x47	Living room Left Fin size x inverse of Internal Walls' Heat Capacity	-113778	2,43E-06
x7:x48	Living room Left Fin size x inverse of Roof's Heat Capacity	-38033,9	6,44E-07
x8:x15	Bedroom_1 Right Fin size x North Axis/ Orientation in the terrain	1,251773	0,031419
x8:x39	Bedroom_1 Right Fin size x inverse of North Axis/ Orientation in the terrain	1187,851	0,002657
x8:x41	Bedroom_1 Right Fin size x inverse of Bedroom_2 Window to Wall Ratio (WWR)	94,34965	0,033376
x8:x48	Bedroom_1 Right Fin size x inverse of Roof's Heat Capacity	13754,79	0,064254
x9:x15	Bedroom_2 Right Fin size x North Axis/ Orientation in the terrain	1,673533	0,003022
x9:x17	Bedroom_2 Right Fin size x Bedroom_2 Window to Wall Ratio (WWR)	2434,638	0,001283
x9:x23	Bedroom_2 Right Fin size x Internal Walls' Heat Capacity	1,85362	0,040696
x9:x24	Bedroom_2 Right Fin size x Roof's Heat Capacity	0,969698	0,048982
x9:x41	Bedroom_2 Right Fin size x inverse of Bedroom_2 Window to Wall Ratio (WWR)	350,1333	0,000117
x9:x47	Bedroom_2 Right Fin size x inverse of Internal Walls' Heat Capacity	83029,7	0,000513
x9:x48	Bedroom_2 Right Fin size x inverse of Roof's Heat Capacity	51610,01	4,08E-08
x10:x14	Living room Right Fin size x Roof's Solar Absorptance	-513,735	0,025839

x10:x18	Living room Right Fin size x Living room Window to Wall Ratio (WWR)	800,5204	0,028759
x10:x48	Living room Right Fin size x inverse of Roof's Heat Capacity	-16831,5	0,02117
x11:x12	Bedroom_1 Overhang size x Bedroom_2 Overhang size	795,0845	0,05541
x11:x14	Bedroom_1 Overhang size x Roof's Solar Absorptance	-504,148	0,028374
x11:x15	Bedroom_1 Overhang size x North Axis/ Orientation in the terrain	1,342506	0,017342
x11:x16	Bedroom_1 Overhang size x Bedroom_1 Window to Wall Ratio (WWR)	997,7483	0,005321
x11:x17	Bedroom_1 Overhang size x Bedroom_2 Window to Wall Ratio (WWR)	-1696,94	0,024549
x11:x19	Bedroom_1 Overhang size x External Walls' U-value	-284,195	5,88E-05
x11:x21	Bedroom_1 Overhang size x Roof's U-Value	-339,883	0,017539
x11:x23	Bedroom_1 Overhang size x Internal Walls' Heat Capacity	-2,1717	0,015469
x11:x41	Bedroom_1 Overhang size x inverse of Bedroom_2 Window to Wall Ratio (WWR)	-263,338	0,003379
x11:x47	Bedroom_1 Overhang size x inverse of Internal Walls' Heat Capacity	-88473,9	0,00013
x11:x48	Bedroom_1 Overhang size x inverse of Roof's Heat Capacity	-24077,2	0,000588
x12:x14	External Walls' Heat Capacity x External Walls' Heat Capacity	-565,314	0,014674
x12:x15	Roof's U-Value x Roof's U-Value	-1,17053	0,042024
x12:x17	External Walls' U-value x External Walls' U-value	2037,285	1,94E-08
x12:x19	Roof's Heat Capacity x Roof's Heat Capacity	-222,394	0,001945
x12:x23	External Walls' Solar Absorptance x External Walls' Solar Absorptance	-3,56782	0,000113
x12:x24	Internal Walls' Heat Capacity x Internal Walls' Heat Capacity	-1,41959	0,004281
x12:x39	Roof's Solar Absorptance x Roof's Solar Absorptance	-1458,48	0,002236
x12:x47	inverse of Roof's Heat Capacity x inverse of Roof's Heat Capacity	-151988	3,36E-10
x12:x48	Bedroom_2 Overhang size x inverse of Roof's Heat Capacity	-71942,7	4,89E-14
x13:x18	Living room Overhang size x Living room Window to Wall Ratio (WWR)	1118,148	0,002388
x13:x23	Living room Overhang size x Internal Walls' Heat Capacity	2,554241	0,006229
x13:x24	Living room Overhang size x Roof's Heat Capacity	1,539743	0,002327
x13:x41	Living room Overhang size x inverse of Bedroom_2 Window to Wall Ratio (WWR)	131,2863	0,002459
x13:x47	Living room Overhang size x inverse of Internal Walls' Heat Capacity	100816,1	4,2E-05
x13:x48	Living room Overhang size x inverse of Roof's Heat Capacity	68930,95	4,81E-13
x14:x15	Roof's Solar Absorptance x North Axis/ Orientation in the terrain	1,062143	0,000999

x14:x18	Roof's Solar Absorptance x Living room Window to Wall Ratio (WWR)	471,3394	0,01923
x14:x19	Roof's Solar Absorptance x External Walls' U-value	498,219	2,26E-39
x14:x21	Roof's Solar Absorptance x Roof's U-Value	-3651,43	0
x14:x23	Roof's Solar Absorptance x Internal Walls' Heat Capacity	2,057037	5,73E-05
x14:x39	Roof's Solar Absorptance x inverse of North Axis/ Orientation in the terrain	1107,284	6E-06
x14:x47	Roof's Solar Absorptance x inverse of Internal Walls' Heat Capacity	87494,02	2,22E-11
x14:x48	Roof's Solar Absorptance x inverse of Roof's Heat Capacity	59679,53	2,35E-49
x15:x16	North Axis/ Orientation in the terrain x Bedroom_1 Window to Wall Ratio (WWR)	-4,17904	3,78E-17
x15:x17	North Axis/ Orientation in the terrain x Bedroom_2 Window to Wall Ratio (WWR)	2,284073	0,029372
x15:x19	North Axis/ Orientation in the terrain x External Walls' U-value	0,266389	0,009415
x15:x21	North Axis/ Orientation in the terrain x Roof's U-Value	0,474984	0,019096
x15:x23	North Axis/ Orientation in the terrain x Internal Walls' Heat Capacity	0,00519	3,53E-05
x15:x24	North Axis/ Orientation in the terrain x Roof's Heat Capacity	0,002092	0,002756
x15:x41	North Axis/ Orientation in the terrain x inverse of Bedroom_2 Window to Wall Ratio (WWR)	0,467003	0,000214
x15:x47	North Axis/ Orientation in the terrain x inverse of Internal Walls' Heat Capacity	190,3256	6,42E-09
x15:x48	North Axis/ Orientation in the terrain x inverse of Roof's Heat Capacity	100,1104	2,34E-13
x16:x17	Bedroom_1 Window to Wall Ratio (WWR) x Bedroom_2 Window to Wall Ratio (WWR)	1048,579	0,000712
x16:x18	Bedroom_1 Window to Wall Ratio (WWR) x Living room Window to Wall Ratio (WWR)	647,0496	0,042999
x16:x19	Bedroom_1 Window to Wall Ratio (WWR) x External Walls' U-value	-130,306	0,0379
x16:x22	Bedroom_1 Window to Wall Ratio (WWR) x External Walls' Heat Capacity	-0,93141	0,035377
x17:x21	Bedroom_2 Window to Wall Ratio (WWR) x Roof's U-Value	725,1015	0,006219
x17:x22	Bedroom_2 Window to Wall Ratio (WWR) x External Walls' Heat Capacity	2,104073	0,021782
x17:x23	Bedroom_2 Window to Wall Ratio (WWR) x Internal Walls' Heat Capacity	6,28843	0,00013
x17:x24	Bedroom_2 Window to Wall Ratio (WWR) x Roof's Heat Capacity	2,351353	0,009602
x17:x47	Bedroom_2 Window to Wall Ratio (WWR) x inverse of Internal Walls' Heat Capacity	233910,8	1,08E-08
x17:x48	Bedroom_2 Window to Wall Ratio (WWR) x inverse of Roof's Heat Capacity	127327,5	3,93E-12
x18:x39	Living room Window to Wall Ratio (WWR) x inverse of North Axis/ Orientation in the terrain	1813,6	0,000292
x18:x41	Living room Window to Wall Ratio (WWR) x inverse of Bedroom_2 Window to Wall Ratio (WWR)	-194,491	3,26E-07

x19:x21	External Walls' U-value x Roof's U-Value	-218,549	6,88E-20
x19:x22	External Walls' U-value x External Walls' Heat Capacity	-0,69686	1,66E-16
x19:x24	External Walls' U-value x Roof's Heat Capacity	-0,16906	0,040065
x19:x39	External Walls' U-value x inverse of North Axis/ Orientation in the terrain	-668,837	0,000175
x19:x41	External Walls' U-value x inverse of Bedroom_2 Window to Wall Ratio (WWR)	27,2388	9,63E-05
x19:x47	External Walls' U-value x inverse of Internal Walls' Heat Capacity	13754,08	1,04E-09
x19:x48	External Walls' U-value x inverse of Roof's Heat Capacity	5654,901	3,6E-05
x21:x23	Roof's U-Value x Internal Walls' Heat Capacity	0,812822	0,00934
x21:x24	Roof's U-Value x Roof's Heat Capacity	-0,42091	0,01508
x21:x39	Roof's U-Value x inverse of North Axis/ Orientation in the terrain	-280,024	0,018208
x21:x41	Roof's U-Value x inverse of Bedroom_2 Window to Wall Ratio (WWR)	121,9251	0,000127
x21:x47	Roof's U-Value x inverse of Internal Walls' Heat Capacity	44061,9	4,34E-08
x21:x48	Roof's U-Value x inverse of Roof's Heat Capacity	22642,77	8,18E-13
x22:x23	External Walls' Heat Capacity x Internal Walls' Heat Capacity	0,003632	0,000994
x22:x24	External Walls' Heat Capacity x Roof's Heat Capacity	0,003173	2,25E-12
x22:x41	External Walls' Heat Capacity x inverse of Bedroom_2 Window to Wall Ratio (WWR)	0,419161	0,00011
x22:x47	External Walls' Heat Capacity x inverse of Internal Walls' Heat Capacity	72,54738	0,012133
x23:x24	Internal Walls' Heat Capacity x Roof's Heat Capacity	0,004758	1,26E-05
x23:x41	Internal Walls' Heat Capacity x inverse of Bedroom_2 Window to Wall Ratio (WWR)	1,223949	2,32E-10
x23:x48	Internal Walls' Heat Capacity x inverse of Roof's Heat Capacity	186,8037	1,32E-19
x24:x39	Roof's Heat Capacity x inverse of North Axis/ Orientation in the terrain	-0,8409	0,065167
x24:x41	Roof's Heat Capacity x inverse of Bedroom_2 Window to Wall Ratio (WWR)	0,404944	0,000146
x24:x47	Roof's Heat Capacity x inverse of Internal Walls' Heat Capacity	151,6058	9,22E-08
x41:x47	inverse of Bedroom_2 Window to Wall Ratio (WWR) x inverse of Internal Walls' Heat Capacity	46847,78	1,12E-22
x41:x48	inverse of Bedroom_2 Window to Wall Ratio (WWR) x inverse of Roof's Heat Capacity	21864,94	2,67E-24
x47:x48	inverse of Internal Walls' Heat Capacity x inverse of Roof's Heat Capacity	8761530	1,16E-59
x4^2	External Walls' Solar Absorptance x External Walls' Solar Absorptance	527,8405	0,000248
x6^2	Bedroom_2 Left Fin size x Bedroom_2 Left Fin size	-941,356	0,043109
x14^2	Roof's Solar Absorptance x Roof's Solar Absorptance	1404,531	9,52E-23
x15^2	North Axis/ Orientation in the terrain x North Axis/ Orientation in the terrain	0,036833	3,6E-304

x19^2	External Walls' U-value x External Walls' U-value	-109,712	1,4E-43
x22^2	External Walls' Heat Capacity x External Walls' Heat Capacity	0,005532	5,52E-16
x24^2	Roof's Heat Capacity x Roof's Heat Capacity	0,001443	0,037068
x39^2	inverse of North Axis/ Orientation in the terrain x inverse of North Axis/ Orientation in the terrain	148,4513	1,64E-14
x47^2	inverse of Internal Walls' Heat Capacity x inverse of Internal Walls' Heat Capacity	1778989	0,001615
x48^2	inverse of Roof's Heat Capacity x inverse of Roof's Heat Capacity	-483967	3,11E-05

7.2 Appendix B - Curitiba/PR Meta-model coefficients – Degree-hours of Discomfort by Heat

Table 31 – Standard approach with regression floor

Coefficient	Parameter Identification	value	p-value
INTERCEPT	INTERCEPT	56,21201	0,003227
x3	Living room Effective window ventilation area	90,89477	3,48E-08
x4	External Walls' Solar Absorptance	-58,35	5,75E-09
x13	Living room Overhang size	103,5655	9,66E-10
x14	Roof's Solar Absorptance	-157,764	1,57E-54
x18	Living room Window to Wall Ratio (WWR)	-5,06523	0,205875
x19	External Walls' U-value	-18,3262	2,11E-44
x21	Roof's U-Value	-59,9842	3,2E-07
x24	Roof's Heat Capacity	0,203004	6,31E-23
x45	inverse of Roof's U-Value	-9,31795	0,248669
x46	inverse of External Walls' Heat Capacity	-5744,54	1E-22
x47	inverse of Internal Walls' Heat Capacity	-3347,65	8,56E-09
x48	inverse of Roof's Heat Capacity	-1980,84	7,37E-07
x3:x21	Living room Effective window ventilation area x Roof's U-Value	-49,0604	5,48E-10
x3:x45	Living room Effective window ventilation area x inverse of Roof's U-Value	-30,8972	2,63E-05
x3:x46	Living room Effective window ventilation area x inverse of External Walls' Heat Capacity	-972,667	0,00025
x3:x47	Living room Effective window ventilation area x inverse of Internal Walls' Heat Capacity	-617,76	0,018928
x4:x14	External Walls' Solar Absorptance x Roof's Solar Absorptance	11,1276	2,1E-05
x4:x19	External Walls' Solar Absorptance x External Walls' U-value	13,62601	3,05E-65
x4:x21	External Walls' Solar Absorptance x Roof's U-Value	20,73743	3,07E-06
x4:x24	External Walls' Solar Absorptance x Roof's Heat Capacity	-0,02653	3,76E-10
x4:x45	External Walls' Solar Absorptance x inverse of	12,41491	0,002711

	Roof's U-Value		
x4:x46	External Walls' Solar Absorptance x inverse of External Walls' Heat Capacity	1323,415	6,63E-19
x4:x47	External Walls' Solar Absorptance x inverse of Internal Walls' Heat Capacity	397,254	0,009521
x13:x14	Living room Overhang size x Roof's Solar Absorptance	-15,1162	0,00146
x13:x21	Living room Overhang size x Roof's U-Value	-50,0336	4,91E-10
x13:x45	Living room Overhang size x inverse of Roof's U-Value	-30,3248	6,26E-05
x13:x46	Living room Overhang size x inverse of External Walls' Heat Capacity	-1100,82	2,66E-05
x13:x47	Living room Overhang size x inverse of Internal Walls' Heat Capacity	-1045,1	0,000123
x13:x48	Living room Overhang size x inverse of Roof's Heat Capacity	-375,549	0,00856
x14:x19	Roof's Solar Absorptance x External Walls' U-value	4,912302	1,62E-10
x14:x21	Roof's Solar Absorptance x Roof's U-Value	75,7089	2,74E-65
x14:x24	Roof's Solar Absorptance x Roof's Heat Capacity	-0,02123	0,000188
x14:x45	Roof's Solar Absorptance x inverse of Roof's U-Value	40,51501	1,66E-22
x14:x46	Roof's Solar Absorptance x inverse of External Walls' Heat Capacity	1773,623	6,39E-34
x14:x47	Roof's Solar Absorptance x inverse of Internal Walls' Heat Capacity	925,5288	5,65E-10
x14:x48	Roof's Solar Absorptance x inverse of Roof's Heat Capacity	1433,689	5,55E-39
x18:x19	Living room Window to Wall Ratio (WWR) x External Walls' U-value	3,131024	0,013169
x18:x21	Living room Window to Wall Ratio (WWR) x Roof's U-Value	6,445681	0,014365
x18:x24	Living room Window to Wall Ratio (WWR) x Roof's Heat Capacity	-0,03225	1,15E-06
x18:x46	Living room Window to Wall Ratio (WWR) x inverse of External Walls' Heat Capacity	896,7809	0,000131
x18:x47	Living room Window to Wall Ratio (WWR) x inverse of Internal Walls' Heat Capacity	682,4573	0,00453
x19:x21	External Walls' U-value x Roof's U-Value	1,579005	0,001159
x19:x24	External Walls' U-value x Roof's Heat Capacity	-0,01408	4,74E-17
x19:x46	External Walls' U-value x inverse of External Walls' Heat Capacity	845,1039	3,41E-80
x19:x47	External Walls' U-value x inverse of Internal Walls' Heat Capacity	309,437	1,17E-11
x19:x48	External Walls' U-value x inverse of Roof's Heat Capacity	62,09573	0,022655
x21:x24	Roof's U-Value x Roof's Heat Capacity	-0,07346	2,43E-14
x21:x46	Roof's U-Value x inverse of External Walls' Heat Capacity	2721,857	2,57E-28
x21:x47	Roof's U-Value x inverse of Internal Walls' Heat Capacity	1794,206	1,2E-12
x21:x48	Roof's U-Value x inverse of Roof's Heat Capacity	1372,534	2,08E-14
x24:x45	Roof's Heat Capacity x inverse of Roof's U-Value	-0,04596	2,72E-07

x24:x46	Roof's Heat Capacity x inverse of External Walls' Heat Capacity	-1,96853	1,33E-09
x24:x47	Roof's Heat Capacity x inverse of Internal Walls' Heat Capacity	-1,36258	2,27E-05
x45:x46	inverse of Roof's U-Value x inverse of External Walls' Heat Capacity	1323,99	2,01E-08
x45:x47	inverse of Roof's U-Value x inverse of Internal Walls' Heat Capacity	865,682	0,000234
x45:x48	inverse of Roof's U-Value x inverse of Roof's Heat Capacity	515,4849	0,002303
x46:x47	inverse of External Walls' Heat Capacity x inverse of Internal Walls' Heat Capacity	96581,18	9,64E-30
x46:x48	inverse of External Walls' Heat Capacity x inverse of Roof's Heat Capacity	57558,36	4,23E-21
x47:x48	inverse of Internal Walls' Heat Capacity x inverse of Roof's Heat Capacity	24868,09	3,91E-05
x4^2	External Walls' Solar Absorptance x External Walls' Solar Absorptance	7,359847	0,012301
x14^2	Roof's Solar Absorptance x Roof's Solar Absorptance	18,52881	1,94E-10
x19^2	External Walls' U-value x External Walls' U-value	1,641649	2,12E-24
x21^2	Roof's U-Value x Roof's U-Value	16,13522	5,97E-10
x48^2	inverse of Roof's Heat Capacity x inverse of Roof's Heat Capacity	-17056,6	4,48E-24

7.3 Appendix C - Curitiba/PR Meta-model coefficients – Degree-hours of discomfort by heat

Table 32 – Non zero approach with regression floor

Coefficient	Parameter Identification	value	p-value
INTERCEPT	INTERCEPT	358,3747	3,02E-12
x4	External Walls' Solar Absorptance	-176,567	5,93E-18
x9	Bedroom_2 Right Fin size	-52,0469	0,000224
x11	Bedroom_1 Overhang size	-8,72256	0,035275
x12	Bedroom_2 Overhang size	-2,7608	0,844729
x13	Living room Overhang size	45,81751	0,000384
x14	Roof's Solar Absorptance	-336,754	3,26E-12
x16	Bedroom_1 Window to Wall Ratio (WWR)	47,6327	0,000125
x17	Bedroom_2 Window to Wall Ratio (WWR)	-14,7976	0,214369
x18	Living room Window to Wall Ratio (WWR)	26,97337	0,001166
x19	External Walls' U-value	-44,9846	1,21E-13
x21	Roof's U-Value	-249,298	6,01E-14
x22	External Walls' Heat Capacity	0,004138	0,951917
x24	Roof's Heat Capacity	0,586081	1,33E-16
x30	inverse of Bedroom_2 Left Fin size	-0,07762	0,812395
x43	inverse of External Walls' U-value	-6,28239	0,166167

x45	inverse of Roof's U-Value	-59,1857	0,000447
x46	inverse of External Walls' Heat Capacity	-14492,7	4,43E-14
x47	inverse of Internal Walls' Heat Capacity	-6040,44	2,4E-10
x4:x12	External Walls' Solar Absorptance x Bedroom_2 Overhang size	-42,2659	0,017261
x4:x14	External Walls' Solar Absorptance x Roof's Solar Absorptance	92,14922	3,08E-10
x4:x17	External Walls' Solar Absorptance x Bedroom_2 Window to Wall Ratio (WWR)	31,99793	0,036676
x4:x19	External Walls' Solar Absorptance x External Walls' U-value	41,88045	1,48E-56
x4:x21	External Walls' Solar Absorptance x Roof's U-Value	52,73584	2,29E-19
x4:x24	External Walls' Solar Absorptance x Roof's Heat Capacity	-0,21619	6,66E-24
x4:x46	External Walls' Solar Absorptance x inverse of External Walls' Heat Capacity	5883,885	1,23E-29
x4:x47	External Walls' Solar Absorptance x inverse of Internal Walls' Heat Capacity	2729,927	2,68E-07
x9:x14	Bedroom_2 Right Fin size x Roof's Solar Absorptance	42,82548	0,019203
x9:x24	Bedroom_2 Right Fin size x Roof's Heat Capacity	0,065345	0,020128
x12:x43	Bedroom_2 Overhang size x inverse of External Walls' U-value	10,66446	0,021182
x13:x21	Living room Overhang size x Roof's U-Value	-34,7	5,53E-05
x13:x47	Living room Overhang size x inverse of Internal Walls' Heat Capacity	-2777,92	0,001667
x14:x16	Roof's Solar Absorptance x Bedroom_1 Window to Wall Ratio (WWR)	-50,6403	0,001423
x14:x19	Roof's Solar Absorptance x External Walls' U-value	18,58297	7,43E-11
x14:x21	Roof's Solar Absorptance x Roof's U-Value	191,2808	1,26E-30
x14:x22	Roof's Solar Absorptance x External Walls' Heat Capacity	-0,15364	0,004051
x14:x24	Roof's Solar Absorptance x Roof's Heat Capacity	-0,29456	2,21E-35
x14:x45	Roof's Solar Absorptance x inverse of Roof's U-Value	56,254	0,000841
x14:x46	Roof's Solar Absorptance x inverse of External Walls' Heat Capacity	3868,094	7,04E-05
x14:x47	Roof's Solar Absorptance x inverse of Internal Walls' Heat Capacity	3724,52	4,84E-10
x16:x43	Bedroom_1 Window to Wall Ratio (WWR) x inverse of External Walls' U-value	12,93459	0,001122
x16:x47	Bedroom_1 Window to Wall Ratio (WWR) x inverse of Internal Walls' Heat Capacity	-2115,81	0,005263
x17:x46	Bedroom_2 Window to Wall Ratio (WWR) x inverse of External Walls' Heat Capacity	1987,836	0,004038
x18:x24	Living room Window to Wall Ratio (WWR) x Roof's Heat Capacity	-0,07456	0,002555
x18:x30	Living room Window to Wall Ratio (WWR) x inverse of Bedroom_2 Left Fin size	-1,25358	0,002534
x18:x46	Living room Window to Wall Ratio (WWR) x inverse of External Walls' Heat Capacity	2890,185	6,53E-05
x19:x21	External Walls' U-value x Roof's U-Value	7,855186	3,9E-05

x19:x22	External Walls' U-value x External Walls' Heat Capacity	-0,05341	3,69E-08
x19:x24	External Walls' U-value x Roof's Heat Capacity	-0,06174	2,8E-41
x19:x46	External Walls' U-value x inverse of External Walls' Heat Capacity	1038,687	2,14E-07
x19:x47	External Walls' U-value x inverse of Internal Walls' Heat Capacity	1171,907	1,12E-20
x21:x22	Roof's U-Value x External Walls' Heat Capacity	-0,08	0,000884
x21:x24	Roof's U-Value x Roof's Heat Capacity	-0,31627	3,4E-38
x21:x30	Roof's U-Value x inverse of Bedroom_2 Left Fin size	0,541511	7,41E-06
x21:x43	Roof's U-Value x inverse of External Walls' U-value	-5,0214	0,032584
x21:x46	Roof's U-Value x inverse of External Walls' Heat Capacity	4088,617	5,32E-07
x21:x47	Roof's U-Value x inverse of Internal Walls' Heat Capacity	3164,67	7,07E-29
x22:x24	External Walls' Heat Capacity x Roof's Heat Capacity	0,000571	1,7E-13
x24:x30	Roof's Heat Capacity x inverse of Bedroom_2 Left Fin size	-0,00124	0,000751
x24:x45	Roof's Heat Capacity x inverse of Roof's U-Value	-0,10499	7,38E-05
x24:x46	Roof's Heat Capacity x inverse of External Walls' Heat Capacity	-6,61937	6,33E-06
x24:x47	Roof's Heat Capacity x inverse of Internal Walls' Heat Capacity	-11,3061	1,69E-32
x30:x47	inverse of Bedroom_2 Left Fin size x inverse of Internal Walls' Heat Capacity	26,18306	0,028809
x45:x46	inverse of Roof's U-Value x inverse of External Walls' Heat Capacity	1511,287	0,046572
x46:x47	inverse of External Walls' Heat Capacity x inverse of Internal Walls' Heat Capacity	225123,5	6,97E-20
x14^2	Roof's Solar Absorptance x Roof's Solar Absorptance	62,80359	2,98E-06
x19^2	External Walls' U-value x External Walls' U-value	3,785869	4,54E-08
x21^2	Roof's U-Value x Roof's U-Value	47,31777	1,5E-09
x22^2	External Walls' Heat Capacity x External Walls' Heat Capacity	0,000288	0,004714
x24^2	Roof's Heat Capacity x Roof's Heat Capacity	0,000526	6,42E-59
x30^2	inverse of Bedroom_2 Left Fin size x inverse of Bedroom_2 Left Fin size	0,005166	0,017999

7.4 Appendix D - São Paulo/SP: Meta-model coefficients – Degree-hours of discomfort by cold

Table 33 – Standard approach with regression floor

Coefficient	Parameter Identification	value	p-value
INTERCEPT	INTERCEPT	3492,212	0
x4	External Walls' Solar Absorptance	-1805,7	2,9E-149

x5	Bedroom_1 Left Fin size	150,607	0,001339
x6	Bedroom_2 Left Fin size	181,8468	0,004163
x7	Living room Left Fin size	-4,07676	0,937628
x8	Bedroom_1 Right Fin size	-17,1501	0,538154
x9	Bedroom_2 Right Fin size	-47,8172	0,361285
x10	Living room Right Fin size	71,5257	0,254192
x11	Bedroom_1 Overhang size	313,6652	6,55E-06
x12	Bedroom_2 Overhang size	170,6565	0,000175
x13	Living room Overhang size	381,4572	6,05E-08
x14	Roof's Solar Absorptance	-1626,23	6,7E-129
x15	North Axis/ Orientation in the terrain	-8,43494	0
x17	Bedroom_2 Window to Wall Ratio (WWR)	-612,262	1,42E-15
x18	Living room Window to Wall Ratio (WWR)	-750,439	3,58E-28
x19	External Walls' U-value	1896,31	0
x21	Roof's U-Value	2671,813	0
x22	External Walls' Heat Capacity	-2,76346	1,28E-45
x23	Internal Walls' Heat Capacity	-0,82868	2,56E-12
x24	Roof's Heat Capacity	-1,04491	1,15E-10
x35	inverse of Bedroom_1 Overhang size	0,968856	6,95E-07
x39	inverse of North Axis/ Orientation in the terrain	-829,156	5,65E-10
x40	inverse of Bedroom_1 Window to Wall Ratio (WWR)	82,86173	5,41E-15
x46	inverse of External Walls' Heat Capacity	-5027,45	0,119784
x48	inverse of Roof's Heat Capacity	7326,963	0,000656
x4:x11	External Walls' Solar Absorptance x Bedroom_1 Overhang size	-115,734	0,022153
x4:x14	External Walls' Solar Absorptance x Roof's Solar Absorptance	797,5468	1,4E-167
x4:x15	External Walls' Solar Absorptance x North Axis/ Orientation in the terrain	0,333428	1,58E-06
x4:x17	External Walls' Solar Absorptance x Bedroom_2 Window to Wall Ratio (WWR)	424,3361	3,6E-22
x4:x18	External Walls' Solar Absorptance x Living room Window to Wall Ratio (WWR)	401,2784	5,98E-21
x4:x19	External Walls' Solar Absorptance x External Walls' U-value	-930,732	0
x4:x21	External Walls' Solar Absorptance x Roof's U-Value	-45,8067	0,007676
x4:x22	External Walls' Solar Absorptance x External Walls' Heat Capacity	-0,24648	0,024791
x4:x40	External Walls' Solar Absorptance x inverse of Bedroom_1 Window to Wall Ratio (WWR)	-43,0326	5,39E-17
x4:x46	External Walls' Solar Absorptance x inverse of External Walls' Heat Capacity	12010,35	2,15E-05
x5:x6	Bedroom_1 Left Fin size x Bedroom_2 Left Fin size	195,6862	0,037671
x5:x14	Bedroom_1 Left Fin size x Roof's Solar Absorptance	-121,834	0,016785
x5:x40	Bedroom_1 Left Fin size x inverse of Bedroom_1 Window to Wall Ratio (WWR)	-19,052	0,043601
x6:x7	Bedroom_2 Left Fin size x Living room Left Fin size	-202,7	0,029376

x6:x14	Bedroom_2 Left Fin size x Roof's Solar Absorptance	-140,855	0,005356
x6:x15	Bedroom_2 Left Fin size x North Axis/ Orientation in the terrain	-0,4445	0,000615
x6:x17	Bedroom_2 Left Fin size x Bedroom_2 Window to Wall Ratio (WWR)	242,9577	0,002577
x6:x39	Bedroom_2 Left Fin size x inverse of North Axis/ Orientation in the terrain	-801,063	7,8E-10
x7:x18	Living room Left Fin size x Living room Window to Wall Ratio (WWR)	190,2675	0,015741
x7:x21	Living room Left Fin size x Roof's U-Value	58,86032	0,057451
x8:x15	Bedroom_1 Right Fin size x North Axis/ Orientation in the terrain	0,493053	0,000154
x8:x39	Bedroom_1 Right Fin size x inverse of North Axis/ Orientation in the terrain	628,9143	0,000139
x9:x14	Bedroom_2 Right Fin size x Roof's Solar Absorptance	-99,0826	0,049068
x9:x17	Bedroom_2 Right Fin size x Bedroom_2 Window to Wall Ratio (WWR)	292,7451	0,000188
x9:x40	Bedroom_2 Right Fin size x inverse of Bedroom_1 Window to Wall Ratio (WWR)	24,63209	0,00857
x10:x18	Living room Right Fin size x Living room Window to Wall Ratio (WWR)	320,7788	3,53E-05
x10:x39	Living room Right Fin size x inverse of North Axis/ Orientation in the terrain	-381,671	0,000392
x11:x14	Bedroom_1 Overhang size x Roof's Solar Absorptance	-235,881	3,11E-06
x11:x15	Bedroom_1 Overhang size x North Axis/ Orientation in the terrain	1,047235	4,47E-16
x11:x19	Bedroom_1 Overhang size x External Walls' U-value	-42,7339	0,006204
x11:x22	Bedroom_1 Overhang size x External Walls' Heat Capacity	0,313453	0,004487
x11:x23	Bedroom_1 Overhang size x Internal Walls' Heat Capacity	0,267591	0,014708
x11:x40	Bedroom_1 Overhang size x inverse of Bedroom_1 Window to Wall Ratio (WWR)	-38,0826	6,54E-05
x11:x48	Bedroom_1 Overhang size x inverse of Roof's Heat Capacity	-6283,54	3,09E-05
x12:x14	Bedroom_2 Overhang size x Roof's Solar Absorptance	-180,868	0,000329
x12:x17	Bedroom_2 Overhang size x Bedroom_2 Window to Wall Ratio (WWR)	451,1494	6,97E-09
x13:x14	Living room Overhang size x Roof's Solar Absorptance	-173,407	0,00064
x13:x15	Living room Overhang size x North Axis/ Orientation in the terrain	-0,25133	0,049674
x13:x17	Living room Overhang size x Bedroom_2 Window to Wall Ratio (WWR)	-214,925	0,007735
x13:x18	Living room Overhang size x Living room Window to Wall Ratio (WWR)	475,6046	1,41E-09
x13:x19	Living room Overhang size x External Walls' U-value	-58,3345	0,000248
x13:x21	Living room Overhang size x Roof's U-Value	-71,392	0,025666
x14:x15	Roof's Solar Absorptance x North Axis/	0,159975	0,023603

	Orientation in the terrain		
x14:x17	Roof's Solar Absorptance x Bedroom_2 Window to Wall Ratio (WWR)	367,3323	2,54E-16
x14:x18	Roof's Solar Absorptance x Living room Window to Wall Ratio (WWR)	494,6006	2,02E-29
x14:x19	Roof's Solar Absorptance x External Walls' U-value	181,8692	8,52E-98
x14:x21	Roof's Solar Absorptance x Roof's U-Value	-2122,23	0
x14:x24	Roof's Solar Absorptance x Roof's Heat Capacity	-0,54307	2,33E-18
x14:x39	Roof's Solar Absorptance x inverse of North Axis/ Orientation in the terrain	-487,504	6,61E-14
x14:x40	Roof's Solar Absorptance x inverse of Bedroom_1 Window to Wall Ratio (WWR)	-57,3359	2,1E-27
x14:x48	Roof's Solar Absorptance x inverse of Roof's Heat Capacity	5720,702	2,78E-06
x15:x19	North Axis/ Orientation in the terrain x External Walls' U-value	0,040484	0,070059
x15:x22	North Axis/ Orientation in the terrain x External Walls' Heat Capacity	0,000447	0,004094
x15:x40	North Axis/ Orientation in the terrain x inverse of Bedroom_1 Window to Wall Ratio (WWR)	0,206795	2,89E-52
x15:x48	North Axis/ Orientation in the terrain x inverse of Roof's Heat Capacity	7,525179	0,001461
x17:x18	Bedroom_2 Window to Wall Ratio (WWR) x Living room Window to Wall Ratio (WWR)	318,7175	3,8E-06
x17:x19	Bedroom_2 Window to Wall Ratio (WWR) x External Walls' U-value	-100,539	3,58E-13
x17:x23	Bedroom_2 Window to Wall Ratio (WWR) x Internal Walls' Heat Capacity	-0,19837	0,039359
x17:x24	Bedroom_2 Window to Wall Ratio (WWR) x Roof's Heat Capacity	-0,3074	1,64E-05
x17:x40	Bedroom_2 Window to Wall Ratio (WWR) x inverse of Bedroom_1 Window to Wall Ratio (WWR)	-43,2287	8,14E-08
x17:x46	Bedroom_2 Window to Wall Ratio (WWR) x inverse of External Walls' Heat Capacity	6268,585	0,011145
x18:x19	Living room Window to Wall Ratio (WWR) x External Walls' U-value	-82,8442	1,7E-10
x18:x24	Living room Window to Wall Ratio (WWR) x Roof's Heat Capacity	-0,31335	7,96E-06
x18:x40	Living room Window to Wall Ratio (WWR) x inverse of Bedroom_1 Window to Wall Ratio (WWR)	-47,2867	3,09E-09
x19:x21	External Walls' U-value x Roof's U-Value	-144,395	5,1E-173
x19:x22	External Walls' U-value x External Walls' Heat Capacity	-0,34184	2,77E-24
x19:x23	External Walls' U-value x Internal Walls' Heat Capacity	-0,23263	1,53E-33
x19:x24	External Walls' U-value x Roof's Heat Capacity	-0,22311	5,6E-35
x19:x39	External Walls' U-value x inverse of North Axis/ Orientation in the terrain	-523,632	1E-29
x19:x40	External Walls' U-value x inverse of Bedroom_1 Window to Wall Ratio (WWR)	10,48896	5,24E-12
x19:x46	External Walls' U-value x inverse of External Walls' Heat Capacity	4767,008	3,6E-08

x19:x48	External Walls' U-value x inverse of Roof's Heat Capacity	1568,278	5,21E-06
x21:x23	Roof's U-Value x Internal Walls' Heat Capacity	-0,14394	0,000114
x21:x24	Roof's U-Value x Roof's Heat Capacity	-0,74904	2,64E-84
x21:x39	Roof's U-Value x inverse of North Axis/ Orientation in the terrain	-248,817	6,23E-09
x21:x46	Roof's U-Value x inverse of External Walls' Heat Capacity	8974,969	2,08E-21
x21:x48	Roof's U-Value x inverse of Roof's Heat Capacity	4216,483	1,42E-08
x22:x24	External Walls' Heat Capacity x Roof's Heat Capacity	0,001281	6,19E-13
x22:x39	External Walls' Heat Capacity x inverse of North Axis/ Orientation in the terrain	2,768684	3,9E-30
x23:x24	Internal Walls' Heat Capacity x Roof's Heat Capacity	0,001017	3,62E-14
x23:x39	Internal Walls' Heat Capacity x inverse of North Axis/ Orientation in the terrain	1,681017	7,49E-19
x23:x40	Internal Walls' Heat Capacity x inverse of Bedroom_1 Window to Wall Ratio (WWR)	0,03713	0,001131
x23:x46	Internal Walls' Heat Capacity x inverse of External Walls' Heat Capacity	-46,8797	1,89E-41
x23:x48	Internal Walls' Heat Capacity x inverse of Roof's Heat Capacity	-15,1352	4,83E-09
x24:x40	Roof's Heat Capacity x inverse of Bedroom_1 Window to Wall Ratio (WWR)	0,030903	0,000226
x24:x46	Roof's Heat Capacity x inverse of External Walls' Heat Capacity	-17,9343	0,000497
x35:x39	inverse of Bedroom_1 Overhang size x inverse of North Axis/ Orientation in the terrain	-17,656	5,95E-09
x39:x40	inverse of North Axis/ Orientation in the terrain x inverse of Bedroom_1 Window to Wall Ratio (WWR)	77,0011	2,38E-10
x39:x46	inverse of North Axis/ Orientation in the terrain x inverse of External Walls' Heat Capacity	52481	1,2E-26
x39:x48	inverse of North Axis/ Orientation in the terrain x inverse of Roof's Heat Capacity	-5069,76	0,072726
x40:x46	inverse of Bedroom_1 Window to Wall Ratio (WWR) x inverse of External Walls' Heat Capacity	-939,124	0,000996
x46:x48	inverse of External Walls' Heat Capacity x inverse of Roof's Heat Capacity	931757,5	6,74E-45
x4^2	External Walls' Solar Absorptance x External Walls' Solar Absorptance	559,2501	3,69E-70
x10^2	Living room Right Fin size x Living room Right Fin size	-243,027	0,017286
x14^2	Roof's Solar Absorptance x Roof's Solar Absorptance	982,538	2,2E-207
x15^2	North Axis/ Orientation in the terrain x North Axis/ Orientation in the terrain	0,017765	0
x19^2	External Walls' U-value x External Walls' U-value	-55,8444	3,5E-210
x22^2	External Walls' Heat Capacity x External Walls' Heat Capacity	0,002656	4,24E-22
x23^2	Internal Walls' Heat Capacity x Internal Walls' Heat Capacity	0,000897	2,44E-09
x24^2	Roof's Heat Capacity x Roof's Heat Capacity	0,001593	1,17E-24
x39^2	inverse of North Axis/ Orientation in the terrain x	32,56589	1,82E-41

	inverse of North Axis/ Orientation in the terrain		
x40^2	inverse of Bedroom_1 Window to Wall Ratio (WWR) x inverse of Bedroom_1 Window to Wall Ratio (WWR)	-2,8693	7,98E-06
x48^2	inverse of Roof's Heat Capacity x inverse of Roof's Heat Capacity	-218561	2,01E-17

7.5 Appendix E - São Paulo/SP: Meta-model coefficients – Degree-hours of discomfort by heat

Table 34 – Standard approach with regression floor

Coefficient	Parameter Identification	value	p-value
INTERCEPT	INTERCEPT	209,0965	3,57E-54
x4	External Walls' Solar Absorptance	-142,318	3,32E-33
x11	Bedroom_1 Overhang size	11,57586	0,248043
x13	Living room Overhang size	35,13246	0,001299
x14	Roof's Solar Absorptance	-313,121	2,2E-121
x16	Bedroom_1 Window to Wall Ratio (WWR)	-58,3168	0,000395
x17	Bedroom_2 Window to Wall Ratio (WWR)	-47,5932	3,94E-07
x18	Living room Window to Wall Ratio (WWR)	-42,1278	0,000443
x19	External Walls' U-value	-47,3152	5,9E-32
x21	Roof's U-Value	-170,638	2,9E-66
x23	Internal Walls' Heat Capacity	0,187527	1,31E-11
x27	inverse of Living room Effective window ventilation area	17,42579	6,2E-05
x33	inverse of Bedroom_2 Right Fin size	0,670124	0,010185
x46	inverse of External Walls' Heat Capacity	-10970	6,84E-59
x48	inverse of Roof's Heat Capacity	-5654,8	2,48E-36
x4:x11	External Walls' Solar Absorptance x Bedroom_1 Overhang size	-25,7689	0,025528
x4:x14	External Walls' Solar Absorptance x Roof's Solar Absorptance	54,79794	1,08E-17
x4:x18	External Walls' Solar Absorptance x Living room Window to Wall Ratio (WWR)	21,50221	0,027303
x4:x19	External Walls' Solar Absorptance x External Walls' U-value	55,77705	4,5E-162
x4:x21	External Walls' Solar Absorptance x Roof's U-Value	32,08197	3,64E-16
x4:x23	External Walls' Solar Absorptance x Internal Walls' Heat Capacity	-0,05415	0,000118
x4:x46	External Walls' Solar Absorptance x inverse of External Walls' Heat Capacity	4866,426	2,07E-41
x4:x48	External Walls' Solar Absorptance x inverse of Roof's Heat Capacity	1934,396	2,15E-21
x11:x19	Bedroom_1 Overhang size x External Walls' U-value	-14,1075	7,87E-05
x11:x23	Bedroom_1 Overhang size x Internal Walls' Heat Capacity	0,066866	0,007631

x11:x48	Bedroom_1 Overhang size x inverse of Roof's Heat Capacity	-1623,67	2,8E-06
x13:x14	Living room Overhang size x Roof's Solar Absorptance	-23,8267	0,040175
x13:x16	Living room Overhang size x Bedroom_1 Window to Wall Ratio (WWR)	-36,9951	0,040171
x13:x19	Living room Overhang size x External Walls' U-value	-13,5123	0,000182
x14:x16	Roof's Solar Absorptance x Bedroom_1 Window to Wall Ratio (WWR)	44,22432	6,39E-06
x14:x17	Roof's Solar Absorptance x Bedroom_2 Window to Wall Ratio (WWR)	46,05074	6,85E-06
x14:x18	Roof's Solar Absorptance x Living room Window to Wall Ratio (WWR)	28,3489	0,004541
x14:x19	Roof's Solar Absorptance x External Walls' U-value	18,92962	2,65E-22
x14:x21	Roof's Solar Absorptance x Roof's U-Value	146,2219	1,9E-267
x14:x23	Roof's Solar Absorptance x Internal Walls' Heat Capacity	-0,12287	2,71E-18
x14:x33	Roof's Solar Absorptance x inverse of Bedroom_2 Right Fin size	0,466267	0,001684
x14:x46	Roof's Solar Absorptance x inverse of External Walls' Heat Capacity	6190,598	2,51E-66
x14:x48	Roof's Solar Absorptance x inverse of Roof's Heat Capacity	6090,088	1,8E-173
x16:x21	Bedroom_1 Window to Wall Ratio (WWR) x Roof's U-Value	30,3961	2,57E-07
x16:x23	Bedroom_1 Window to Wall Ratio (WWR) x Internal Walls' Heat Capacity	-0,074	0,00058
x16:x46	Bedroom_1 Window to Wall Ratio (WWR) x inverse of External Walls' Heat Capacity	2535,154	2,46E-06
x16:x48	Bedroom_1 Window to Wall Ratio (WWR) x inverse of Roof's Heat Capacity	1360,055	1,3E-05
x17:x21	Bedroom_2 Window to Wall Ratio (WWR) x Roof's U-Value	20,89712	0,000575
x17:x33	Bedroom_2 Window to Wall Ratio (WWR) x inverse of Bedroom_2 Right Fin size	-0,5553	0,012045
x17:x46	Bedroom_2 Window to Wall Ratio (WWR) x inverse of External Walls' Heat Capacity	2039,182	0,000288
x17:x48	Bedroom_2 Window to Wall Ratio (WWR) x inverse of Roof's Heat Capacity	1533,531	1,4E-06
x18:x21	Living room Window to Wall Ratio (WWR) x Roof's U-Value	26,28055	1,72E-05
x18:x23	Living room Window to Wall Ratio (WWR) x Internal Walls' Heat Capacity	-0,057	0,008634
x18:x46	Living room Window to Wall Ratio (WWR) x inverse of External Walls' Heat Capacity	2040,648	0,00023
x18:x48	Living room Window to Wall Ratio (WWR) x inverse of Roof's Heat Capacity	1879,125	1,54E-09
x19:x21	External Walls' U-value x Roof's U-Value	4,114495	0,00029
x19:x23	External Walls' U-value x Internal Walls' Heat Capacity	-0,03756	1,15E-17
x19:x27	External Walls' U-value x inverse of Living room Effective window ventilation area	-4,72156	0,009332
x19:x33	External Walls' U-value x inverse of Bedroom_2	0,206007	3,08E-06

	Right Fin size		
x19:x46	External Walls' U-value x inverse of External Walls' Heat Capacity	2940,155	1,1E-158
x19:x48	External Walls' U-value x inverse of Roof's Heat Capacity	767,2884	4,3E-37
x21:x23	Roof's U-Value x Internal Walls' Heat Capacity	-0,04472	1,66E-07
x21:x27	Roof's U-Value x inverse of Living room Effective window ventilation area	-8,44865	0,021323
x21:x33	Roof's U-Value x inverse of Bedroom_2 Right Fin size	-0,17966	0,046587
x21:x46	Roof's U-Value x inverse of External Walls' Heat Capacity	3366,082	4,61E-54
x21:x48	Roof's U-Value x inverse of Roof's Heat Capacity	3748,863	8,3E-180
x23:x33	Internal Walls' Heat Capacity x inverse of Bedroom_2 Right Fin size	-0,0008	0,011919
x23:x46	Internal Walls' Heat Capacity x inverse of External Walls' Heat Capacity	-7,31071	1,85E-20
x23:x48	Internal Walls' Heat Capacity x inverse of Roof's Heat Capacity	-4,61654	8,5E-26
x27:x33	inverse of Living room Effective window ventilation area x inverse of Bedroom_2 Right Fin size	-0,49387	0,000127
x27:x48	inverse of Living room Effective window ventilation area x inverse of Roof's Heat Capacity	-735,039	4,12E-05
x33:x48	inverse of Bedroom_2 Right Fin size x inverse of Roof's Heat Capacity	14,26025	0,005877
x46:x48	inverse of External Walls' Heat Capacity x inverse of Roof's Heat Capacity	293633,9	1,7E-145
x4^2	External Walls' Solar Absorptance x External Walls' Solar Absorptance	28,60354	6,04E-05
x14^2	Roof's Solar Absorptance x Roof's Solar Absorptance	78,87161	4,51E-29
x16^2	Bedroom_1 Window to Wall Ratio (WWR) x Bedroom_1 Window to Wall Ratio (WWR)	26,923	0,036682
x19^2	External Walls' U-value x External Walls' U-value	4,881887	9,24E-35
x21^2	Roof's U-Value x Roof's U-Value	22,18825	8,19E-22
x23^2	Internal Walls' Heat Capacity x Internal Walls' Heat Capacity	0,000133	0,000115
x33^2	inverse of Bedroom_2 Right Fin size x inverse of Bedroom_2 Right Fin size	0,003711	0,008683
x46^2	inverse of External Walls' Heat Capacity x inverse of External Walls' Heat Capacity	-56791,2	0,000216
x48^2	inverse of Roof's Heat Capacity x inverse of Roof's Heat Capacity	-52405,2	1,57E-66

7.6 Appendix F - São Paulo/SP: Meta-model coefficients – Degree-hours of discomfort by heat

Table 35 – Non zero approach with regression floor

Coefficient	Parameter Identification	value	p-value

INTERCEPT	INTERCEPT	378,9731	9,43E-15
x4	External Walls' Solar Absorptance	-205,863	6,73E-17
x5	Bedroom_1 Left Fin size	-11,5254	0,003621
x11	Bedroom_1 Overhang size	58,04928	3,77E-05
x12	Bedroom_2 Overhang size	-32,1959	0,004398
x13	Living room Overhang size	9,071032	0,366586
x14	Roof's Solar Absorptance	-671,798	6,08E-48
x16	Bedroom_1 Window to Wall Ratio (WWR)	24,80705	0,172697
x17	Bedroom_2 Window to Wall Ratio (WWR)	-23,8698	0,234426
x18	Living room Window to Wall Ratio (WWR)	-55,8355	0,012285
x19	External Walls' U-value	-55,0305	7,43E-25
x21	Roof's U-Value	-362,528	3,83E-30
x22	External Walls' Heat Capacity	0,275397	0,000188
x23	Internal Walls' Heat Capacity	0,304049	1,16E-08
x24	Roof's Heat Capacity	0,69502	5,8E-20
x33	inverse of Bedroom_2 Right Fin size	-0,04448	0,866359
x41	inverse of Bedroom_2 Window to Wall Ratio (WWR)	5,104988	0,000508
x45	inverse of Roof's U-Value	-85,2232	5,93E-09
x46	inverse of External Walls' Heat Capacity	-8705,61	9,45E-12
x48	inverse of Roof's Heat Capacity	-4156,2	1,24E-07
x4:x11	External Walls' Solar Absorptance x Bedroom_1 Overhang size	-55,7242	0,000497
x4:x14	External Walls' Solar Absorptance x Roof's Solar Absorptance	194,791	2,41E-55
x4:x18	External Walls' Solar Absorptance x Living room Window to Wall Ratio (WWR)	43,68695	0,001157
x4:x19	External Walls' Solar Absorptance x External Walls' U-value	102,2987	4,9E-294
x4:x21	External Walls' Solar Absorptance x Roof's U-Value	94,48206	1,62E-63
x4:x22	External Walls' Solar Absorptance x External Walls' Heat Capacity	-0,34993	3,29E-20
x4:x23	External Walls' Solar Absorptance x Internal Walls' Heat Capacity	-0,17166	2,01E-16
x4:x24	External Walls' Solar Absorptance x Roof's Heat Capacity	-0,30419	4,44E-39
x4:x41	External Walls' Solar Absorptance x inverse of Bedroom_2 Window to Wall Ratio (WWR)	-4,87267	0,007654
x4:x46	External Walls' Solar Absorptance x inverse of External Walls' Heat Capacity	4625,35	7,72E-09
x4:x48	External Walls' Solar Absorptance x inverse of Roof's Heat Capacity	1471,436	1,81E-06
x11:x19	Bedroom_1 Overhang size x External Walls' U-value	-18,6852	7E-07
x11:x46	Bedroom_1 Overhang size x inverse of External Walls' Heat Capacity	-1926,78	0,011736
x11:x48	Bedroom_1 Overhang size x inverse of Roof's Heat Capacity	-1447,7	0,000145
x12:x18	Bedroom_2 Overhang size x Living room Window to Wall Ratio (WWR)	46,07613	0,04825

x13:x19	Living room Overhang size x External Walls' U-value	-9,30435	0,014397
x13:x33	Living room Overhang size x inverse of Bedroom_2 Right Fin size	1,061089	0,012862
x13:x46	Living room Overhang size x inverse of External Walls' Heat Capacity	-2430,05	0,001618
x13:x48	Living room Overhang size x inverse of Roof's Heat Capacity	-826,618	0,034632
x14:x16	Roof's Solar Absorptance x Bedroom_1 Window to Wall Ratio (WWR)	60,48912	8,27E-05
x14:x17	Roof's Solar Absorptance x Bedroom_2 Window to Wall Ratio (WWR)	59,37387	0,000205
x14:x18	Roof's Solar Absorptance x Living room Window to Wall Ratio (WWR)	45,38299	0,003385
x14:x19	Roof's Solar Absorptance x External Walls' U-value	41,25817	7,63E-47
x14:x21	Roof's Solar Absorptance x Roof's U-Value	402,8104	1,7E-132
x14:x22	Roof's Solar Absorptance x External Walls' Heat Capacity	-0,4033	9,72E-19
x14:x23	Roof's Solar Absorptance x Internal Walls' Heat Capacity	-0,24136	7,18E-24
x14:x24	Roof's Solar Absorptance x Roof's Heat Capacity	-0,4663	5,65E-73
x14:x33	Roof's Solar Absorptance x inverse of Bedroom_2 Right Fin size	0,980809	0,000141
x14:x45	Roof's Solar Absorptance x inverse of Roof's U-Value	118,8332	3,47E-14
x14:x46	Roof's Solar Absorptance x inverse of External Walls' Heat Capacity	6141,33	3,98E-12
x14:x48	Roof's Solar Absorptance x inverse of Roof's Heat Capacity	5420,793	4,18E-50
x16:x21	Bedroom_1 Window to Wall Ratio (WWR) x Roof's U-Value	28,51599	8,56E-05
x16:x22	Bedroom_1 Window to Wall Ratio (WWR) x External Walls' Heat Capacity	-0,11861	8,43E-05
x16:x23	Bedroom_1 Window to Wall Ratio (WWR) x Internal Walls' Heat Capacity	-0,1004	0,000673
x16:x24	Bedroom_1 Window to Wall Ratio (WWR) x Roof's Heat Capacity	-0,09137	0,002248
x16:x48	Bedroom_1 Window to Wall Ratio (WWR) x inverse of Roof's Heat Capacity	2599,851	1,13E-08
x17:x21	Bedroom_2 Window to Wall Ratio (WWR) x Roof's U-Value	33,57022	1,16E-05
x17:x23	Bedroom_2 Window to Wall Ratio (WWR) x Internal Walls' Heat Capacity	-0,09893	0,000829
x17:x24	Bedroom_2 Window to Wall Ratio (WWR) x Roof's Heat Capacity	-0,06203	0,043406
x17:x46	Bedroom_2 Window to Wall Ratio (WWR) x inverse of External Walls' Heat Capacity	4256,2	1,23E-09
x17:x48	Bedroom_2 Window to Wall Ratio (WWR) x inverse of Roof's Heat Capacity	2649,202	4,41E-09
x18:x21	Living room Window to Wall Ratio (WWR) x Roof's U-Value	43,14944	6,09E-09
x18:x23	Living room Window to Wall Ratio (WWR) x Internal Walls' Heat Capacity	-0,10453	0,000308
x18:x24	Living room Window to Wall Ratio (WWR) x Roof's	-0,12446	3,97E-05

	Heat Capacity		
x18:x46	Living room Window to Wall Ratio (WWR) x inverse of External Walls' Heat Capacity	3660,921	5,07E-08
x18:x48	Living room Window to Wall Ratio (WWR) x inverse of Roof's Heat Capacity	1654,549	0,000214
x19:x21	External Walls' U-value x Roof's U-Value	22,09194	3,51E-60
x19:x22	External Walls' U-value x External Walls' Heat Capacity	-0,1062	3,88E-30
x19:x23	External Walls' U-value x Internal Walls' Heat Capacity	-0,07222	6,1E-44
x19:x24	External Walls' U-value x Roof's Heat Capacity	-0,09551	1,12E-74
x19:x33	External Walls' U-value x inverse of Bedroom_2 Right Fin size	0,218991	2,26E-05
x19:x46	External Walls' U-value x inverse of External Walls' Heat Capacity	2175,135	2,64E-25
x19:x48	External Walls' U-value x inverse of Roof's Heat Capacity	258,3311	0,000736
x21:x22	Roof's U-Value x External Walls' Heat Capacity	-0,23472	1,9E-30
x21:x23	Roof's U-Value x Internal Walls' Heat Capacity	-0,12132	3,93E-27
x21:x24	Roof's U-Value x Roof's Heat Capacity	-0,40882	1,47E-66
x21:x46	Roof's U-Value x inverse of External Walls' Heat Capacity	1864,055	7,52E-06
x21:x48	Roof's U-Value x inverse of Roof's Heat Capacity	2268,019	3,55E-37
x22:x23	External Walls' Heat Capacity x Internal Walls' Heat Capacity	0,000335	1,18E-05
x22:x24	External Walls' Heat Capacity x Roof's Heat Capacity	0,000551	1,75E-10
x22:x33	External Walls' Heat Capacity x inverse of Bedroom_2 Right Fin size	-0,00146	0,008529
x22:x48	External Walls' Heat Capacity x inverse of Roof's Heat Capacity	-6,16094	2,99E-07
x23:x24	Internal Walls' Heat Capacity x Roof's Heat Capacity	0,000398	1,84E-18
x23:x33	Internal Walls' Heat Capacity x inverse of Bedroom_2 Right Fin size	-0,0021	2,98E-05
x23:x46	Internal Walls' Heat Capacity x inverse of External Walls' Heat Capacity	-5,87328	0,000391
x23:x48	Internal Walls' Heat Capacity x inverse of Roof's Heat Capacity	-5,30587	7,77E-16
x24:x33	Roof's Heat Capacity x inverse of Bedroom_2 Right Fin size	-0,00088	0,017034
x24:x45	Roof's Heat Capacity x inverse of Roof's U-Value	-0,08679	0,000156
x24:x46	Roof's Heat Capacity x inverse of External Walls' Heat Capacity	-11,2287	4,22E-10
x46:x48	inverse of External Walls' Heat Capacity x inverse of Roof's Heat Capacity	126041,4	3,8E-06
x4^2	External Walls' Solar Absorptance x External Walls' Solar Absorptance	64,23986	5,1E-10
x14^2	Roof's Solar Absorptance x Roof's Solar Absorptance	124,8602	6,76E-24
x19^2	External Walls' U-value x External Walls' U-value	6,95283	2,36E-47
x21^2	Roof's U-Value x Roof's U-Value	65,10893	1,5E-16
x22^2	External Walls' Heat Capacity x External Walls'	0,000747	8,15E-17

	Heat Capacity		
x23^2	Internal Walls' Heat Capacity x Internal Walls' Heat Capacity	0,00032	6,93E-12
x24^2	Roof's Heat Capacity x Roof's Heat Capacity	0,000632	7,72E-36
x48^2	inverse of Roof's Heat Capacity x inverse of Roof's Heat Capacity	-42880,6	3,58E-12

7.7 Appendix G - Manaus/AM: Meta-model coefficients – Degree-hours of discomfort by heat

Table 36 – Standard approach with regression floor

Coefficient	Parameter Identification	value	p-value
INTERCEPT	INTERCEPT	911,8894	4,62E-13
x4	External Walls' Solar Absorptance	-1850,12	2,44E-82
x5	Bedroom_1 Left Fin size	308,6149	0,004451
x6	Bedroom_2 Left Fin size	48,42138	0,475329
x8	Bedroom_1 Right Fin size	468,2416	0,000621
x9	Bedroom_2 Right Fin size	390,6307	4,08E-05
x11	Bedroom_1 Overhang size	393,9732	1,18E-05
x12	Bedroom_2 Overhang size	155,6619	0,164865
x13	Living room Overhang size	580,1741	6,48E-12
x14	Roof's Solar Absorptance	-3010,46	2,1E-199
x15	North Axis/ Orientation in the terrain	-0,27827	0,012303
x16	Bedroom_1 Window to Wall Ratio (WWR)	-296,258	0,019323
x17	Bedroom_2 Window to Wall Ratio (WWR)	-539,48	1,65E-05
x18	Living room Window to Wall Ratio (WWR)	-666,16	2,38E-07
x19	External Walls' U-value	-216,528	3,45E-23
x21	Roof's U-Value	-1243,23	3,8E-118
x24	Roof's Heat Capacity	1,68734	2,87E-15
x25	inverse of Bedroom_1 Effective window ventilation area	67,28971	0,0075
x31	inverse of Living room Left Fin size	-5,02796	9,85E-06
x32	inverse of Bedroom_1 Right Fin size	-0,52004	0,510173
x34	inverse of Living room Right Fin size	0,52491	0,498399
x43	inverse of External Walls' U-value	235,9633	6,54E-15
x46	inverse of External Walls' Heat Capacity	-28572,8	2,28E-07
x47	inverse of Internal Walls' Heat Capacity	-20062,9	1,21E-05
x48	inverse of Roof's Heat Capacity	-39261,2	4,97E-23
x4:x6	External Walls' Solar Absorptance x Bedroom_2 Left Fin size	-161,352	0,016394
x4:x11	External Walls' Solar Absorptance x Bedroom_1 Overhang size	-155,998	0,019908
x4:x12	External Walls' Solar Absorptance x Bedroom_2 Overhang size	-197,806	0,002829
x4:x13	External Walls' Solar Absorptance x Living room Overhang size	-183,121	0,005272
x4:x14	External Walls' Solar Absorptance x Roof's Solar	792,1097	1,1E-101

	Absorptance		
x4:x16	External Walls' Solar Absorptance x Bedroom_1 Window to Wall Ratio (WWR)	270,5399	2,58E-06
x4:x17	External Walls' Solar Absorptance x Bedroom_2 Window to Wall Ratio (WWR)	226,356	7,85E-05
x4:x18	External Walls' Solar Absorptance x Living room Window to Wall Ratio (WWR)	284,6164	7,47E-07
x4:x19	External Walls' Solar Absorptance x External Walls' U-value	907,7453	0
x4:x21	External Walls' Solar Absorptance x Roof's U-Value	253,1698	7,86E-30
x4:x24	External Walls' Solar Absorptance x Roof's Heat Capacity	-0,53998	1,1E-11
x4:x32	External Walls' Solar Absorptance x inverse of Bedroom_1 Right Fin size	1,868761	0,020749
x4:x43	External Walls' Solar Absorptance x inverse of External Walls' U-value	110,1346	8,89E-11
x4:x46	External Walls' Solar Absorptance x inverse of External Walls' Heat Capacity	51882,5	2,2E-124
x4:x47	External Walls' Solar Absorptance x inverse of Internal Walls' Heat Capacity	12085,61	7,03E-09
x4:x48	External Walls' Solar Absorptance x inverse of Roof's Heat Capacity	6593,142	2,66E-05
x5:x12	Bedroom_1 Left Fin size x Bedroom_2 Overhang size	243,9179	0,046649
x5:x14	Bedroom_1 Left Fin size x Roof's Solar Absorptance	-140,524	0,035856
x5:x18	Bedroom_1 Left Fin size x Living room Window to Wall Ratio (WWR)	-206,912	0,04961
x5:x19	Bedroom_1 Left Fin size x External Walls' U-value	-92,8213	0,005869
x5:x32	Bedroom_1 Left Fin size x inverse of Bedroom_1 Right Fin size	-3,09938	0,039812
x5:x43	Bedroom_1 Left Fin size x inverse of External Walls' U-value	-66,3944	0,035854
x5:x46	Bedroom_1 Left Fin size x inverse of External Walls' Heat Capacity	-10676	0,007401
x6:x17	Bedroom_2 Left Fin size x Bedroom_2 Window to Wall Ratio (WWR)	-217,089	0,038712
x6:x24	Bedroom_2 Left Fin size x Roof's Heat Capacity	0,303552	0,004626
x8:x19	Bedroom_1 Right Fin size x External Walls' U-value	-169,982	2,95E-07
x8:x43	Bedroom_1 Right Fin size x inverse of External Walls' U-value	-86,3336	0,005826
x8:x46	Bedroom_1 Right Fin size x inverse of External Walls' Heat Capacity	11726,31	0,018486
x8:x48	Bedroom_1 Right Fin size x inverse of Roof's Heat Capacity	-4275,67	0,035669
x9:x14	Bedroom_2 Right Fin size x Roof's Solar Absorptance	-133,26	0,044852
x9:x17	Bedroom_2 Right Fin size x Bedroom_2 Window to Wall Ratio (WWR)	-270,203	0,009488
x9:x47	Bedroom_2 Right Fin size x inverse of Internal Walls' Heat Capacity	-11684,8	0,001533
x11:x14	Bedroom_1 Overhang size x Roof's Solar Absorptance	-300,391	6,87E-06

x11:x16	Bedroom_1 Overhang size x Bedroom_1 Window to Wall Ratio (WWR)	-283,935	0,007
x11:x21	Bedroom_1 Overhang size x Roof's U-Value	-137,172	0,000702
x11:x24	Bedroom_1 Overhang size x Roof's Heat Capacity	0,267408	0,01369
x11:x34	Bedroom_1 Overhang size x inverse of Living room Right Fin size	-3,91906	0,008649
x11:x46	Bedroom_1 Overhang size x inverse of External Walls' Heat Capacity	-9792,22	0,012519
x12:x14	Bedroom_2 Overhang size x Roof's Solar Absorptance	-272,818	5,04E-05
x12:x17	Bedroom_2 Overhang size x Bedroom_2 Window to Wall Ratio (WWR)	-565,38	6,28E-08
x12:x24	Bedroom_2 Overhang size x Roof's Heat Capacity	0,297132	0,005684
x12:x46	Bedroom_2 Overhang size x inverse of External Walls' Heat Capacity	-8479,82	0,030252
x12:x47	Bedroom_2 Overhang size x inverse of Internal Walls' Heat Capacity	-8393,31	0,028185
x13:x14	Living room Overhang size x Roof's Solar Absorptance	-209,114	0,001508
x13:x18	Living room Overhang size x Living room Window to Wall Ratio (WWR)	-421,627	5,6E-05
x13:x21	Living room Overhang size x Roof's U-Value	-140,294	0,000354
x13:x34	Living room Overhang size x inverse of Living room Right Fin size	-3,42052	0,016614
x13:x47	Living room Overhang size x inverse of Internal Walls' Heat Capacity	-13082,2	0,000561
x13:x48	Living room Overhang size x inverse of Roof's Heat Capacity	-12577,4	8,91E-10
x14:x15	Roof's Solar Absorptance x North Axis/ Orientation in the terrain	0,300336	0,001014
x14:x16	Roof's Solar Absorptance x Bedroom_1 Window to Wall Ratio (WWR)	606,2887	3,69E-26
x14:x17	Roof's Solar Absorptance x Bedroom_2 Window to Wall Ratio (WWR)	547,5171	1,32E-21
x14:x18	Roof's Solar Absorptance x Living room Window to Wall Ratio (WWR)	497,4884	4,53E-18
x14:x19	Roof's Solar Absorptance x External Walls' U-value	101,4124	8,63E-09
x14:x21	Roof's Solar Absorptance x Roof's U-Value	1926,697	0
x14:x24	Roof's Solar Absorptance x Roof's Heat Capacity	-1,70997	5,2E-97
x14:x43	Roof's Solar Absorptance x inverse of External Walls' U-value	-70,9483	2,83E-05
x14:x46	Roof's Solar Absorptance x inverse of External Walls' Heat Capacity	48938,73	4,7E-112
x14:x47	Roof's Solar Absorptance x inverse of Internal Walls' Heat Capacity	19379,41	4,61E-20
x14:x48	Roof's Solar Absorptance x inverse of Roof's Heat Capacity	36554,19	1,2E-121
x15:x18	North Axis/ Orientation in the terrain x Living room Window to Wall Ratio (WWR)	0,316551	0,026577
x15:x21	North Axis/ Orientation in the terrain x Roof's U-Value	0,106798	0,051286

x15:x24	North Axis/ Orientation in the terrain x Roof's Heat Capacity	-0,00034	0,019017
x15:x46	North Axis/ Orientation in the terrain x inverse of External Walls' Heat Capacity	10,23942	0,051698
x16:x17	Bedroom_1 Window to Wall Ratio (WWR) x Bedroom_2 Window to Wall Ratio (WWR)	245,7963	0,005512
x16:x18	Bedroom_1 Window to Wall Ratio (WWR) x Living room Window to Wall Ratio (WWR)	266,7729	0,002918
x16:x21	Bedroom_1 Window to Wall Ratio (WWR) x Roof's U-Value	90,80791	0,008612
x16:x24	Bedroom_1 Window to Wall Ratio (WWR) x Roof's Heat Capacity	-0,38619	0,001751
x16:x25	Bedroom_1 Window to Wall Ratio (WWR) x inverse of Bedroom_1 Effective window ventilation area	-143,52	0,006686
x16:x46	Bedroom_1 Window to Wall Ratio (WWR) x inverse of External Walls' Heat Capacity	14812,75	2,11E-05
x16:x47	Bedroom_1 Window to Wall Ratio (WWR) x inverse of Internal Walls' Heat Capacity	8711,905	0,005764
x16:x48	Bedroom_1 Window to Wall Ratio (WWR) x inverse of Roof's Heat Capacity	14835,55	5,84E-11
x17:x18	Bedroom_2 Window to Wall Ratio (WWR) x Living room Window to Wall Ratio (WWR)	307,7179	0,000633
x17:x21	Bedroom_2 Window to Wall Ratio (WWR) x Roof's U-Value	188,6714	4,79E-08
x17:x24	Bedroom_2 Window to Wall Ratio (WWR) x Roof's Heat Capacity	-0,45313	0,000317
x17:x46	Bedroom_2 Window to Wall Ratio (WWR) x inverse of External Walls' Heat Capacity	14969,28	3,81E-06
x17:x47	Bedroom_2 Window to Wall Ratio (WWR) x inverse of Internal Walls' Heat Capacity	13441,73	5,19E-05
x17:x48	Bedroom_2 Window to Wall Ratio (WWR) x inverse of Roof's Heat Capacity	16297,15	2,47E-11
x18:x21	Living room Window to Wall Ratio (WWR) x Roof's U-Value	81,86552	0,01702
x18:x24	Living room Window to Wall Ratio (WWR) x Roof's Heat Capacity	-0,36643	0,003386
x18:x34	Living room Window to Wall Ratio (WWR) x inverse of Living room Right Fin size	3,231787	0,012141
x18:x46	Living room Window to Wall Ratio (WWR) x inverse of External Walls' Heat Capacity	18605,07	4,26E-08
x18:x47	Living room Window to Wall Ratio (WWR) x inverse of Internal Walls' Heat Capacity	12246,53	0,000138
x18:x48	Living room Window to Wall Ratio (WWR) x inverse of Roof's Heat Capacity	9196,268	0,000112
x19:x24	External Walls' U-value x Roof's Heat Capacity	-0,24571	2,47E-24
x19:x31	External Walls' U-value x inverse of Living room Left Fin size	2,500773	2,75E-08
x19:x46	External Walls' U-value x inverse of External Walls' Heat Capacity	19191,14	2,69E-83
x19:x47	External Walls' U-value x inverse of Internal Walls' Heat Capacity	5209,872	4,44E-18
x19:x48	External Walls' U-value x inverse of Roof's Heat Capacity	1689,813	0,000436
x21:x24	Roof's U-Value x Roof's Heat Capacity	-1,16593	2,6E-126
x21:x31	Roof's U-Value x inverse of Living room Left Fin	1,126068	0,026995

	size		
x21:x46	Roof's U-Value x inverse of External Walls' Heat Capacity	16682,36	1,58E-38
x21:x47	Roof's U-Value x inverse of Internal Walls' Heat Capacity	12566,95	1E-23
x21:x48	Roof's U-Value x inverse of Roof's Heat Capacity	15021,79	1,7E-60
x24:x46	Roof's Heat Capacity x inverse of External Walls' Heat Capacity	-62,1312	4,03E-41
x24:x47	Roof's Heat Capacity x inverse of Internal Walls' Heat Capacity	-31,2748	2,96E-12
x25:x48	inverse of Bedroom_1 Effective window ventilation area x inverse of Roof's Heat Capacity	2753,509	0,006277
x31:x43	inverse of Living room Left Fin size x inverse of External Walls' U-value	1,076889	0,003813
x31:x48	inverse of Living room Left Fin size x inverse of Roof's Heat Capacity	88,7408	0,000912
x32:x46	inverse of Bedroom_1 Right Fin size x inverse of External Walls' Heat Capacity	256,1624	3,93E-05
x34:x48	inverse of Living room Right Fin size x inverse of Roof's Heat Capacity	54,14534	0,033488
x43:x46	inverse of External Walls' U-value x inverse of External Walls' Heat Capacity	-5646,37	1,44E-08
x46:x47	inverse of External Walls' Heat Capacity x inverse of Internal Walls' Heat Capacity	1493300	4,85E-32
x46:x48	inverse of External Walls' Heat Capacity x inverse of Roof's Heat Capacity	1628899	1,89E-77
x47:x48	inverse of Internal Walls' Heat Capacity x inverse of Roof's Heat Capacity	741422,3	2,46E-20
x4^2	External Walls' Solar Absorptance x External Walls' Solar Absorptance	286,135	3,22E-12
x8^2	Bedroom_1 Right Fin size x Bedroom_1 Right Fin size	-431,147	0,015436
x9^2	Bedroom_2 Right Fin size x Bedroom_2 Right Fin size	-336,007	0,012734
x12^2	Bedroom_2 Overhang size x Bedroom_2 Overhang size	326,389	0,01687
x14^2	Roof's Solar Absorptance x Roof's Solar Absorptance	1043,219	1,4E-136
x17^2	Bedroom_2 Window to Wall Ratio (WWR) x Bedroom_2 Window to Wall Ratio (WWR)	224,3875	0,003441
x18^2	Living room Window to Wall Ratio (WWR) x Living room Window to Wall Ratio (WWR)	193,6553	0,011336
x21^2	Roof's U-Value x Roof's U-Value	237,8337	3,07E-72
x24^2	Roof's Heat Capacity x Roof's Heat Capacity	0,002055	9,13E-24
x43^2	inverse of External Walls' U-value x inverse of External Walls' U-value	-33,5901	2,27E-09
x46^2	inverse of External Walls' Heat Capacity x inverse of External Walls' Heat Capacity	-1833500	5,88E-85
x47^2	inverse of Internal Walls' Heat Capacity x inverse of Internal Walls' Heat Capacity	-549903	2,53E-10
x48^2	inverse of Roof's Heat Capacity x inverse of Roof's Heat Capacity	-428602	1,19E-34

7.8 Appendix H – Excerpt from Database – Windows

Table 37 – LCH windows' specification

ID	Type	# Floors	# Of Bedrooms	Windows' Distribution	# Façade w/ window/ Tot FWW	Type of window	wwr (%)	EWVA (%)
HISB01	Building	from 7 to 11	2	Single Wall	2/4	Bedrooms and Living Room (1,4x1,32m) **Living Room** 2 sliding pieces (1,4x1,32x1,23) **Bedrooms** 2 glass sliding pieces, 2 exterior venetian blinds (sliding)	18%	
HISB02	Building	12	2	Single Wall	2/4			
HISB03	Building	Ground floor + 4	2	Adjacent walls		**Bedrooms** (1,36x1,55x1,10) sliding window 04 pieces: 2 blind **Living Room** (3,16x1,35x1,30) "L" window. Amount of sliding pieces vary.	25%	1,04

7.9 Appendix I – Excerpt from Database - Geometry

Table 38 – LCH geometry description

ID	Type	# of Floors	# Of Bedrooms	Attic	Floor-to-ceiling height (m)	Overhang Description	Geometrical Proportion	AREAS (m2)		OBS.
								Unit	Floor	
HIS B01	Building	from 7 to 11	2	NO	2,55	-	2,38	45,01	1021,15	
HIS B02	Building	12	2	NO	2,77	Concrete overhang on main façade	1,53	51,73	635,50	
HIS B03	Building	Ground floor + 4	2	NO	2,68	Concrete overhang with waterproof and fire resistant resin in all windows except living room		48,19	227,57	
HIS B04	Building	Ground floor + 4	2	NO	2,64	Concrete overhang with waterproof and fire resistant resin in all windows except living room		48,19	227,57	
HIS B05	Building		2	YES	2,50	Concrete overhang with waterproof and fire resistant resin in all windows	1,34	50,79	619,91	Data from Unit type 02 from 3° Floor. of Blocks A & B

7.10 Appendix J – Excerpt from Database - Construction

Table 39 – LCH Constructive systems' description

ID	Constructive System			Painting		OBS.
	Roof	External Seal	Internal Seal	Roof	External Wall	
HISB01	Waterproofed slab: area where water tank will be placed, waterproofed concrete with asphalt layer. Roof: Metallic roof tile in galvanized steel plates, 5% slant	Structural blocks thickness=19cm	Ceramic blocks thickness =9cm	Light color	Not specified	
HISB02	Waterproofed slab: area where water tank will be placed, waterproofed concrete with asphalt layer. Roof: Metallic roof tile in galvanized steel plates, 5% slant	Ceramic blocks w/ 9 wholes thickness=14cm	Ceramic blocks thickness =9cm. Solid ceramic brick b/w bedrooms and living room	Light color	Not specified	
HISB03	Trapezoidal Metallic roof tile in most of it. Central area covered with waterproof layer.	Ceramic blocks w/ 9 wholes thickness =14cm. exterior finish in latex acrylic	Ceramic blocks thickness =9cm. Solid ceramic brick b/w bedrooms and living room	Light color	Not specified	Concrete perforated shading element (*cobogó*) suspended b concrete structure
HISB04	Trapezoidal Metallic roof tile. Central area covered with waterproof layer.	Ceramic blocks w/ 9 wholes thickness = 14cm	Ceramic blocks thickness =9cm. Solid ceramic brick b/w bedrooms	Light color	Not specified	Concrete perforated shading element (*cobogó*) suspended b concrete structure
HISB05	Metallic roof tile in galvanized steel plates, 5% slant	Structural blocks thickness =19cm	Ceramic blocks thickness = 9cm		Not specified	Concrete perforated shading element (*cobogó*) painted with waterproof and fire resistant paint